

67-13,439

**KIMMEL, Howard S., 1938-  
INFRARED STUDIES OF METHYLSTANNANE.**

**The City University of New York, Ph.D., 1967  
Chemistry, physical**

**University Microfilms, Inc., Ann Arbor, Michigan**

INFRARED STUDIES OF METHYLSTANNANE

By

Howard S. Kimmel

A dissertation submitted to the  
Graduate Faculty in Chemistry in partial  
fulfillment of the requirements for the  
degree of Doctor of Philosophy, The City  
University of New York.

1967

This manuscript has been read and accepted for the University Committee in Chemistry in satisfaction of the dissertation requirement for the degree of Doctor of Philosophy.

May 5, 1967  
Date

Clyde R. Dillard  
Chairman of Examining Committee

May 4, 1967  
Date

Richard Wiley  
Executive Officer

Freyner  
Walter Blumey  
Clyde R. Dillard  
Supervisory Committee

## ACKNOWLEDGMENT

The author wishes to thank Professor C. R. Dillard for his help and encouragement in the course of this work. Appreciation is also extended to Professors U. Blukis, J. Wijnen, and S. Radel for their criticisms and suggestions.

The contributions of Professor R. P. Bauman, Professor J. Steigman and Mr. H. Toltz of Brooklyn Polytechnic Institute, Brooklyn, New York, Professor T. D. Goldfarb of the State University of New York at Stony Brook, New York, Mr. L. Clougherty of Beckman Instruments, Inc., Mountainside, New Jersey, Professor W. A. Fletcher of the University of Tennessee, Knoxville, and Professor M. Pei and Mrs. Ann File of the City College of New York Computation Center are gratefully acknowledged.

The author expresses his gratitude to his wife, Barbara, for her patience and encouragement.

## TABLE OF CONTENTS

	<u>Page</u>
I. INTRODUCTION	1
II. EXPERIMENTAL METHOD	4
A. Preparation of Compounds Studied	4
B. Instrumentation	8
III. ANALYSIS OF THE INFRARED SPECTRA	11
A. Vibrational Spectra and Assignments of the Vibrational Bands	11
B. Thermodynamic Properties	30
IV. VIBRATION-ROTATION ANALYSIS	31
A. Parallel Bands	35
B. Perpendicular Bands	38
V. NORMAL COORDINATE ANALYSIS	60
A. Anharmonic Corrections	62
B. Model Force Fields	77
C. The Vibrational Secular Equation	86
D. The Force Constant Refinement	90
E. The Calculation of the Potential Energy Distributions and Coriolis Constants	103
1. The Potential Energy Distributions	103
2. Coriolis Constants	109
VI. FORCE CONSTANT CORRELATIONS	113
A. Relationships Among the Force Constants	115
B. "Model" Force Constants and the Prediction of Vibrational Frequencies	123
APPENDIX I. TABLES OF THERMODYNAMIC PROPERTIES	137
APPENDIX II. TABLES OF VIBRATION-ROTATION LINES	141
APPENDIX III. COMPUTER PROGRAMS	151
BIBLIOGRAPHY	181

## LIST OF TABLES

<u>Table</u>	<u>Page</u>
I. Infrared Spectrum of Methylstannane	16
II. Infrared Spectrum of Methylstannane-d <sub>3</sub>	17
III. Infrared Spectrum of Methyl-d <sub>3</sub> -stannane	18
IV. Fundamental Vibrations of the Methylstannanes	19
V. Teller-Redlich Product-Rule Ratios	25
VI. Torsional Energy Levels for Methylstannane	29
VII. Structural Constants of Methylstannane	34
VIII. Ground State Rotational Constants of the Methylstannanes	34
IX. P-R Separations	37
X. Results of Combinations and Differences Analysis of CH <sub>3</sub> SnH <sub>3</sub>	43
XI. Rotational Constants from the Perpendicular Bands of CH <sub>3</sub> SnH <sub>3</sub>	44
XII. Results of Combinations and Differences Analysis for the CH <sub>3</sub> Rock and SnH <sub>3</sub> Asym. Deform. Vibrations of Methylstannane	53
XIII. Results of Combinations and Differences Analysis of CD <sub>3</sub> SnH <sub>3</sub>	55
XIV. Rotational Constants from the Perpendicular Bands of CD <sub>3</sub> SnH <sub>3</sub>	56
XV. Anharmonicity Constants, Anharmonic and Harmonic Frequencies for the Methylstannanes	75
XVI. Product Rule Ratios for Harmonic Frequencies	76
XVII. Symbols for the Independent Force Constants for CH <sub>3</sub> XH <sub>3</sub> Type Molecules	79
XVIII. Symmetry Coordinates for Methylstannane in Terms of Internal Coordinates	92
XIX. Harmonic Force Constants, and Calculated and Observed Frequencies. A <sub>1</sub> Symmetry Species	98

<u>Table</u>	<u>Page</u>
XX. Harmonic Force Constants, Calculated and Observed Frequencies, and Calculated and Observed Coriolis Constants. E Symmetry Species	100
XXI. L-Matrices of the Methylstannanes. A <sub>1</sub> Symmetry Species	101
XXII. L-Matrices of the Methylstannanes. E Symmetry Species	102
XXIII. Force Constants of the CH <sub>3</sub> XH <sub>3</sub> Series of Molecules	104
XXIV. Potential Energy Distributions. A <sub>1</sub> Symmetry Species	105
XXV. Potential Energy Distributions. E Symmetry Species	106
XXVI. P.E.D. Among the CH <sub>3</sub> Rocking, XH <sub>3</sub> Asymmetric Deformation and XH <sub>3</sub> Rocking Modes of CH <sub>3</sub> SiH <sub>3</sub> and CH <sub>3</sub> GeH <sub>3</sub>	108
XXVII. Coriolis Constants of Methylstannane	110
XXVIII. Coriolis Constants for the CH <sub>3</sub> XH <sub>3</sub> Molecules	112
XXIX. Bond Lengths (A) for CH <sub>3</sub> XH <sub>3</sub> Molecules	114
XXX. Equations Used for Calculating the "Model" Force Constants	124
XXXI. "Model" Force Constants	126
XXXII. Vibrational Frequencies of CH <sub>3</sub> SiH <sub>3</sub> Calculated from the "Model" Force Constants	127
XXXIII. Vibrational Frequencies of CH <sub>3</sub> GeH <sub>3</sub> Calculated from the "Model" Force Constants	128
XXXIV. Vibrational Frequencies of CH <sub>3</sub> SnH <sub>3</sub> Calculated from the "Model" Force Constants	129
XXXV. "Model" Force Constants and Calculated Frequencies for the Methyl Group in Methyltriethyltin	133
XXXVI. "Model" Force Constants and Calculated Frequencies for Germylsilane	135
XXXVII. Vibrational Frequencies for Germylsilane	136

## LIST OF FIGURES

<u>Figure</u>	<u>Page</u>
1. Reaction System for Preparation of $\text{CD}_3\text{SnCl}_3$	7
2. Infrared Spectrum of $\text{CH}_3\text{SnH}_3$	13
3. Infrared Spectrum of $\text{CH}_3\text{SnD}_3$	14
4. Infrared Spectrum of $\text{CD}_3\text{SnH}_3$	15
5. Potential Energy Curve for Hindered Rotation Drawn to Scale for Methylstannane	27
6. CH Asym. Str. ( $\nu_7$ ) and Sym. Str. ( $\nu_1$ ) Bands of $\text{CH}_3\text{SnH}_3$	48
7. SnH Asym. Str. Band of $\text{CH}_3\text{SnH}_3$	49
8. $\text{CH}_3$ Asym. Deform. ( $\nu_9$ ) and Sym. Deform. ( $\nu_3$ ) Bands of $\text{CH}_3\text{SnH}_3$	50
9. $\text{SnH}_3$ Sym. Deform. ( $\nu_4$ ) and Rock ( $\nu_{12}$ ) Bands of $\text{CH}_3\text{SnH}_3$	51
10. $\text{CH}_3$ Rock ( $\nu_{10}$ ) and $\text{SnH}_3$ Asym. Deform. ( $\nu_{11}$ ) Bands of $\text{CH}_3\text{SnH}_3$	52
11. SnH Asym. Str. Band of $\text{CD}_3\text{SnH}_3$	57
12. $\text{SnH}_3$ Asym. Deform. Band of $\text{CD}_3\text{SnH}_3$	58
13. $\text{CD}_3$ Rock Band of $\text{CD}_3\text{SnH}_3$	59
14. Plot of $x_e$ vs. $x$ for the CH Asym. Str. Vibration of $\text{CH}_3\text{X}$ Molecules	69
15. Plot of $x_e$ vs. $x$ for the $\text{CH}_3$ Sym. Deform. Vibration of $\text{CH}_3\text{X}$ Molecules	71
16. Plot of $x_{\text{SD}}$ vs. $x_{\text{R}}$ of $\text{CH}_3\text{X}$ Molecules	73
17. Plot of Angular Dependence of the $F_{\text{AD-R}}$ with Negative Values	87
18. Valence Coordinates for Methylstannane	93
19. Plot of XH Bond Lengths vs. $\text{XH}_3$ Sym. Deform. Force Constants	118
20. Plot of XH Bond Lengths vs. $\text{XH}_3$ Asym. Deform. Force Constants	119
21. Plot of XH Bond Lengths vs. $\text{XH}_3$ Rock Force Constants	120

## CHAPTER I

### INTRODUCTION

This study is concerned with the detailed vibrational and vibration-rotational analysis of methylstannane,  $\text{CH}_3\text{SnH}_3$ . The goal of this investigation is to develop a technique by means of which force constants, that are related to the structures of the molecules, can be derived for the series  $\text{CH}_3\text{XH}_3$ . Further, these force constants should be transferable to other molecules not in this series provided that the appropriate structural parameters are known.

The vibration and vibration-rotation spectra of structurally similar molecules,  $\text{CH}_3\text{XH}_3$ , where X is C, Si, and Ge have been studied in some detail (5, 26, 27, 54, 61, 63). The infrared spectrum of  $\text{CH}_3\text{SnH}_3$  has been reported by Dillard and May (16) who made tentative vibrational assignments. However, because of lack of data on isotopically substituted methylstannanes, Dillard and May were unable to make a complete vibrational analysis.

The complete vibrational analysis of methylstannane made in this research extends the knowledge of the spectra of  $\text{CH}_3\text{XH}_3$  type molecules, and provides some insights about the effect of changing the nature of the central atom, X, on the observed spectra. By use of empirical and theoretical methods to obtain force constants it is now possible to predict the vibrational frequencies for this series of molecules.

Ward (62) established empirical relationships of the frequencies in the series  $(\text{CH}_3)_n\text{XCl}_{(4-n)}$  where X is C, Si, Ge, and Sn and n is an integer 1 to 3. Dillard and May (16)

made similar correlations for the frequencies of the series  $(\text{CH}_3)_n \text{XH}_{(4-n)}$ . However, these empirical correlations can be used only to show trends in the frequencies. Moreover, the relationships obtained are not applicable outside the specified series.

Factors which are needed in order to make reliable and quantitative predictions about the spectra of a series of related molecules include (1) the knowledge of how the potential energy is distributed among the respective vibrational modes; (2) the relationships between the force constants which will make them transferable between members of the series; and (3) the knowledge of how the structures of the molecules affect the force constants and the rotational constants. In this work we have obtained the potential energy distributions of the entire series of  $\text{CH}_3\text{XH}_3$  molecules. Our analysis shows that the force constants are related to the bond lengths of the  $\text{CH}_3$  and  $\text{XH}_3$  groups and are transferable among the molecules.

For molecules in the  $\text{CH}_3\text{XH}_3$  series it is impossible to uniquely determine the General Harmonic Force Field without making simplifying assumptions because (1) there is usually insufficient data to compute the anharmonicity corrections to the observed vibrational frequencies and to calculate unique general harmonic force constants; and (2) it is necessary to solve a complicated set of equations in order to calculate the force constants from the observed data. The anharmonicity effects were determined by empirically transferring known anharmonicity constants of related molecules. The complicated set of equations were solved by choosing a force field with the minimum number of independent parameters and taking advantage of the symmetry of the molecule.

The approach used in this study consisted of the several steps outlined below. First, a complete vibrational analysis was performed because accurate and correctly assigned frequencies are necessary to calculate the force constants. Data on isotopic species and related molecules were used when available to confirm the assignments.

Second, a vibration-rotation analysis was performed to obtain accurate frequencies, ground and excited state rotational constants and Coriolis constants. The Coriolis constants would be expected to show a dependence upon the nature of the X atom in the  $\text{CH}_3\text{XH}_3$  series of molecules. However, because of the complicated structure of the vibration-rotation bands, the experimental error was large and sufficiently accurate Coriolis constants were not obtained. On the other hand, the vibration-rotation analysis did provide the accurate frequencies necessary for the force constant calculations.

Third, the observed vibrational frequencies were corrected for anharmonicity effects. A suitable force field was chosen. Then a normal coordinate analysis was performed using a computer program which yielded the best set of force constants, the eigenvectors and the potential energy distribution. From the force constant computations a unique solution to the secular equation was obtained. The eigenvectors were used to calculate the Coriolis constants and the calculated and experimental values were comparable within the limits of experimental error.

Finally, "model" force constants were derived which were transferable between the molecules of the  $\text{CH}_3\text{XH}_3$  series. Furthermore, these force constants were shown to be transferable to molecules not in this series.

CHAPTER II  
EXPERIMENTAL

A. Preparation of Compounds Studied

Methylstannane and methylstannane-d<sub>3</sub> were prepared by reacting CH<sub>3</sub>SnCl<sub>3</sub> with LiAlH<sub>4</sub> and LiAlD<sub>4</sub>, respectively (22). The methyltin chloride was prepared by bubbling methyl chloride through melted anhydrous tin (II) chloride at 365°C (62).

Descriptions of the reaction chamber and the reaction train used in the preparation of CH<sub>3</sub>SnCl<sub>3</sub> were given by Ward (62). About 80 grams of pure anhydrous tin (II) chloride (Matheson Coleman & Bell, Reagent Grade) were introduced into the reaction chamber. The tin (II) chloride was then melted and brought to 365°C in an atmosphere of methyl chloride (Matheson Co.). The methyl chloride was allowed to bubble through the molten tin (II) chloride at a rate of 20 to 25 ml per minute. Within an hour, tiny droplets of a clear liquid were observed in the product receiver. The reaction was allowed to run for 9 hours. The final product was a clear solid at room temperature. The CH<sub>3</sub>SnCl<sub>3</sub> was used in the preparation of CH<sub>3</sub>SnH<sub>3</sub> without purification.

To prepare methylstannane, about 3.4 mmoles of LiAlH<sub>4</sub> (Metal Hydrides Co.) were dissolved in anhydrous diglyme (b.p.: 160-164°C) and placed in a reaction flask. A dropping funnel containing about 1.7 mmoles of CH<sub>3</sub>SnCl<sub>3</sub> which was dissolved in diglyme was placed in the neck of the flask. The reaction flask was then evacuated. The reaction was carried out at dry ice temperatures with vigorous stirring. The solution of methyltin chloride was added very slowly

and the reaction was carried out over a period of four hours. The gaseous product was passed through a  $-78.5^{\circ}\text{C}$  bath and collected in a liquid nitrogen bath. The vapor pressure of the impure product was 28mm at  $-78.5^{\circ}\text{C}$ . Pure methylstannane has a vapor pressure of 9.5mm at  $-78.5^{\circ}\text{C}$  (22). The molecular weight of the sample and its infrared spectrum were used as the criteria of its purity. The sample was purified by successively passing it through traps at  $-95^{\circ}$ ,  $-112^{\circ}$ , and  $-150^{\circ}\text{C}$ . The material in the  $-95^{\circ}\text{C}$  trap showed a vapor pressure of 9.5mm at  $-78.5^{\circ}\text{C}$ . Its molecular weight was found to be 134 g/mole, which is within experimental error of the calculated molecular weight of 137 for methylstannane. The infrared spectrum of the product agreed with the spectrum reported for methylstannane (16). A yield of 46% was obtained.

Pure methylstannane- $\text{d}_3$  was prepared by reacting about 0.16 mmoles of  $\text{CH}_3\text{SnCl}_3$  with 0.117 moles of  $\text{LiAlD}_4$  (Metal Hydrides Co., 98.4%). The final product had a vapor pressure of 11mm at  $-78.5^{\circ}\text{C}$ . Repeated distillation of the sample showed no change in the vapor pressure or in the infrared spectrum. The infrared spectrum of the product gave the expected shifts due to isotopic substitution. A very weak absorption band at about  $1880\text{ cm}^{-1}$  indicated the presence of  $\text{CH}_3\text{SnH}_3$  as an impurity. A yield of 37% was obtained. Because of the small quantity of the rather unstable compound, the molecular weight and other physical properties were not determined.

A modification of the procedure reported by Ward (62) was used to prepare  $\text{CD}_3\text{SnCl}_3$  as described below. The reaction system for the preparation of  $\text{CD}_3\text{SnCl}_3$  is shown in Figure 1.

A large excess of tin (II) chloride (about 10.6 mmoles) was added to the reaction flask through A. After 8.7 mmoles of  $\text{CD}_3\text{Cl}$  (Tracerlab, 99 atom % D) were added through A, the glass tube was sealed. The reaction was run at a temperature of  $350^\circ\text{C}$  for 4 days. After 16 hours, liquid was noted in the received. The yield of  $\text{CD}_3\text{SnCl}_3$  was 44%. This material was used in the preparation of  $\text{CD}_3\text{SnH}_3$  without further purification.

Methyl- $\text{d}_3$ -stannane was prepared by reacting approximately 3.0 mmoles of  $\text{CD}_3\text{SnCl}_3$  with 6.6 mmoles of  $\text{LiAlH}_4$  using the method described above. Distillation of the impure methyl- $\text{d}_3$ -stannane through traps at  $-80^\circ$  and  $-112^\circ\text{C}$  into a liquid nitrogen trap was repeated until a constant vapor pressure of 14mm at  $-78.5^\circ\text{C}$  was obtained. Absorption bands at 2940, 2900 and  $1180\text{ cm}^{-1}$  in the infrared spectrum of the product indicated the presence of dimethylether as an impurity. The infrared bands due to the impurity were further identified by obtaining infrared spectra of the sample at several of the early steps of purification when there were changes in the measured physical properties of the product. The molecular weight of the sample was 123 as compared to the calculated molecular weight of 139 for  $\text{CD}_3\text{SnH}_3$ . From the molecular weights it was estimated that the methyl- $\text{d}_3$ -stannane was about 86% pure. The yield of  $\text{CD}_3\text{SnH}_3$  was 18%.

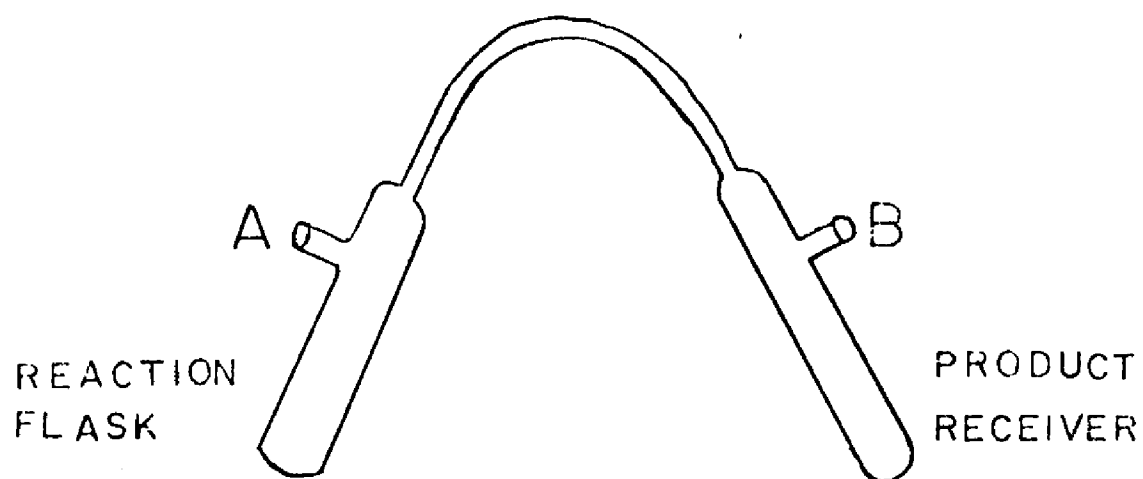


Figure 1. Reaction System for Preparation of  $\text{CD}_3\text{SnCl}_3$

## B. Instrumentation

The infrared spectra were obtained using a Perkin-Elmer Model 521 spectrophotometer<sup>1</sup>, and Beckman IR-9<sup>1</sup> and IR-12 spectrophotometers. Perkin-Elmer Model 21 and Model 337 infrared spectrophotometers were used to check the purity of the methylstannanes during their preparation.

The Perkin-Elmer Model 521 infrared spectrophotometer is a double-beam, double grating instrument with a range of 4000-250  $\text{cm}^{-1}$ . Both Beckman spectrophotometers are double-beam instruments. The IR-9 employs a double monochromator consisting of a KBr foreprism and two gratings, and has a range of 4000-400  $\text{cm}^{-1}$ . The IR-12 employs a single monochromator consisting of four gratings which gives the instrument a range of 4000-200  $\text{cm}^{-1}$ .

All high resolution spectra were obtained at a scanning speed of 2 - 4  $\text{cm}^{-1}/\text{min}$ . Each absorption band was examined at a constant slit width. The slit widths were manually adjusted for each band so as to obtain optimum resolution and signal to noise ratio.

---

<sup>1</sup> The use of the Perkin-Elmer Model 521 infrared spectrometer was made possible by Professor R. P. Bauman, Professor J. Steigman and Mr. H. Toltz of Brooklyn Polytechnic Institute, Brooklyn, New York. The use of the Beckman IR-11 infrared spectrophotometer at the Beckman Laboratories, Mountainside, New Jersey was made possible by Mr. L. Clougherty of Beckman Instruments, Inc. These kindnesses are gratefully acknowledged.

In order to compare spectra obtained on different instruments and to transfer spectral absorption data between instruments, the resolution was expressed in terms of the spectral slit width. The spectral slit width is the frequency interval between the two points at which the energy passing through the exit slit of a monochromator is one-half its maximum value. Spectral slit widths of about  $1.5 \text{ cm}^{-1}$  for the  $4000\text{-}1600 \text{ cm}^{-1}$  region and about  $1.0 \text{ cm}^{-1}$  for the  $1600\text{-}250 \text{ cm}^{-1}$  region gave the best high resolution spectral data for the methylstannanes. The mechanical slit widths corresponding to these spectral slit widths varied with the instrument used. The methods for converting from one to the other are described in the instruction manuals for the instruments.

The instruments were calibrated against  $\text{HCl}$ ,  $\text{NH}_3$ ,  $\text{CO}_2$ , and  $\text{H}_2\text{O}$ . The frequencies of the vibration-rotation lines of the compounds were taken from the IUPAC tables (34) and from the papers of Plyler, Blaine, and co-workers (6, 53). Each band was scanned three times and average values for the measured frequencies were used. The probable error of a spectral line wave number assignment was about  $1.0 \text{ cm}^{-1}$  from  $4000\text{-}2000 \text{ cm}^{-1}$  and about  $0.6 \text{ cm}^{-1}$  from  $2000\text{-}250 \text{ cm}^{-1}$ .

A standard 10 cm gas absorption cell made of pyrex glass and equipped with  $\text{KBr}$  and  $\text{CsBr}$  windows was used for the high resolution spectra. The methylstannanes were kept in the gas cell for periods up to six hours without any significant decomposition. Both the intensity of the band and the resolution had to be considered in determining suitable pressures for obtaining the spectra of the individual bands. The pressures used ranged from 6mm for the vibration-rotation lines of the  $\text{Sn-H}$  stretching vibrations to more than

100mm for the weak C-H stretching vibrations.

For the very weak overtone and combination bands involving the torsional vibration, it was necessary to use a Perkin-Elmer 1-meter gas absorption cell (Model #127-0061) equipped with CsBr windows<sup>2</sup>.

---

<sup>2</sup> The kindness of Professor T. D. Goldfarb, of the State University of New York at Stony Brook, New York in making available the Perkin-Elmer 1-meter gas absorption cell and a Perkin-Elmer Model 521 infrared spectrophotometer is gratefully acknowledged.

## CHAPTER III

### ANALYSIS OF THE INFRARED SPECTRA

#### A. Vibrational Spectra and Assignments of the Vibrational Bands

Methylstannane is a member of the structurally similar class of molecules of the type  $\text{CH}_3\text{XH}_3$  where X is C, Si, Ge or Sn. Vibrational studies have been made on ethane (27, 61) and methylgermane (26) where infrared spectra of several isotopic species were available. For methylsilane only the  $\text{CH}_3\text{SiH}_3$  and  $\text{CH}_3\text{SiD}_3$  species have been studied (5, 63). Dillard and May (16) have reported on the infrared spectrum of  $\text{CH}_3\text{SnH}_3$ , however they lacked data on the isotopically substituted methylstannanes and a complete vibrational analysis was not made. In other works, the vibrational assignments for  $\text{CH}_3\text{SnCl}_3$  (47, 61) and  $\text{CH}_3\text{GeCl}_3$  (45) have been reported.

The infrared spectra of  $\text{CH}_3\text{SnH}_3$ ,  $\text{CH}_3\text{SnD}_3$ , and  $\text{CD}_3\text{SnH}_3$  are shown in Figures 2, 3, and 4. These three molecules have  $\text{C}_{3v}$  symmetry.

Thus there are 12 fundamental vibrations, of which 5 are of the nondegenerate species,  $\text{A}_1$ , 6 are of the doubly degenerate E species, while the remaining one is of type  $\text{A}_2$ . The  $\text{A}_1$  and E vibrations are infrared active. The  $\text{A}_2$  vibration which is due to the torsional motion is inactive in the infrared. Of the 11 active fundamentals, 5 may be considered to be vibrations of the  $\text{CH}_3$  group and 5 arise from the vibrations of the  $\text{SnH}_3$  group. The remaining band arises from the Sn-C stretching mode.

The vibrational assignments reported here were made by (1) comparison with assignments reported for similar molecules, (2) consideration of the relationships with isotopic species, and (3) considerations of the contours of the bands. By comparison with the assignments for the other members of the series  $\text{CH}_3\text{XH}_3$ , where X is C, Si and Ge (26, 27, 63) it is seen that the carbon-hydrogen vibrations occur at approximately the same frequencies throughout the series. The frequencies associated with the tin-hydrogen motions were readily identified by the observed shifts upon isotopic substitution. Band contours of these  $\text{C}_{3v}$  type molecules were used to identify the nondegenerate and degenerate vibrations. Nondegenerate vibrations showed two broad absorption bands of medium intensity (P and R branches) on either side of a strong, sharp band (Q branch). Degenerate vibrations showed a single broad absorption band.

The frequencies and vibrational assignments of  $\text{CH}_3\text{SnH}_3$ ,  $\text{CH}_3\text{SnD}_3$ , and  $\text{CD}_3\text{SnH}_3$  are listed in Tables I - III. The fundamental vibrations and their descriptions for the methylstannanes are summarized in Table IV where the notation is adapted from that used by Herzberg (32). Assignments of the fundamental frequencies to normal modes are done in an analogous manner for all three isotopic species. Therefore, the discussion will center on methylstannane and comments on the isotopic molecules will be made only to support the assignments.

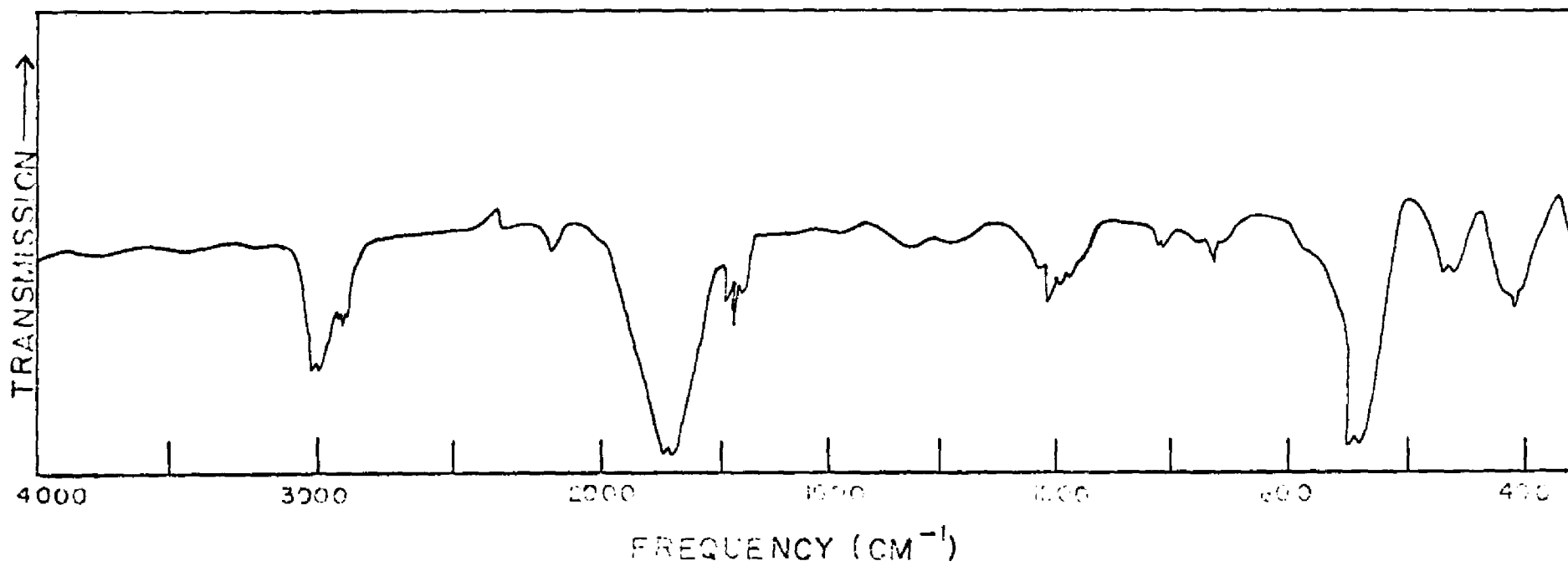


Figure 2. Infrared Spectrum of  $\text{CH}_3\text{SnH}_3$

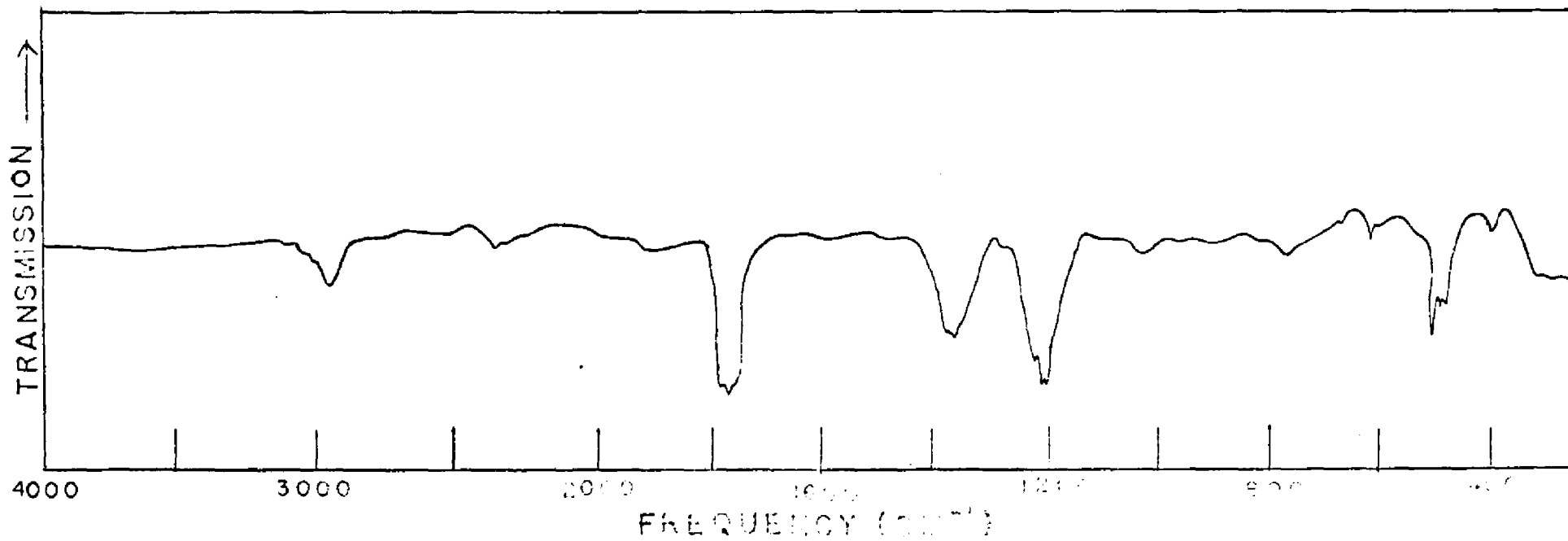


Figure 3. Infrared Spectrum of  $\text{CH}_3\text{SnD}_3$

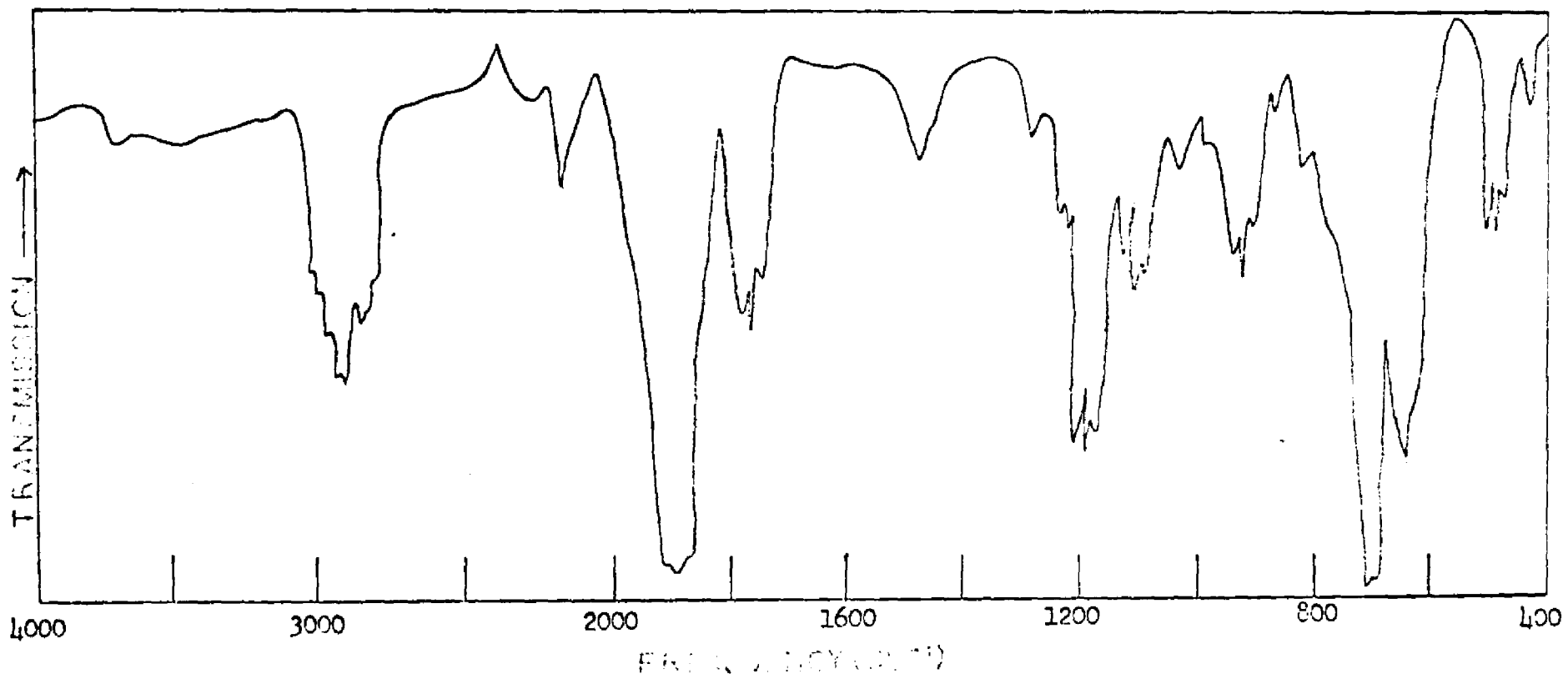


Figure 4. Infrared Spectrum of  $\text{CD}_3\text{SnH}_3$

TABLE I

Infrared Spectrum of Methylstannane (cm<sup>-1</sup>)

<u>Frequency</u>	<u>Intensity</u>	<u>Assignment</u>	
3710	w	$\nu_1 + \nu_{10}$	(E)
3005.4	w	$\nu_7$	(E)
2932.5	w	$\nu_1$	(A <sub>1</sub> )
2827.6	w	$2\nu_9$	(A <sub>1</sub> + E)
1874.5	s	$\nu_8$ (E), $\nu_2$ (A <sub>1</sub> )	
1755.8	m	$\nu_3 + \nu_5$	(A <sub>1</sub> )
1417.0	w	$\nu_9$	(E)
1209.3	w	$\nu_3$	(A <sub>1</sub> )
1168.2	w	$\nu_{10} + \nu_{12}$	(A <sub>1</sub> + A <sub>2</sub> + E)
931	vw	$\nu_5 + \nu_{12}$	(E)
910	vw	$\nu_4 + 2\nu_6$	(A <sub>1</sub> )
774.1	m	$\nu_{10}$	(E)
741.3	m	$\nu_{11}$	(E)
694.5	s	$\nu_4$	(A <sub>1</sub> )
570	vw		
526.9	m	$\nu_5$	(A <sub>1</sub> )
416.3	m	$\nu_{12}$	(E)
340	vw		
320	vw	$\nu_5 - 2\nu_6$	(A <sub>1</sub> )
298	vw	$\nu_{12} - \nu_6$	(E)

TABLE II

Infrared Spectrum of Methylstannane-d<sub>3</sub> (cm<sup>-1</sup>)

<u>Frequency</u>	<u>Intensity</u>	<u>Assignment</u>	
3000	w	$\nu_7$	(E)
2930	m	$\nu_1$	(A <sub>1</sub> )
1756.4	s	$\nu_3 + \nu_5$	(A <sub>1</sub> )
1550	w	$2\nu_{10}$	(A <sub>1</sub> + E)
1400	w	$\nu_8$	(E)
1352.0	s	$\nu_9$ (E), $\nu_2$ (A <sub>1</sub> )	
1204.5	s	$\nu_3$	(A <sub>1</sub> )
1182	m		
1170	m		
1055	w	$\nu_{10} + \nu_{12}$	(A <sub>1</sub> +A <sub>2</sub> +E)
1012	w	$2\nu_5; 2\nu_{11}; \nu_4 + \nu_5; \nu_5 + \nu_{11}$	
908	w		
765	w	$\nu_{10}$	(E)
612	w	$2\nu_{12}$	(A <sub>1</sub> + E)
509.1	m	$\nu_4$	(A <sub>1</sub> )
502.5	s	$\nu_{11}$	(E)
493.0	s	$\nu_5$	(A <sub>1</sub> )
390	w		
316.6	m	$\nu_{12}$	(E)

TABLE III

Infrared Spectrum of Methyl-d<sub>3</sub>-stannane (cm<sup>-1</sup>)

<u>Frequency</u>	<u>Intensity</u>	<u>Assignment</u>	
2254.5	m	$\nu_7$	(E)
2144.3	m	$\nu_1$	(A <sub>1</sub> )
1889.0	s	$\nu_8$ (E), $\nu_2$ (A <sub>1</sub> )	
1759.0	m	$\nu_9 + \nu_{10}$	(A <sub>1</sub> + A <sub>2</sub> + E)
1606	w	$\nu_3 + \nu_4$	(A <sub>1</sub> )
1462.9	m	$\nu_4 + \nu_{10}$	(E)
1117.5	m	$\nu_{10} + \nu_{12}$	(A <sub>1</sub> + A <sub>2</sub> + E)
1017.1	w	$\nu_9$	(E)
920.2	m	$\nu_3$	(A <sub>1</sub> )
738.1	m	$\nu_{10}$	(E)
703.5	s	$\nu_4$	(A <sub>1</sub> )
628.4	s	$\nu_{11}$	(E)
478.0	m	$\nu_5$	(A <sub>1</sub> )
392.4	w	$\nu_{12}$	(E)

TABLE IV

Fundamental Vibrations of the Methylstannanes (cm<sup>-1</sup>)

<u>Description</u>	<u>Vibn.</u> <u>No.</u>	<u>CH<sub>3</sub>SnH<sub>3</sub></u>	<u>Vibn.</u> <u>No.</u>	<u>CH<sub>3</sub>SnD<sub>3</sub></u>	<u>Vibn.</u> <u>No.</u>	<u>CD<sub>3</sub>SnH<sub>3</sub></u>
<u>A<sub>1</sub> Species</u>						
CH sym. str.	1	2932.5	1	2930 <sup>b</sup>	1	2144.3
SnH sym. str.	2	1874.5	2	1352.0	2	1889.0
CH <sub>3</sub> sym. deform.	3	1209.3	3	1204.5	3	920.2
SnH <sub>3</sub> sym. deform.	4	694.5	5	493.0	4	703.5
SnC str.	5	526.9	4	509.1	5	478.0
<u>A<sub>2</sub> Species</u>						
Torsion <sup>a</sup>	6	109	6	101	6	89
<u>E Species</u>						
CH asym. str.	7	3005.4	7	3000 <sup>b</sup>	7	2254.5
SnH asym. str.	8	1874.5	9	1352.0	8	1889.0
CH <sub>3</sub> asym. deform.	9	1417.0	8	1400 <sup>b</sup>	9	1017.1
SnH <sub>3</sub> asym. deform.	11	741.3	11	502.5	10	738.1
Ch <sub>3</sub> rock	10	774.1	10	765 <sup>b</sup>	11	628.4
SnH <sub>3</sub> rock	12	416.3	12	316.6	12	392.4

<sup>a</sup> Calculated from the barrier to internal rotation (9)

<sup>b</sup> Frequencies were measured to + 10 cm<sup>-1</sup>.

The asymmetric and symmetric stretching motions of the C-H bonds are assigned to the bands at 3005.4 and 2932.5  $\text{cm}^{-1}$ , respectively. The analogous modes for the  $\text{CD}_3\text{SnH}_3$  molecule are shifted to 2254.5 and 2144.3  $\text{cm}^{-1}$ , respectively. The asymmetric and symmetric  $\text{CH}_3$  deformation vibrations are observed at 1417.0 and 1209.3  $\text{cm}^{-1}$ , respectively while the same modes for the  $\text{CD}_3$  group in  $\text{CD}_3\text{SnH}_3$  occur 1017.1 and 920.2  $\text{cm}^{-1}$ . Dillard and May (16) have reported a value of 1143  $\text{cm}^{-1}$  for the  $\text{CH}_3$  symmetric deformation vibration of methylstannane. In reports on other methyltin compounds (16, 48, 62) the assigned frequency for this vibration was between 1200 and 1220  $\text{cm}^{-1}$ . In this work the frequency at 1209.3  $\text{cm}^{-1}$  is assigned to the  $\text{CH}_3$  symmetric deformation vibration. The product rule ratios for the  $A_1$  species substantiates this assignment (Table V).

The strong band at 1874.5  $\text{cm}^{-1}$  which appears only in the spectra of  $\text{CH}_3\text{SnH}_3$  and  $\text{CD}_3\text{SnH}_3$  must arise from the Sn-H asymmetric and Sn-H symmetric stretch vibrations. As will be pointed out in the section on the high resolution analysis of the methylstannanes, this band shows the rotational structure of the Q branch arising from the asymmetric stretching motion. The data on  $\text{CH}_3\text{SiH}_3$  (63) and  $\text{CH}_3\text{GeH}_3$  (26) indicate that both stretching modes would be expected to appear close together and there are no other bands in this region that could be assigned to the symmetric stretching motion. Hence the symmetric stretching vibration must be buried in this strong absorption band. Also, it can be seen that for  $\text{CH}_3\text{SnD}_3$  only one band appears at 1352.0  $\text{cm}^{-1}$  which can be assigned to the two Sn-D stretching modes. The parallel band between 1750 and

1760  $\text{cm}^{-1}$  in the spectrum of  $\text{CH}_3\text{SnH}_3$  can not be assigned to the  $\text{SnH}_3$  symmetric stretch because the band also appears in the spectra of the other two isotopic species. This absorption band has been assigned to a combination band.

Three bands are observed in the region 690-780  $\text{cm}^{-1}$  for  $\text{CH}_3\text{SnH}_3$ . One parallel band due to the  $\text{SnH}_3$  symmetric deformation vibration and two perpendicular bands due to the  $\text{SnH}_3$  asymmetric deformation and  $\text{CH}_3$  rocking vibrations would be expected to appear in this region. Unambiguous assignments for these bands are possible if the band contours and data on the isotopic species are considered. Consideration of the moments of inertia for methylstannane indicates that the parallel band of species  $A_1$  should show a definite PQR branch structure with a strong sharp Q branch while the perpendicular band of species E should show a single broad bell-shaped absorption curve (23). The band at 694.5  $\text{cm}^{-1}$  is observed to be a parallel band and thus can be assigned to the  $\text{SnH}_3$  symmetric deformation vibration. This band has a frequency of 703.5  $\text{cm}^{-1}$  in  $\text{CD}_3\text{SnH}_3$  but is seen to shift to 493  $\text{cm}^{-1}$  in  $\text{CH}_3\text{SnD}_3$ . The other two bands of  $\text{CH}_3\text{SnH}_3$  in the 690-780  $\text{cm}^{-1}$  region have the contour of perpendicular bands with frequencies of 741.3 and 774.1  $\text{cm}^{-1}$ . In the  $\text{CH}_3\text{SnD}_3$  molecule only one band remains at 765  $\text{cm}^{-1}$  while for  $\text{CD}_3\text{SnH}_3$  a band at 739.8  $\text{cm}^{-1}$  is observed. Thus, the band at 774.1  $\text{cm}^{-1}$  can be assigned as the  $\text{CH}_3$  rocking mode and the absorption peak at 741.3  $\text{cm}^{-1}$  must arise from the  $\text{SnH}_3$  asymmetric deformation vibration. In  $\text{CD}_3\text{SnH}_3$ , the  $\text{CD}_3$  rocking vibration can be observed at 628.4  $\text{cm}^{-1}$  while the  $\text{SnD}_3$  asymmetric deformation vibration in  $\text{CH}_3\text{SnD}_3$  appears at 502.5  $\text{cm}^{-1}$ .

The Sn-C stretching mode and the SnH<sub>3</sub> rocking mode remain to be assigned. The absorptions at 526.9 cm<sup>-1</sup> in CH<sub>3</sub>SnH<sub>3</sub> and 509.1 cm<sup>-1</sup> in CH<sub>3</sub>SnD<sub>3</sub> have the contours of parallel bands and thus can be assigned to the stretching vibration of the Sn-C bond. In the case of CD<sub>3</sub>SnH<sub>3</sub>, this band is displaced to 478.0 cm<sup>-1</sup>. The SnH<sub>3</sub> rocking mode can be correlated with the perpendicular bands appearing at 416.3 cm<sup>-1</sup> in CH<sub>3</sub>SnH<sub>3</sub>, and 392.4 cm<sup>-1</sup> in CD<sub>3</sub>SnH<sub>3</sub>. Substitution of D for H on tin causes the appearance of the SnD<sub>3</sub> rocking mode at 316.6 cm<sup>-1</sup>.

The existence of the three infrared bands of CH<sub>3</sub>SnD<sub>3</sub> in the region of 490 to 510 cm<sup>-1</sup> have already been cited as evidence supporting the assignments of the CH<sub>3</sub> rocking SnH<sub>3</sub> symmetric deformation and SnH<sub>3</sub> asymmetric deformation vibrations of CH<sub>3</sub>SnH<sub>3</sub>. However, due to the complexity of the spectrum in this region, some further comments should be made on the assignments of the three bands. One perpendicular band due to the SnD<sub>3</sub> asymmetric deformation vibration and two parallel bands due to the SnD<sub>3</sub> symmetric deformation and Sn-C stretching vibrations would be expected to appear in this region. Examination of the contour of the bands indicates a weak absorption peak on the high frequency side of the band at 509.1 cm<sup>-1</sup> probably due to the R branch of a parallel band, and a weak absorption maximum on the low frequency side of the band at 493.0 cm<sup>-1</sup> probably due to the P branch of a parallel band. Thus the bands at 509.1 and 493.0 cm<sup>-1</sup> can be attributed to Q branches of parallel-type bands. The latter can be assigned to the SnD<sub>3</sub> symmetric deformation mode since this vibration would be expected to occur at approximately  $694.5/(2)^{1/2} = 490$  cm<sup>-1</sup>.

The other parallel band at  $509.1 \text{ cm}^{-1}$  must be due to the Sn-C stretching mode. The remaining band at  $502.5 \text{ cm}^{-1}$ , which is a perpendicular type, must arise from the  $\text{SnD}_3$  asymmetric deformation vibration.

The assignments of the fundamental vibration frequencies of the  $A_1$  and E species for the three isotopic molecules are substantiated by Teller-Redlich product rule calculations which appear in Table V. Good agreement is obtained for the observed and calculated product rule ratios. Molecular constants from microwave studies (38) were used in the calculations. The constants are listed in Table VIII of Chapter IV. The observed product rule ratios for anharmonic frequencies listed in Table V, should be greater than the calculated ratios. In the case of the  $\text{CH}_3\text{SnD}_3/\text{CH}_3\text{SnH}_3$  ratio for the  $A_1$  species the observed value is less than the calculated value. This reversal of the  $A_1$  species product ratio was observed for the methylgermanes (6).

Since all the combination bands except binary combinations of torsional vibrations with  $A_1$  type vibrations are infrared active, 400 binary and ternary overtones and combination bands could exist for each of these isotopic species. Only 10 such bands for  $\text{CH}_3\text{SnH}_3$ , 9 such bands for  $\text{CH}_3\text{SnD}_3$  and 4 such bands for  $\text{CD}_3\text{SnH}_3$  were actually observed. The assignments of combination and overtone bands were made using the method suggested by Glass and Pullin (13). In this procedure frequencies of all possible binary and ternary combination bands and overtones were calculated. Additivity of all fundamental frequencies were assumed. Combinations and overtones were assigned to those bands which were observed in the range 1.01 to 0.98 times the calculated frequency. Where several combinations and

overtone could be assigned to an observed band, other evidence, such as band contours (i.e., the parallel or perpendicular character of the band) and comparison with related compounds, were used to select the appropriate assignment. The assignments for the methylstannanes are shown in Tables I - III.

The rotation of a methyl group relative to the  $\text{SnH}_3$  group work is opposed by a threefold potential barrier. If the barrier to the internal rotation is sufficiently high the rotation reduces to a torsional oscillation. Although the frequency of the torsional motion cannot be directly observed in the infrared, it can be determined from overtones and combination bands which are infrared active, or from the barrier to internal rotation by the method described by Fateley and Miller (21).

Methylstannane may be considered as a molecule in which a rigid symmetric top (i.e., the methyl group) is attached to a rigid framework (i.e., the stanyl group), and in which there are three identical potential minima. Since the top has a threefold symmetry axis, the potential energy hindering rotation  $V(\alpha)$  is expressed in a Fourier series as

$$V(\alpha) = V_3(1 - \cos 3\alpha) / 2 + V_6(1 - \cos 6\alpha) / 2 + \dots \quad (1)$$

where  $V_3$  is the height of the threefold potential barrier,  $V_6$  is that of the sixfold one, and  $\alpha$  is the angle of internal rotation, i.e., the angle between the two parts of the molecule. Fateley and Miller (21) have taken  $V_6$  to be much smaller than  $V_3$ . Thus, all terms after the first were neglected. The height of the potential barrier has been determined from the microwave spectrum of methylstannane to be 650 cal/mole ( $227 \text{ cm}^{-1}$ ) (9).

TABLE V

Teller-Redlich Product-Rule Ratios

<u>Species Type</u>	<u>CD<sub>3</sub>SnH<sub>3</sub>/CH<sub>3</sub>SnH<sub>3</sub></u>		<u>CH<sub>3</sub>SnD<sub>3</sub>/CH<sub>3</sub>SnH<sub>3</sub></u>	
	<u>(obs.)</u>	<u>(calc.)</u>	<u>(obs.)</u>	<u>(calc.)</u>
A <sub>1</sub>	0.5152	0.5055	0.4923	0.5055
E	0.4136	0.3980	0.3622	0.3740

Using equation 1, the potential energy for hindered rotation was calculated and plotted in Figure 5. The graph shows the assumed threefold potential barrier and the torsional energy levels each of which are split into two sublevels, one of which is non-degenerate (symmetry species A), and the other doubly degenerate (species E). It can be seen that the A-sublevel is alternately lower and higher than the corresponding E-sublevel and the splitting becomes greater as the levels approach the top of the barrier. The torsional energy,  $E_{v\sigma}$ , is given by:

$$E_{v\sigma} = 2.25Fb_{v\sigma} \quad (2)$$

where  $v$  is the principal torsional quantum number,  $\sigma$  is an index designating either the A- or E- levels,  $b_{v\sigma}$  is an eigenvalue of the solution obtained when the potential function is put in the Schrodinger equation for the torsional motion, and  $F$  is related to the reduced moments of inertia for internal rotation.  $F$  is given by the equation:

$$F = (h/8\pi^2c) (1/I_a + 1/I_b) \quad (3)$$

In this equation  $I_a$  and  $I_b$  are the moments of inertia of the internal top (i.e.,  $\text{CH}_3$ ) and of the rigid framework (i.e.,  $\text{SnH}_3$ ), respectively about their symmetry axes. Energies of the first four torsional levels are given in Table VI. The difference between two of the energy levels gives  $\nu_1$  the infrared frequency of the transition between the two levels.

Thus

$$\nu = \Delta E_{v\sigma} = 2.25F(\Delta b_{v\sigma}) \quad (4)$$

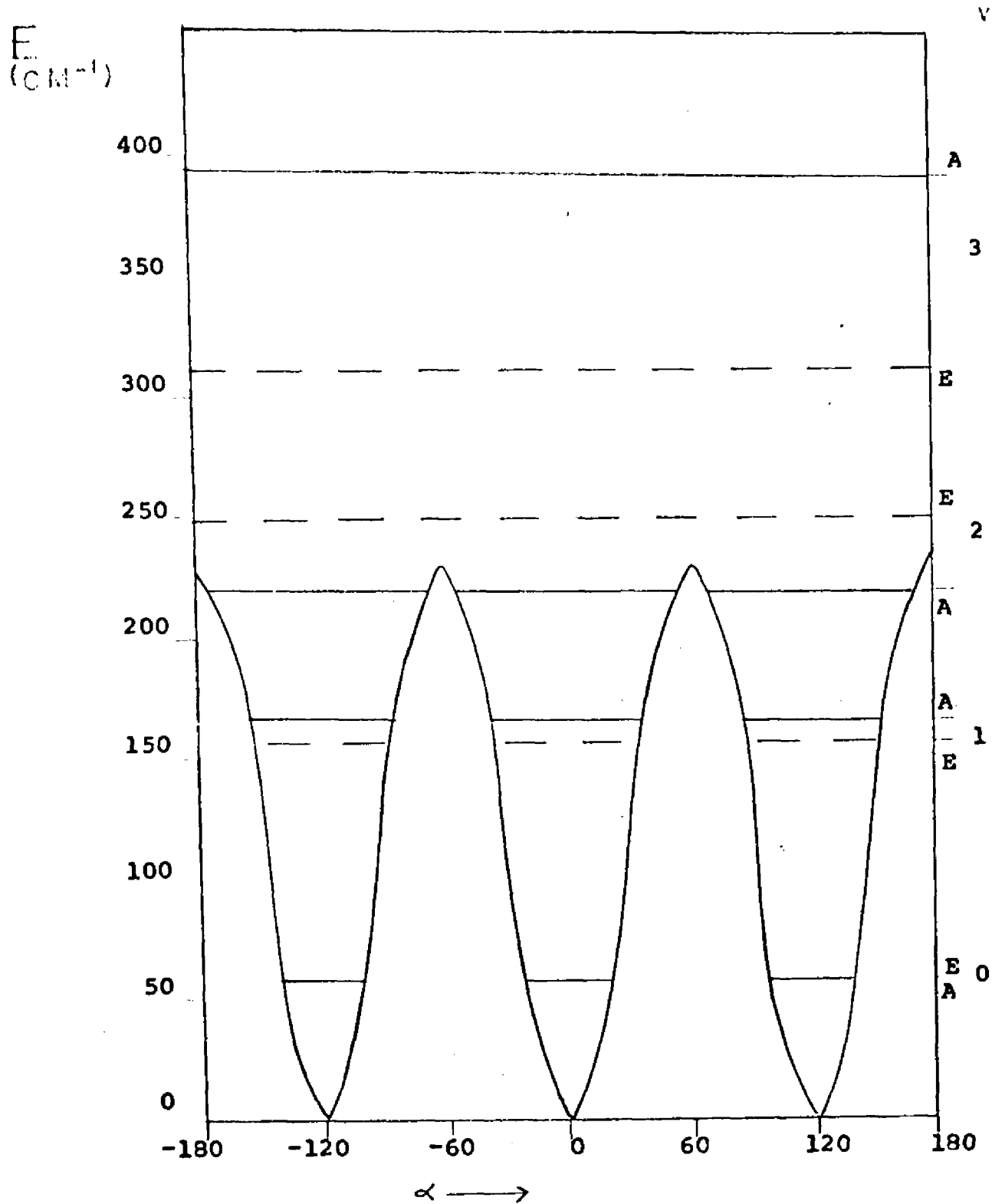


Figure 5. Potential Energy Curve for Hindered Rotation Drawn to Scale for Methylstannane.

where  $\Delta E_{\nu_0}$  is in  $\text{cm}^{-1}$ . The barrier height,  $V_3$ , is related to  $F$  by the equation

$$V_3 = 2.25Fs \quad (5)$$

where  $s$  is a dimensionless parameter.

The torsional frequency can be calculated using equations 4 and 5 and the value of the barrier height which has been determined by microwave measurements (9).  $F$  is determined from the moments of inertia using equation 3. Using the values of  $F$  and  $V_3$ ,  $s$  can be calculated by equation 5. Tables of  $b_{\nu_0}$  versus  $s$  are available (31) hence  $\Delta b_{\nu_0}$  can be evaluated. Thus, using equation 4 and the barrier height of 650 cal./mole ( $227 \text{ cm}^{-1}$ ), a value of  $109 \text{ cm}^{-1}$  is obtained for the torsional frequency of  $\text{CH}_3\text{SnH}_3$ . Assuming the same barrier to internal rotation for  $\text{CH}_3\text{SnD}_3$  and  $\text{CD}_3\text{SnH}_3$ , the torsional frequencies for the two isotopic species are 101 and  $88 \text{ cm}^{-1}$ , respectively.

Several combination bands of  $\text{CH}_3\text{SnH}_3$  involving the torsional mode and listed in Table I can now be assigned. The following combinations,  $(\nu_4 + 2\nu_6)$  at  $910 \text{ cm}^{-1}$ ;  $(\nu_5 - 2\nu_6)$  at  $320 \text{ cm}^{-1}$ ; and  $(\nu_{12} - \nu_6)$  at  $298 \text{ cm}^{-1}$  yield frequencies of 108, 104, and  $118 \text{ cm}^{-1}$ , respectively, for the torsional vibration. These results are in good agreement with the frequency calculated from the rotational barrier.

TABLE VI

Torsional Energy Levels for Methylstannanes

<u>v</u>	<u>Sublevel</u>	<u>Energy (Cm<sup>-1</sup>)</u>
0	A	57.0
	E	57.6
1	E	157.5
	A	166.3
2	A	220.9
(Barrier)		227.0
	E	249.6
3	E	313.2
	A	391.6

## B. Calculation of Thermodynamic Properties

The complete vibrational assignment makes possible the calculation of the thermodynamic properties of the methylstannanes. In making the thermodynamic calculations of the heat content, free energy, entropy, and heat capacity, four different contributions to the partition functions are considered: translation, vibration, rotation, and internal rotation. Standard methods of statistical mechanics were used for the calculations (37). The determination of the vibrational contributions to the thermodynamic functions were carried out with the aid of a 1620 computer. The program is listed in Appendix III. The calculated properties, based on a rigid-rotor harmonic-oscillator approximation, and assuming an ideal gas at 1 atmosphere pressure in the temperature range from 273.16° to 1000°K, are listed in Appendix I.

## CHAPTER IV

### VIBRATION-ROTATION ANALYSIS

High resolution studies yielding P-R branch separations of parallel bands, excited state rotational constants and Coriolis constants have been made for ethane (27), methylsilane (54, 63), and methylgermane (26). The vibration-rotation analysis of methylstannane further extends the data on  $\text{CH}_3\text{XH}_3$  type molecules.

For the purposes of the vibration-rotation analysis methylstannane is classified as a symmetric top molecule, that is, a molecule having two identical moments of inertia, the third moment being different but not equal to zero. The axis of this third moment of inertia is the symmetry axis. Two types of vibration-rotation bands are observed in the infrared spectra of symmetric top molecules, namely, parallel bands which are due to transitions in which the change of dipole moment is in the direction of the symmetry axis, and perpendicular bands where the change of dipole moment is perpendicular to the symmetry axis. Equations have been derived from the application of quantum mechanics to the problem of vibration-rotation energies of symmetric top molecules by Dennison (13), Nielsen (49, 50), and Allen and Cross (3). The total energy of vibration and rotation,  $E$ , of a symmetric top molecule, which is assumed to be a rigid rotor and whose vibrations are strictly harmonic, may be expressed as the sum of two factors;

$$E = G(v_1, v_2, v_3, \dots) + F(J, K) \quad (6)$$

where the vibrational energy is

$$G(v_1, v_2, v_3, \dots) = \sum_i \omega_i (v_i + d_i/2); \quad (7)$$

F (J,K) gives the rotational energy levels associated with each vibrational state; and  $v_1, v_2, \dots, v_i$  are the vibrational quantum numbers of the fundamental modes. J is a quantum number associated with the total momentum of the molecule and K is the quantum number associated with the component of the angular momentum about the symmetry axis. J can take on values of 0, 1, 2, 3, ... and K can take on (2J + 1) values of 0,  $\pm 1, \pm 2, \pm 3, \dots, \pm J$  for each value of J.

All allowed infrared transitions between two nondegenerate vibrational states (parallel type,  $A_1$ , fundamentals) have for the rotational selection rules:

$$\Delta K = 0, \quad \Delta J = \pm 1, \text{ if } K = 0 \quad (8)$$

$$\Delta K = 0, \quad \Delta J = 0, \pm 1, \text{ if } K \neq 0$$

For the perpendicular type (E) bands the rotational selection rules are

$$\Delta J = 0, \pm 1, \quad \Delta K = \pm 1 \quad (9)$$

Corresponding to every value of K and  $\Delta K$ , there are sub-bands consisting of three branches where for

$\Delta J = -1$ , a P-branch arises (low frequency side),

$\Delta J = 0$ , a Q-branch arises

$\Delta J = +1$ , an R-branch arises (high frequency side)

The rotational energy levels are given by the expression

$$F(J,K) = BJ (J + 1) + (A-B)K^2 \quad (10)$$

where the rotational constants A and B are expressed in wavenumbers and are defined by the relations

$$\begin{aligned} A &= h/8\pi^2 c I_A \\ \text{and} \\ B &= h/8\pi^2 c I_B \end{aligned} \tag{11}$$

A, refers to the symmetry axis and B, refers to the axes perpendicular to the symmetry axis. In equation 10 (A-B) is greater than zero for a prolate top ( $I_A < I_B = I_C$ ) and the level having  $K = 0$  is the level of lowest energy in a given J. Since K enters into the energy expressions as a square, each level, except for  $K = 0$ , is doubly degenerate. The influence of the vibration-rotation interaction is reflected in the dependence of A and B upon the vibrational quantum number, v.

The structure of the methylstannane molecule has been reported by Lide (38). The molecular parameters are listed in Table VII. The atomic weights given in Table VII are based on the carbon-12 scale (10). Using these parameters the ground state rotational constants were calculated for the three isotopic species and are listed in Table VIII.

The results of the high resolution study are best discussed by considering the analyses of parallel bands and perpendicular bands separately.

TABLE VII

Structural Constants of Methylstannane

Sn-C distance	$2.143 \pm 0.002A$	$m_{Sn} = 118.69$
C -H distance	$1.083 \pm 0.005A$	$m_C = 12.011$
Sn-H distance	$1.700 \pm 0.015A$	$m_H = 1.0080$
Angle H-C-H	$108^{\circ}25'$	$m_D = 2.0147$
Angle H-Sn-H	$109^{\circ}28'$	

TABLE VIII

Ground State Rotational Constants of the Methylstannanes

	A	B
$CH_3SnH_3$	$1.539 \pm 0.027$	$0.2286 \pm 0.0055$
$CH_3SnD_3$	$0.898 \pm 0.016$	$0.2095 \pm 0.0050$
$CD_3SnH_3$	$1.197 \pm 0.021$	$0.1849 \pm 0.0044$

### A. Parallel Bands

The contours of the infrared bands of symmetric top molecules should depend mainly on the moments of inertia and the type of band involved (23). For the case of methylstannane, the parallel bands show a definite P, Q, R structure such as is shown in Figure 8 for the CH<sub>3</sub> symmetric deformation vibration.

The distance between the fine structure lines in the P or R branches of a parallel band is calculated from equation 10. Let the ground state quantities be labelled with double primes and the excited states with a single prime. Since  $K' = K''$  and  $J' = J'' + 1$ , then the position of the rotational lines are given by the expression

$$\nu = F(J', K') - F(J'', K'') = 2BJ' \quad (12)$$

The distance between the fine structure lines in the P or R branches should be approximately 2B. From Table VIII it is seen that for methylstannane 2B is equal to 0.46 cm<sup>-1</sup> which is less than the resolution of the instrument. Therefore the rotational fine structure of the parallel bands could not be resolved. On the other hand, useful information may be obtained from the contours of the bands.

Gerhard and Dennison (23) have derived approximate formulas (equations 13, 14, and 15) which relate the separations,  $\Delta\nu$ , of P and R branch maxima in parallel bands to the moments of inertia, I, of the molecules

$$\Delta\nu = \frac{S(\beta)}{\pi c} \left( \frac{kT}{I_B} \right)^{1/2} \quad (13)$$

where  $k$  is the Boltzmann constant, and

$$\beta = \left( \frac{I_B}{I_A} - 1 \right) \quad (14)$$

$S(\beta)$  is defined by

$$\log_{10} S(\beta) = 0.721 / (\beta + 4)^{1.13} \quad (15)$$

In this study, applying equation 13, P-R separations of the parallel bands were obtained for each of the isotopic species of methylstannane. The results are shown in Table IX. The observed separation was taken as the average of several parallel bands of the molecules. Consideration was restricted by the treatment to those fundamentals whose band envelopes were symmetrical and which were not obviously overlapped (25). A band was considered symmetrical if the Q branch was not displaced from the band center by more than 10% of the observed separation. The symbol  $\Delta$  is defined as the difference between the observed separation and the calculated separation. It is seen that the observed and calculated separations are in agreement.

TABLE IX  
P-R Separations

Molecule	P-R Separations Calculated	(cm <sup>-1</sup> ) Observed	$\Delta$ (cm <sup>-1</sup> )
CH <sub>3</sub> SnH <sub>3</sub>	22.2	20.0 $\pm$ 1.0	-2.2
CH <sub>3</sub> SnD <sub>3</sub>	22.3	20.1 $\pm$ 1.0	-2.2
CD <sub>3</sub> SnH <sub>3</sub>	20.0	22.4 $\pm$ 1.0	+2.4

## B. Perpendicular Bands

In the case of the perpendicular bands, the P and R branches form a more or less unresolved background between the Q branches. Thus the rotational fine structure consists of a series of evenly spaced Q branches. In most cases these Q branches do not have their structure resolved.

The series of Q branches in a perpendicular band are subdivided into P, Q and R subbands depending on whether  $\Delta K = 1, 0,$  or  $-1$ . Symbolically the subbands of the Q branches are indicated by left superscripts, P, Q, or R, and with a subscript which designates the lower state K level; e.g.,  ${}^R Q_0$  : K = +1, lower state K level is zero.

While the approximations expressed in equation 10 are adequate for calculating the nondegenerate rotational energy levels, the influence of the Coriolis interactions must be considered in order to satisfactorily interpret the spectra of the degenerate vibrational levels.

When a symmetric top molecule rotates, the atoms move in elliptical paths about their equilibrium positions during the vibration. This excitation of a vibration, caused by the Coriolis forces acting on each of the atoms, can excite another vibration but with the frequency of the first vibration. If the frequencies of the two vibrations are different, then the excitation of one vibration by the other will be weak. However, if the frequencies of the two vibrations are nearly the same, or exactly the same, as in the case of doubly degenerate vibrations, the excitation of one of these vibrations by the Coriolis forces would strongly excite the other vibration.. Thus, there is

an angular momentum of vibration associated with each degenerate mode which interacts with the angular momentum of rotation. As a result of this interaction the expression for the energy levels should include a constant known as the Coriolis coupling coefficient or zeta constant,  $\zeta$ .

The zeta constant can have any value from -1 to +1 for the first vibrational state. A negative value of zeta means that the velocity of rotation of the vibrating dipole moment is greater than it would be if no angular momentum of vibration were present. A positive value indicates that the velocity of rotation is less than it would be if no angular momentum of vibration were present. A zero value for the zeta constant corresponds to a zero vibrational angular momentum.

Due to the Coriolis coupling, the expression for the rotational energy levels of a symmetric rotor in a degenerate vibrational state becomes

$$F(J, K) = BJ(J + 1) + (A - B)K^2 \mp 2A\zeta K \quad (16)$$

For the Q branch,  $\Delta J = 0$ . Thus, the expression for the frequencies of the Q branches in a perpendicular band, obtained from equation 16, is

$$\begin{aligned} \nu &= F(J', K') - F(J'', K'') \\ \nu &= \nu_0 + [A'(1 - 2\zeta) - B'] \pm 2[A'(1 - \zeta) - B']K + [(A' - B') - (A'' - B'')]K^2 \end{aligned} \quad (17)$$

Equation 17 gives the frequencies of the zero positions of the various sub-bands and represents a series of Q branches separated in wave numbers by  $2[A'(1 - \zeta) - B']$ .

As a result of this energy correction the band origin,  $R_{Q_0}$ , is displaced from the band center by  $[A'(1-2\zeta)-B']$ .

The final result of any high resolution infrared analysis of perpendicular bands can be verified with the aid of two sum rules. It has been shown that, assuming harmonic oscillations, the sum of the zeta constants of the vibrations in a given degenerate symmetry species is independent of the potential energy function (7, 43). This relation depends only on the principal moments of inertia. Thus for a  $C_{3v}$  molecule the sum rule is  $\sum_i \zeta_i =$  (number of atoms on the symmetry axis)  $- 2 + (B/2A)$  (18)

Hence, for  $CH_3XH_3$  type molecules, equation 18 reduces to

$$\sum_i \zeta_i = \frac{B}{2A} \quad (19)$$

Combining equation 19 with equation 17 gives a second sum rule which relates the sum of the Q branch spacings in the perpendicular bands to the rotational constants. This relationship is independent of the potential function of the molecule. If it is assumed in equation 17 that A and B are the same for all the excited states, then the expression

$$\sum_i \Delta \nu_i = 12A - 13B \quad (20)$$

is obtained.

In the case of the methylstannanes the form of a perpendicular band is that of a broad spread of Q branches with no clear-cut maximum. Hence the location of the band origin,  $R_{Q_0}$ , is not immediately obvious. There is nothing unique in the spacing between  $R_{Q_0}$  and  $P_{Q_1}$  since the spacing

between Q branches is approximately constant and there is no unambiguous way to assign a band origin. Fortunately, in most cases the derived values of the rotational constants are not sensitive to the rotational assignment.

The following criteria can be used to fix  $R_{Q_0}$ :

- a) There should be an even distribution of the Q branches on either side of the band center and the lines with even K values should be the stronger components (12).
- b) Generally, but not necessarily,  $R_{Q_0}$  should be the most intense Q branch in the band.
- c) The intensity of the branches in a band for a  $C_{3v}$  molecule should show a strong, weak, weak, strong, .... alternation (63).

On the other hand, the assignment of any  $R_{Q_K}$  line depends on the choice of  $R_{Q_0}$ . However, any choice of values may be substantiated by the calculation of the theoretical spectrum.

When the line assignments are completed, the vibration-rotation bands are analyzed by the Method of Combinations and Differences (3). If a transition between two  $P_Q$  levels and the transitions between two  $R_Q$  levels with the same value of K in the excited state are considered, the energy difference between these two transitions is independent of the excited states and represents the energy differences between the two ground state levels appearing in the two transitions. The expression for this difference  $\Delta_2^{F''}$ , is deduced from equation 17 and is seen to be

$$\Delta_2^{F''} = R_Q(K-1) - P_Q(K+1) = 4 (A'' - B'' - A'\zeta)K \quad (21)$$

A similar expression can be set up for the excited state. If this difference is  $\Delta_2 F'$ , then

$$\Delta_2 F' = R_{Q_K} - P_{Q_K} = 4(A' - B' - A'\zeta)K \quad (22)$$

By this method it is possible to separate the rotational constants for the upper and lower states. The band center can then be located using the sum relation

$$R_{Q_K} + P_{Q_K} = 2 \left[ \nu_0 + (A' - B' - 2A'\zeta) \right] + 2 \left[ (A' - B') - (A'' - B'') \right] K^2 \quad (23)$$

Equations 21-23 can be solved either graphically or by the method of least squares.

The results of the combinations and differences analysis can be used in the calculation of a theoretical spectrum which can be compared with the experimental data. In the calculations using equation 23,  $B' - B''$  was assumed to be negligible. The bands of the C-H asymmetric stretching vibration, the Sn-H asymmetric vibration, the  $\text{CH}_3$  asymmetric deformation vibration, and the  $\text{SnH}_3$  rocking vibration of  $\text{CH}_3\text{SnH}_3$  are shown in Figures 6, 7, 8, and 9, respectively. All four bands were studied using the combinations and differences expressions (Equations 21-23). The results are given in Table X. The rotational constants obtained from this analysis are shown in Table XI. The probable errors were calculated by the method of the propagation of errors (65). The values of the differences relationships shown in Table X have probable errors of up to 25%. The probable errors of the Coriolis constants are quite large. Thus no significance can be attached to their magnitudes. However, the sign of the Coriolis constant is meaningful.

TABLE X

Results of Combinations and Differences Analysis of  $\text{CH}_3\text{SnH}_3$  ( $\text{Cm}^{-1}$ )

	CH Asym. Str.	SnH Asym.Str.	$\text{CH}_3$ Asym.Deform.	$\text{SnH}_3$ Rock
$A''-A'_\zeta-B''$	$1.25 \pm 0.06$	$1.40 \pm 0.03$	$1.50 \pm 0.07$	$0.892 \pm 0.021$
$A'-A'_\zeta-B'$	$1.25 \pm 0.08$	$1.39 \pm 0.03$	$1.50 \pm 0.12$	$0.910 \pm 0.025$
$\nu_{\text{O}}+A'(1-2\zeta)-B'$	$3006.6 \pm 0.2$	$1876.0 \pm 0.3$	$1418.7 \pm 0.1$	$416.8 \pm 0.1$
$(A'-B') - (A''-B'')$	$-0.0357 \pm 0.0045$	$-0.0071 \pm 0.0018$	$-0.0074 \pm 0.0015$	$+0.00203 \pm 0.00038$

TABLE XI

Rotational Constants for Methylstannane

	CH Asym. Str.	SnH Asym. Str.	CH <sub>3</sub> Asym. Deform.	SnH <sub>3</sub> Rock
$\nu_0$ (cm <sup>-1</sup> )	3005.4 ± 0.2	1874.5 ± 0.3	1417.0 ± 0.2	416.3 ± 0.1
A'' (cm <sup>-1</sup> )	1.539 ± 0.027	1.539 ± 0.027	1.539 ± 0.027	1.539 ± 0.027
B'' (cm <sup>-1</sup> )	0.2302	0.2302	0.2302	0.2302
A' (cm <sup>-1</sup> )	1.503 ± 0.027	1.532 ± 0.030	1.532 ± 0.027	1.541 ± 0.027
B' (cm <sup>-1</sup> )	0.2302	0.2302	0.2302	0.2302
$\zeta$	+0.0153 ± 0.056	-0.0574 ± 0.030	-0.129 ± 0.081	+0.260 ± 0.021

In the case of near-degeneracy between two degenerate vibrations, there is a Coriolis interaction between the two fundamental modes in addition to the interaction between the degenerate vibrations of each fundamental given by equation 16. The interactions between two near-degenerate modes have been discussed in detail by Nielsen (49, 50) and de Heer (12) who have shown that the energy,  $G(J, K)$ , for the interacting vibrational-rotational levels of the two states, S and T, can be obtained from the following expression:

$$G(J, K) = \frac{1}{2} \left( \left[ F_S(J, K) + F_T(J, K) \right] \pm \left[ F_S(J, K) - F_T(J, K) \right]^2 + 4 \zeta_{S,T}^2 K^2 A^2 \left[ \left( \frac{\nu_S}{\nu_T} \right)^{1/2} + \left( \frac{\nu_T}{\nu_S} \right)^{1/2} \right]^2 \right)^{1/2} \quad (24)$$

where the plus sign refers to the R branch and the negative sign refers to the P branch. The terms  $F_S(J, K)$  and  $F_T(J, K)$  are the energy terms for the first excited levels of states S and T, respectively. These energy terms are given by equation 16.

Using equation 24, Lord and Venkateswarlu (44) have shown that the frequencies of the Q branches are given by

$$\nu = \frac{\nu_S + \nu_T}{2} + (A-B) - A(\zeta_S + \zeta_T) \pm 2 \left[ \left[ 1 - \left( \frac{\zeta_S + \zeta_T}{2} \right) \right] A - B \right] K \pm \frac{1}{2} \left[ \left[ \left( \nu_S - \nu_T \right) \mp 2A(K \pm 1)(\zeta_S - \zeta_T) \right]^2 + 4 \zeta_{S,T}^2 A^2 (K \pm 1)^2 \left[ \left( \frac{\nu_S}{\nu_T} \right)^{1/2} + \left( \frac{\nu_T}{\nu_S} \right)^{1/2} \right]^2 \right]^{1/2} \quad (25)$$

Here  $\zeta_S$  and  $\zeta_T$  are the Coriolis constants for  $\nu_S$  and  $\nu_T$  and  $\zeta_{S,T}$  is the constant for the interaction of the two vibrations.

The first  $\pm$  sign corresponds to the P branches (-) and R branches (+); the second  $\pm$  sign gives the bands for  $\nu_s$  (+) and  $\nu_T$  (-); and the  $\pm$  and  $\mp$  signs within the square brackets enclosing the last term go with the P branches (+) and R branches (-). In this expression, it is assumed that  $A' = A''$ . As a result of this correction, the principal Q branches converge on the R side of the lower frequency band and on the P side of the higher frequency band.

Due to their symmetry and proximity, the  $\text{SnH}_3$  asymmetric deformation vibration,  $\nu_{10}$ , and the  $\text{CH}_3$  rocking vibration,  $\nu_{11}$ , of methylstannane interact with each other by this type of Coriolis interaction. Equation 25 must be used to obtain values of  $\nu_{10}$ ,  $\nu_{11}$ ,  $\zeta_{10}$  and  $\zeta_{11}$ .

In the rotational analysis of  $\nu_{10}$  and  $\nu_{11}$ , the main problem is to assign  $R_{Q_0}$  for each band. As a consequence of the perturbation, the values of A and  $\zeta$  are sensitive to the choice of  $R_{Q_0}$ . After the  $R_{Q_0}$  for the two bands has been located, the Q branches can be assigned K values and the bands can be analyzed by the method of combinations and differences. The following combination relations have been derived from equation 25 (44):

$$\begin{aligned}
 R_{Q_K}(\nu_{10}) + R_{Q_K}(\nu_{11}) + P_{Q_K}(\nu_{10}) + P_{Q_K}(\nu_{11}) \\
 = 4 \left[ (\nu_{10} + \nu_{11}) / 2 + (A-B) - A(\zeta_{10} + \zeta_{11}) \right] = 4 C
 \end{aligned}
 \tag{26}$$

$$R_{Q_K}(\nu_{10}) + R_{Q_K}(\nu_{11}) = 2 C + 4 \left[ A \left( 1 - \frac{\zeta_{10} + \zeta_{11}}{2} \right) - B \right] K
 \tag{27}$$

$${}^P Q_K(\nu_{10}) + {}^P Q_K(\nu_{11}) = 2C - 4 \left[ A \left( 1 - \frac{\zeta_{10} + \zeta_{11}}{2} \right) - B \right] K \quad (28)$$

and

$$\left[ \frac{{}^P Q_K(\nu_{10}) - {}^P Q_K(\nu_{11})}{2} \right]^2 = \left[ \frac{\nu_{10} - \nu_{11}}{2} \right]^2 + A(\zeta_{10} - \zeta_{11})(\nu_{10} - \nu_{11})K' + \left[ A^2(\zeta_{10} - \zeta_{11})^2 + A^2 \zeta_{10,11}^2 \left[ \left( \frac{\nu_{10}}{\nu_{11}} \right)^{1/2} + \left( \frac{\nu_{11}}{\nu_{10}} \right)^{1/2} \right]^2 \right] K'^2 \quad (29)$$

where  $K' = (K + 1)$  for differences between  ${}^R Q_K$  lines and  $K' = -(K - 1)$  for differences  ${}^P Q_K$  lines.

The spectrum of the  $\nu_{10}$  and  $\nu_{11}$  bands is shown in Figure 10. The results of the combinations and differences analysis and the rotational constants for the  $\text{SnH}_3$  asymmetric deformation and  $\text{CH}_3$  rocking vibrations are given in Table XII.

The sum rules for the Q branch spacings and for the zeta constants, equations 19 and 20, can now be used to check the results of this analysis. Using the values of A and B given in Table VIII,  $\sum_i \Delta \nu_i = 12A - 13B = 15.48 \text{ cm}^{-1}$ . The sum of the observed Q branches spacings is given by

$$\sum_i \Delta \nu_i = 2 \left( \left[ A(1 - \zeta_7) - B \right] + \left[ A(1 - \zeta_8) - B \right] + \left[ A(1 - \zeta_9) - B \right] + 2 \left[ A \left( 1 - \frac{\zeta_{10} + \zeta_{11}}{2} \right) - B \right] + 2 \left[ A(1 - \zeta_{12}) - B \right] \right) = 15.30 \text{ cm}^{-1}.$$

In a similar fashion

$$\sum_i \zeta_i = \frac{B}{2A} = 0.075$$

$$\sum_i \zeta_i (\text{obs}) = 0.103$$

In both cases the agreement is within experimental error.

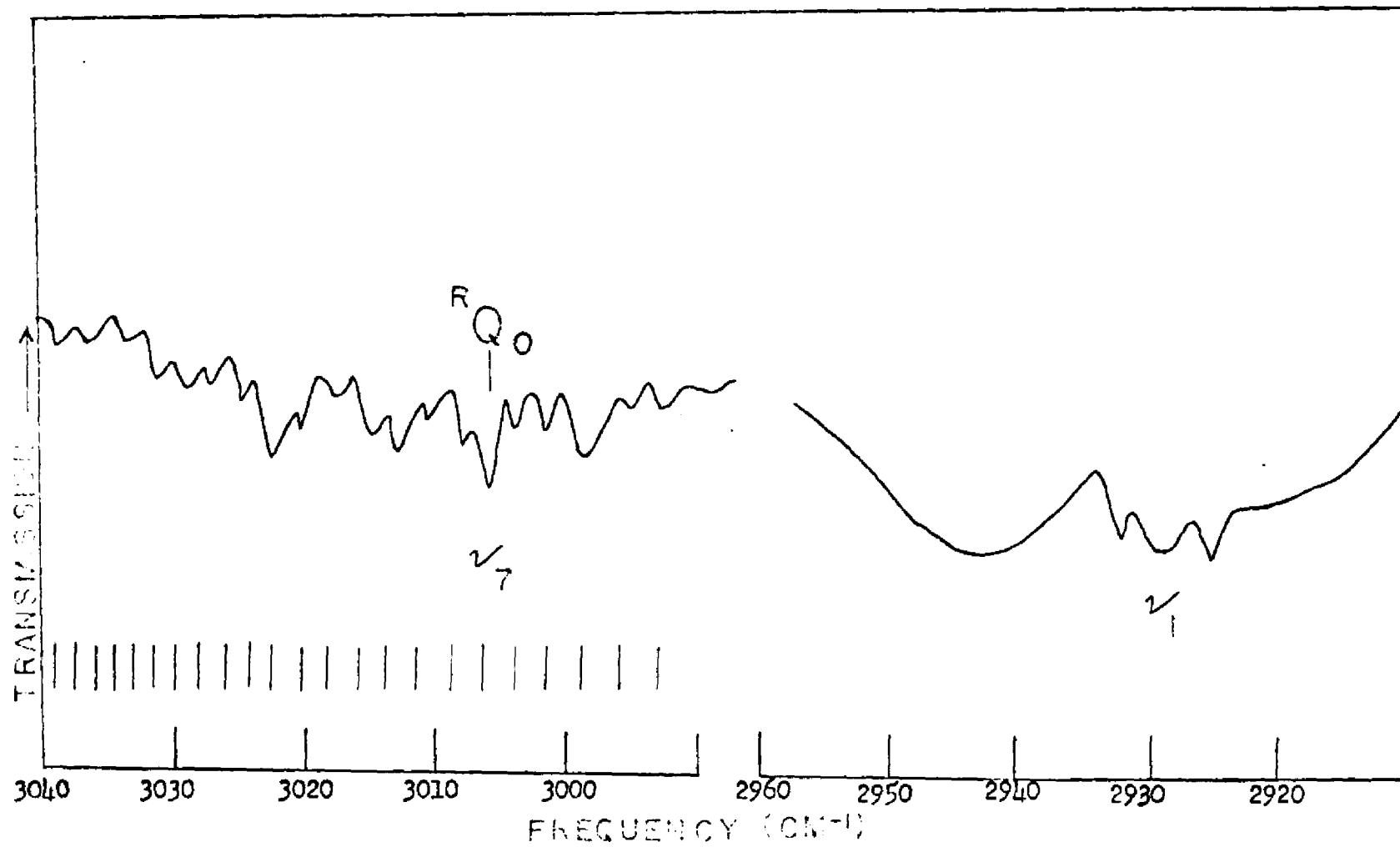


Figure 6. The CH Asymmetric Stretch ( $\nu_7$ ) and Symmetric Stretch ( $\nu_1$ ) Bands of  $\text{CH}_3\text{SnH}_3$ .

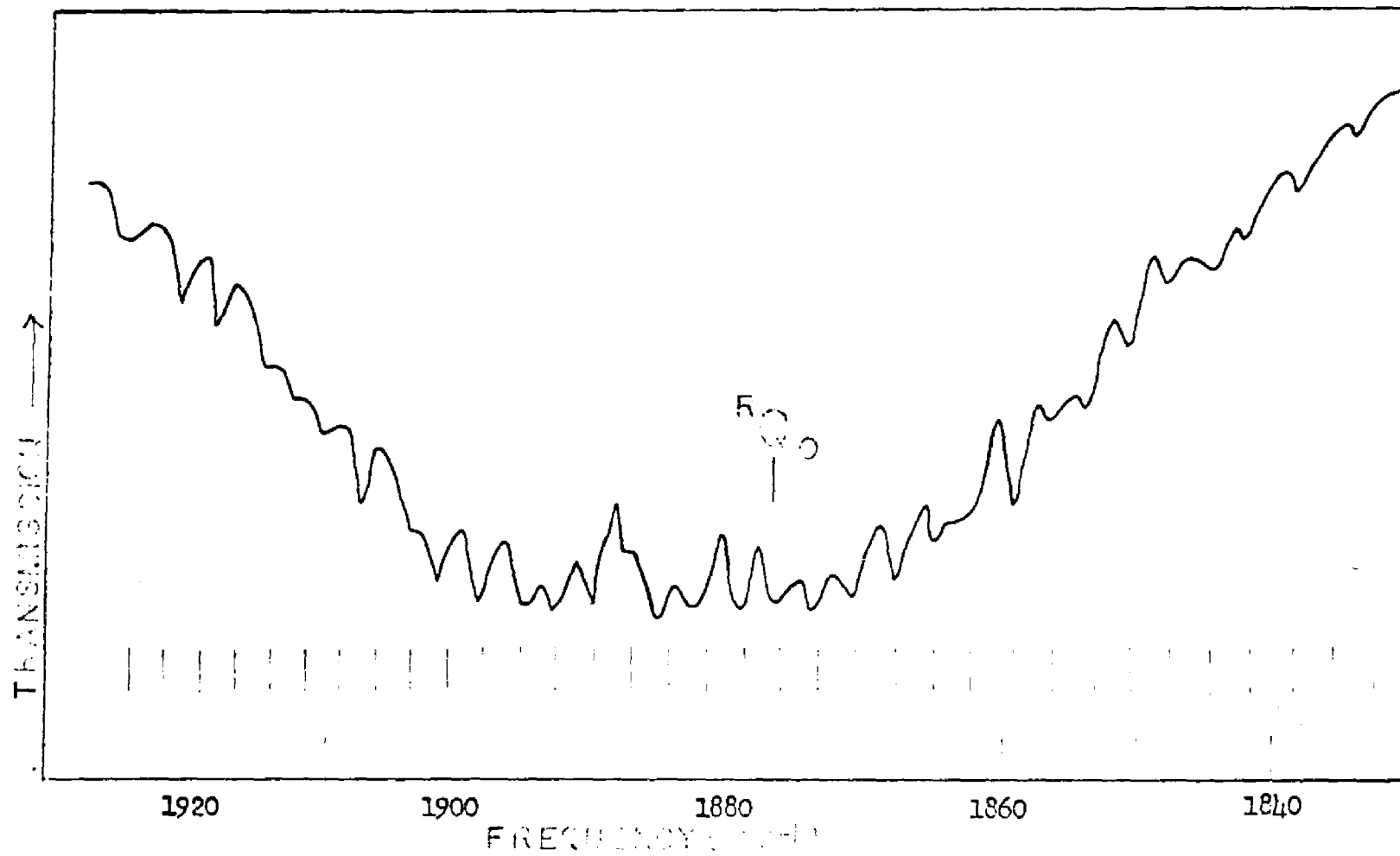


Figure 7. The SnH Asymmetric Stretch Band of  $\text{CH}_3\text{SnH}_3$

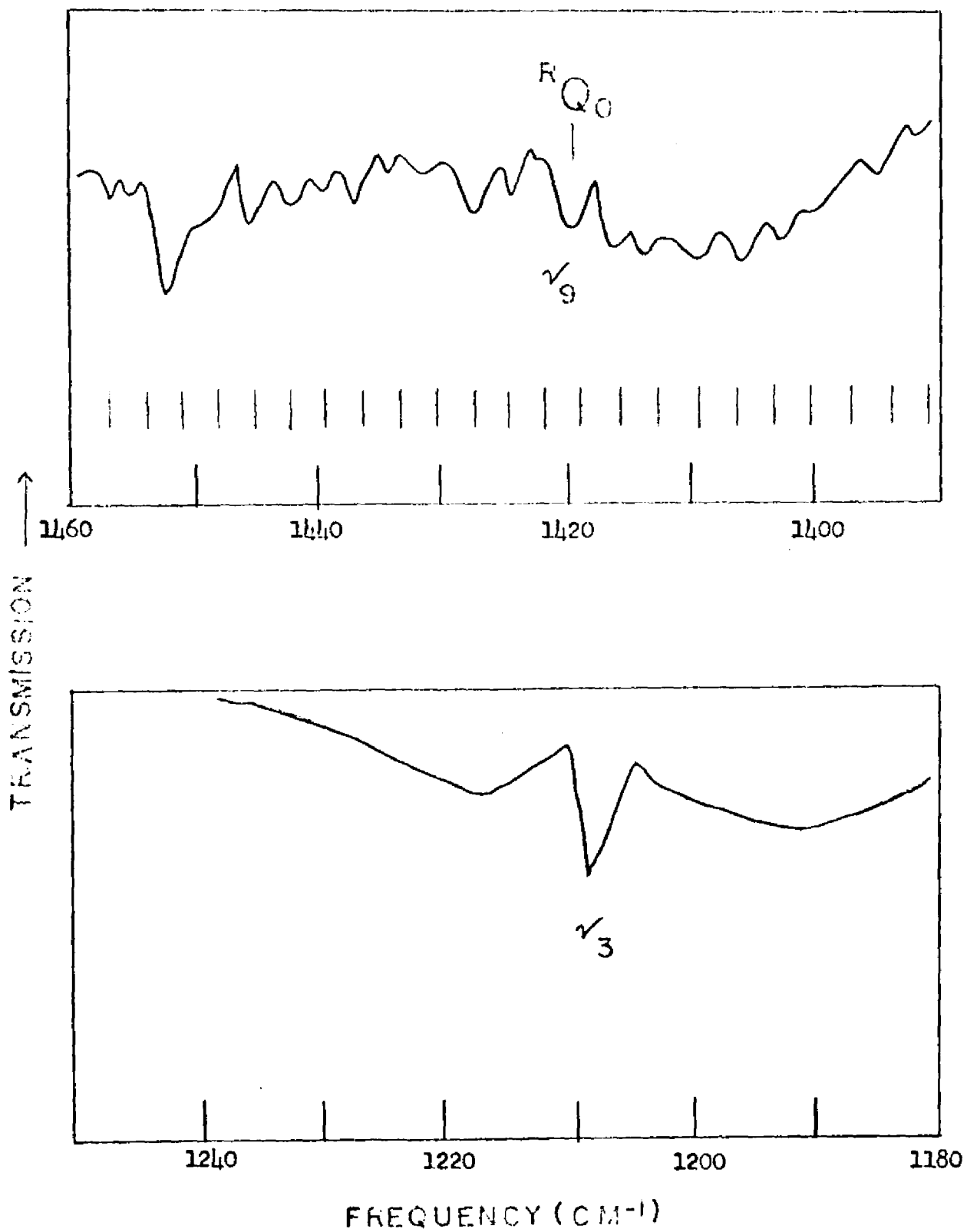


Figure 8. The CH<sub>3</sub> Asymmetric Deformation ( $\nu_9$ ) and Symmetric Deformation ( $\nu_3$ ) Bands of CH<sub>3</sub>SnH<sub>3</sub>.

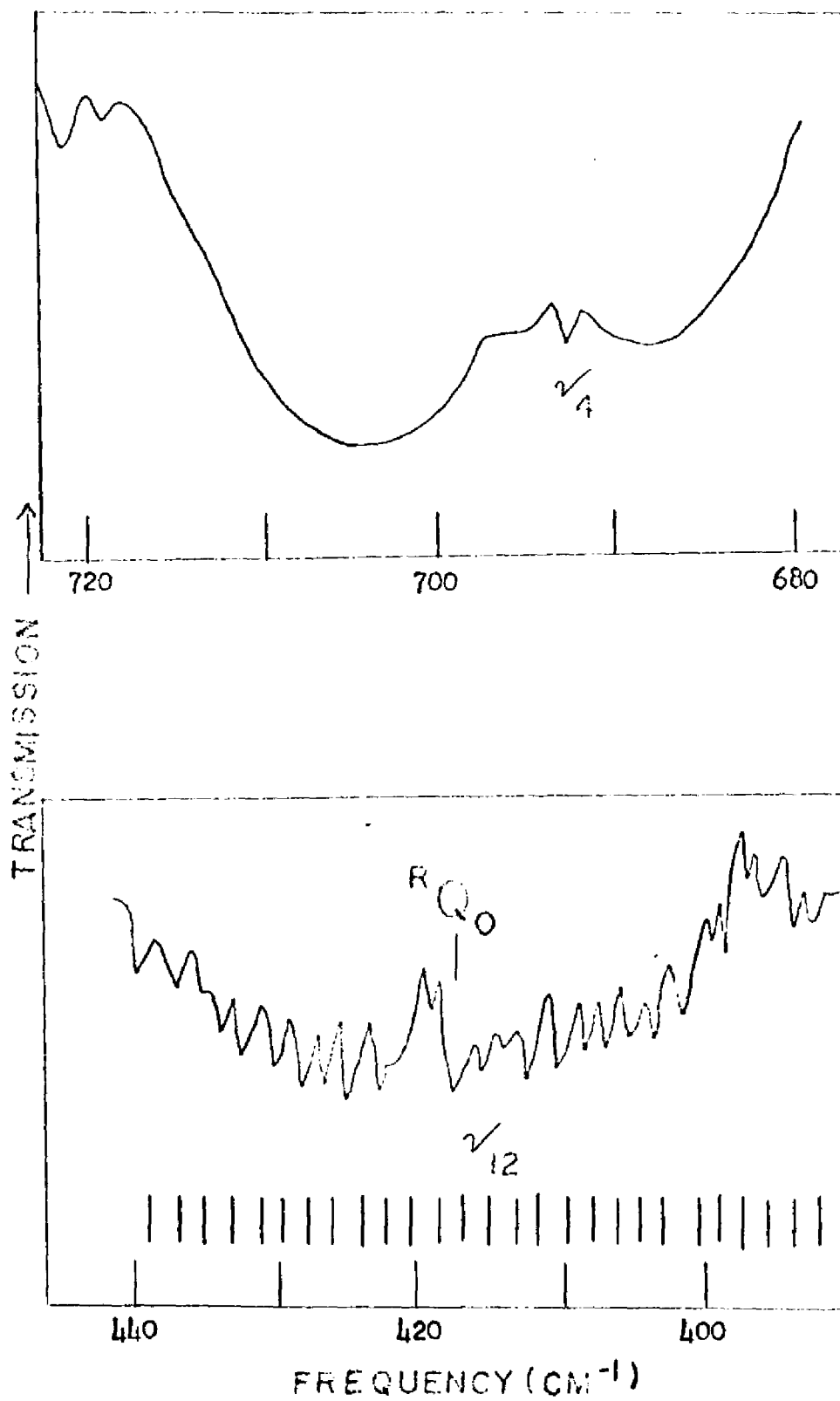


Figure 9. The  $\text{SnH}_3$  Symmetric Deformation ( $\nu_4$ ) and Rocking ( $\nu_{12}$ ) Bands of  $\text{CH}_3\text{SnH}_3$ .

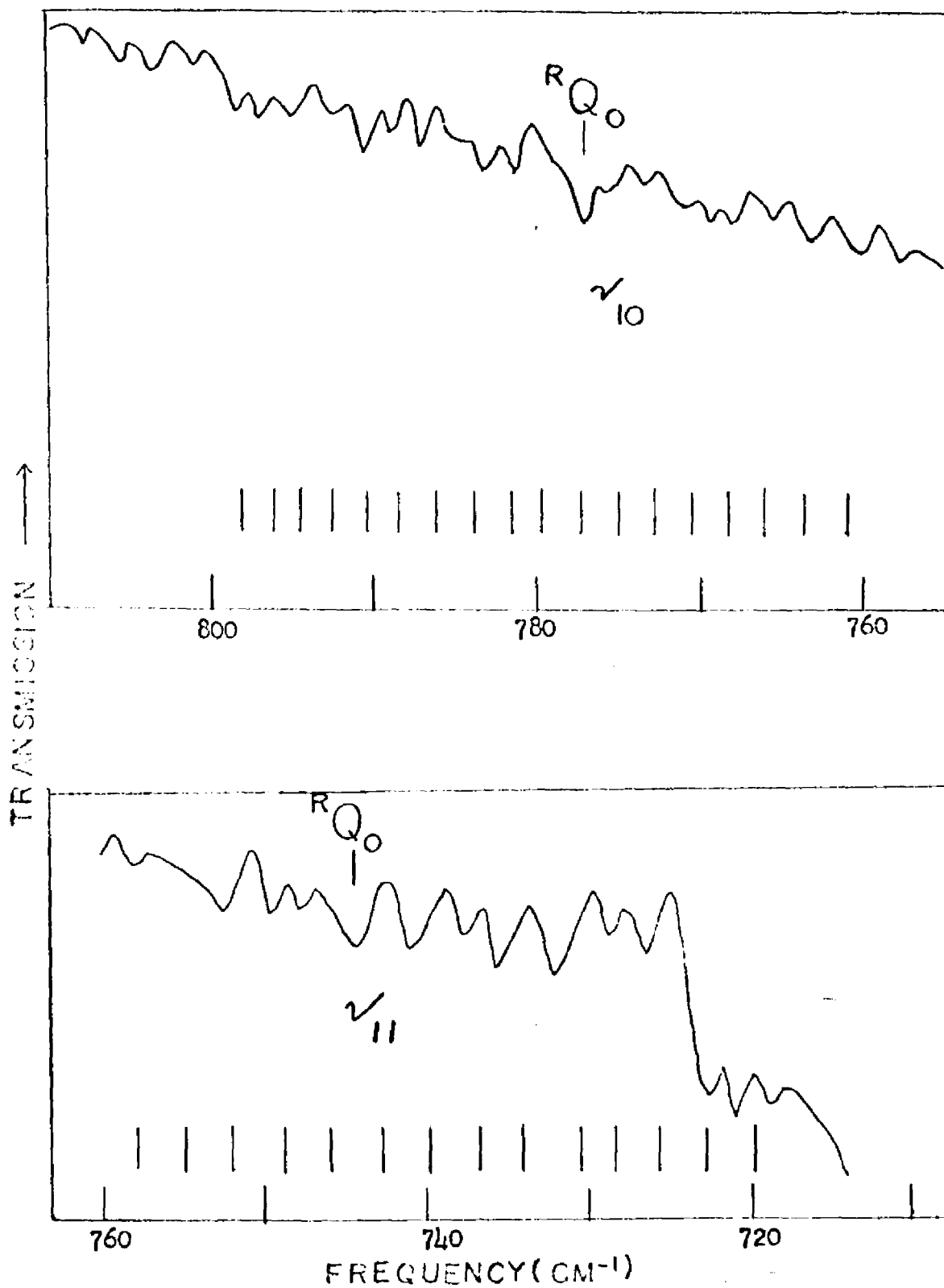


Figure 10. The CH<sub>3</sub> Rocking (ν<sub>10</sub>) and SnH<sub>3</sub> Asymmetric Deformation (ν<sub>11</sub>) Bands of CH<sub>3</sub>SnH<sub>3</sub>.

TABLE XII

Results of Combinations and Differences Analysis

For the CH<sub>3</sub> Rock and SnH<sub>3</sub>

Asymmetric Deformation Vibrations of Methylstannane

$A [1 - (\zeta_{10} + \zeta_{11})/2] - B$	$1.30 \pm 0.10$
$[(\nu_{10} + \nu_{11})/2] + (A-B) - A(\zeta_{10} + \zeta_{11})$	$759.0 \pm 0.2$
$[(\nu_{10} - \nu_{11})/2]^2$	$269.2 \pm 3.5$
$A(\zeta_{10} - \zeta_{11})(\nu_{10} - \nu_{11})$	$10.59 \pm 0.46$
$A^2 (\zeta_{10,11})^2 \left[ \left( \frac{\nu_{10}}{\nu_{11}} \right)^{1/2} \left( \frac{\nu_{11}}{\nu_{10}} \right)^{1/2} \right]^2 +$	
$A^2 (\zeta_{10} - \zeta_{11})^2$	$-0.23 \pm 0.36$
$\zeta_{10}$	$+0.112 \pm 0.077$
$\zeta_{11}$	$-0.098 \pm 0.084$
$\nu_{10}$	$774.1 \pm 0.4$
$\nu_{11}$	$741.3 \pm 0.4$

The spectra of the SnH asymmetric stretching vibration, the SnH<sub>3</sub> asymmetric deformation vibration, and the CD<sub>3</sub> rocking vibration of CD<sub>3</sub>SnH<sub>3</sub> are shown in Figures 11 - 13. The bands were analyzed by the method of combinations and differences using expressions 21 - 23. The results are shown in Table XIII. The rotational constants obtained from this analysis are given in Table XIV.

The results for all the bands studies under high resolution were used to calculate the frequencies of the lines of the Q branches. The observed and the calculated frequencies are listed in Appendix II. The calculated vibration-rotation lines of methylstannane are shown in Figures 6 - 10.

TABLE XIII

Results of Combinations and DifferencesAnalysis of  $\text{CD}_3\text{SnH}_3$ 

	SnH asym str	SnH <sub>3</sub> asym deform	CD <sub>3</sub> rock
$A'' - A'\zeta - B''$	1.09±0.04	1.21±0.07	0.721±0.032
$A' - A'\zeta - B'$	1.06±0.03	1.20±0.05	0.713±0.031
$\nu_{\text{O}} + A'(1-2\zeta) - B'$	1890.1±0.3	739.5±0.2	628.8±0.1
$(A' - B') - (A'' - B'')$	+0.00666±0.00175	+0.0227±0.0090	-0.0116±0.0020

TABLE XIV

Rotational Constants from the  
Perpendicular Bands of CD<sub>3</sub>SnH<sub>3</sub>

	SnH asym str	SnH <sub>3</sub> asym deform	CD <sub>3</sub> rock
$\nu_0$	1889.0 $\pm$ 0.3	738.1 $\pm$ 0.2	628.4 $\pm$ 0.1
A''	1.197 $\pm$ 0.027	1.197 $\pm$ 0.027	1.197 $\pm$ 0.027
B''	0.1849	0.1849	0.1849
A'	1.204 $\pm$ 0.027	1.220 $\pm$ 0.029	1.185 $\pm$ 0.027
B'	0.1849	0.1849	0.1849
$\zeta$	-0.0299 $\pm$ 0.0107	-0.131 $\pm$ 0.049	+0.242 $\pm$ 0.031

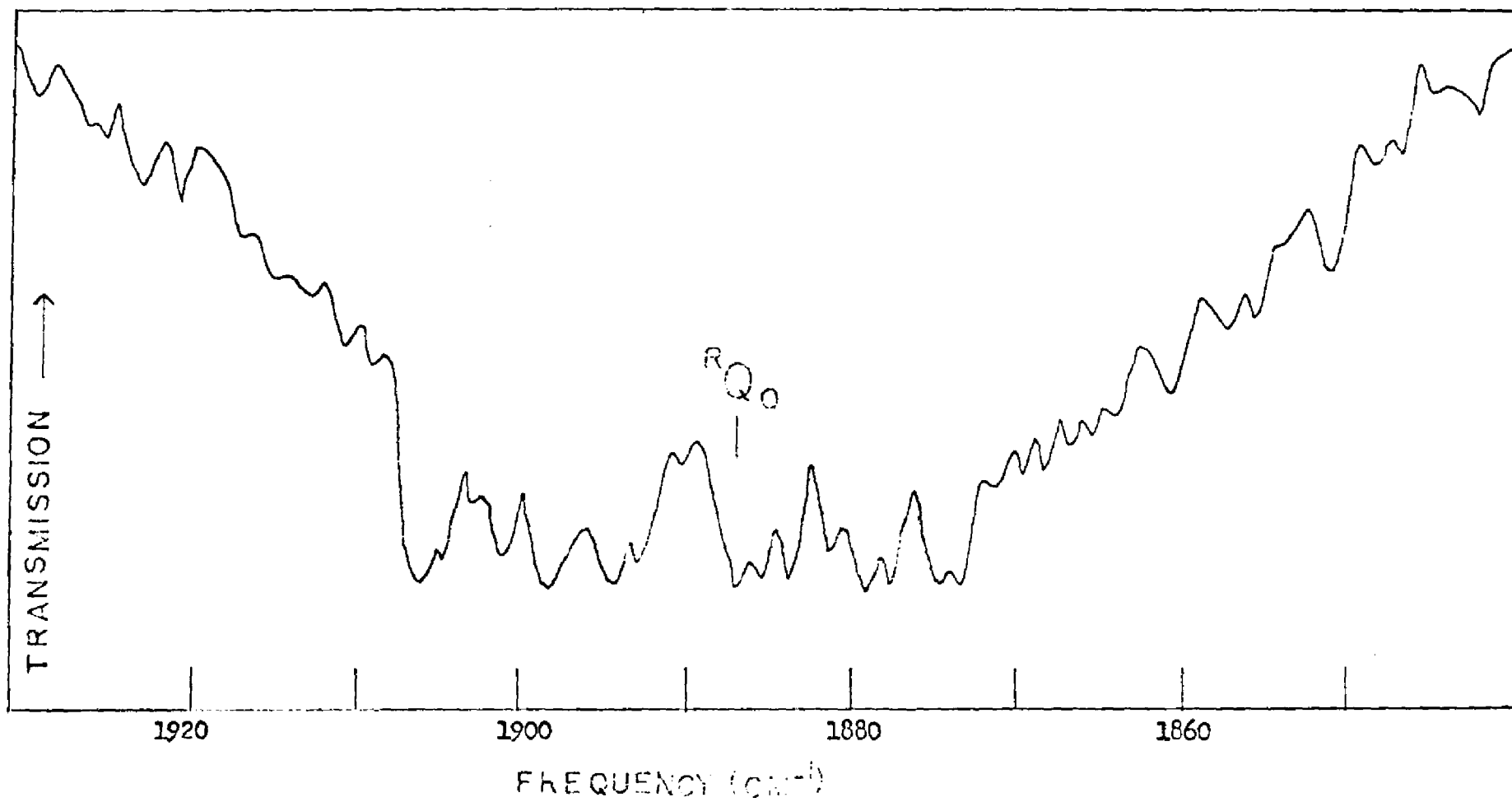


Figure 11. The SnH Asymmetric Stretch Band of  $CD_3SnH_3$

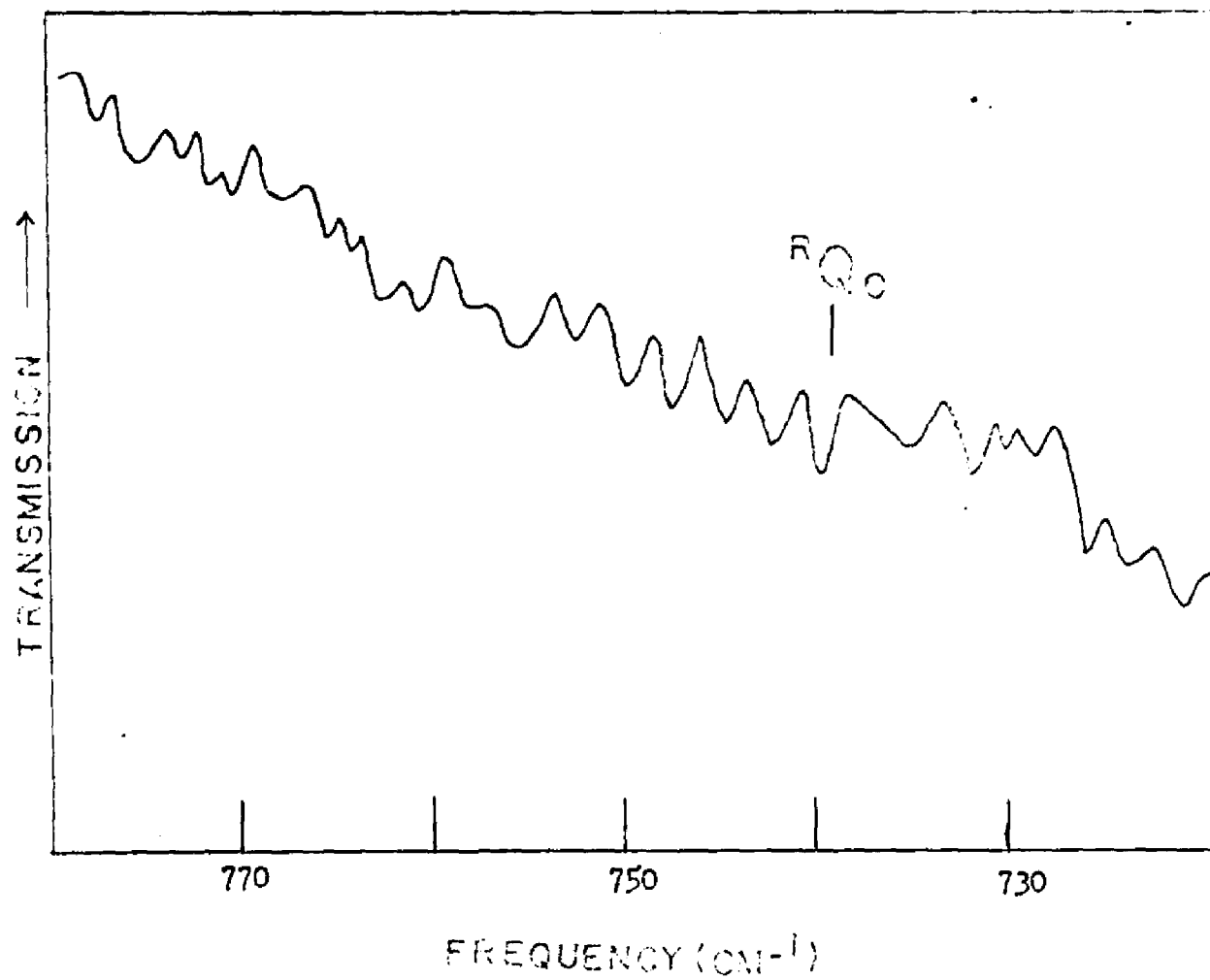


Figure 12. The SnH<sub>3</sub> Asymmetric Deformation Band of CD<sub>3</sub>SnH<sub>3</sub>

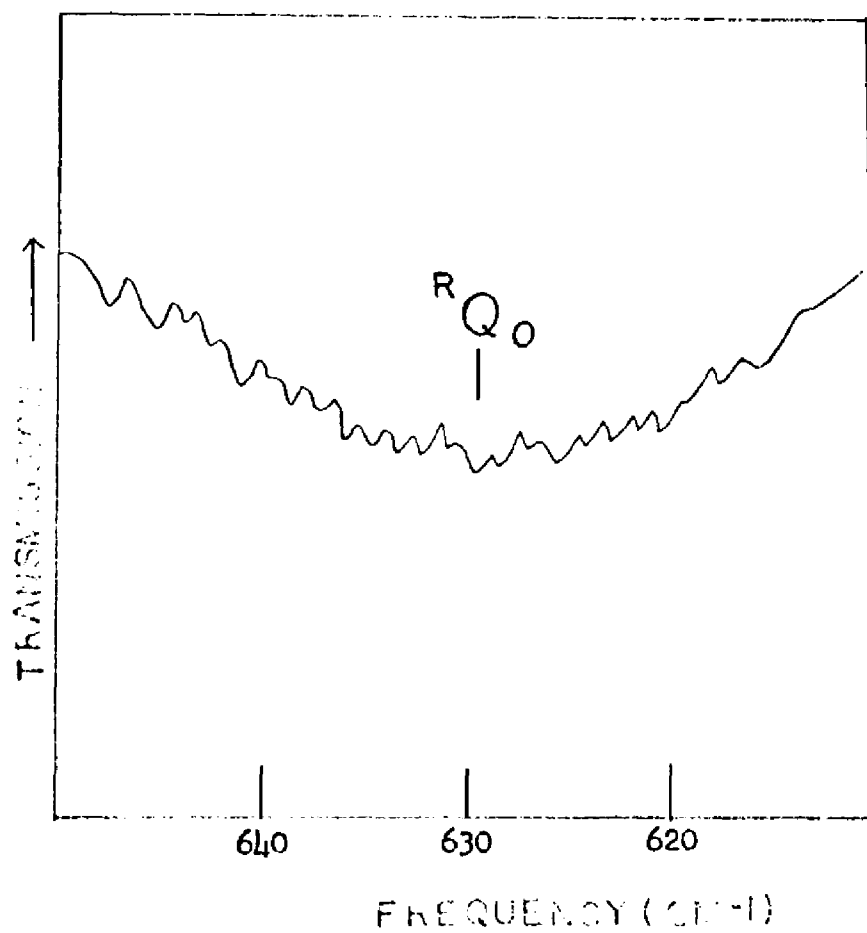


Figure 13. The CD<sub>3</sub> Rocking Band of CD<sub>3</sub>SnH<sub>3</sub>.

CHAPTER V

NORMAL COORDINATE ANALYSIS

This chapter describes the calculation of force constants for  $\text{CH}_3\text{XH}_3$  type molecules, where  $X = \text{C}, \text{Si}, \text{Ge},$  and  $\text{Sn}$ , and the determination of coriolis constants and potential energy distributions for these molecules. The calculation of force constants from observed vibrational frequencies involves (1) obtaining accurate frequencies; (2) correcting the observed frequencies for anharmonicity effects; and (3) solving a set of rather complex secular equations. The first problem has been discussed in Chapters III and IV. Theoretical and semi-empirical approaches to solve the last two problems are described below.

A molecule can be described as a collection of point masses held together by forces that are determined by its electronic structure and nuclear configuration. For a set of independent internal coordinates,  $R_i$ , which measure the changes in the bond lengths and interbond angles from the equilibrium configuration of the molecule (so that  $R_i = 0$  in equilibrium), the potential energy of the molecule is given by the expression (32, 64)

$$\begin{aligned}
 V = V_0 & + \sum_i \left( \frac{\partial V}{\partial R} \right) R_i + \frac{1}{2} \sum_i \sum_j \left( \frac{\partial^2 V}{\partial R_i \partial R_j} \right) R_i R_j \\
 & + \frac{1}{6} \sum_i \sum_j \sum_k \left( \frac{\partial^3 V}{\partial R_i \partial R_j \partial R_k} \right) R_i R_j R_k + \dots \text{higher} \\
 & \text{order terms} \quad (30)
 \end{aligned}$$

The first term,  $V_0$ , defines the zero of the energy scale and is taken to be zero at the equilibrium position. The coefficients of  $R_i$  in the second term are all zero since the derivatives are all to be taken in the equilibrium configuration, in which, by definition,  $V$  is a minimum with respect to all the  $R_i$ . The coefficients in the third term are the harmonic force constants,  $F_{ij}$ , which is defined by the equation

$$F_{ij} = \left( \frac{\partial^2 V}{\partial R_i \partial R_j} \right) \quad (31)$$

The coefficients of the cubic and higher order terms in  $R$  are the anharmonic force constants.

For symmetric top molecules, symmetry coordinates may be used instead of internal coordinates to define the potential energy function. Symmetry coordinates are simple linear combinations of internal coordinates chosen to take advantage of the molecular symmetry. The symmetry coordinates,  $S_i$ , are related to the internal coordinates,  $R_i$ , by means of a transformation matrix,  $U$ , according to the equation,

$$S = UR$$

where

$$S_i = \sum_j U_{ij} R_j \quad (32)$$

The symmetry coordinates of any molecule can be classified into symmetry species. The normal modes of vibrations are similarly classified into symmetry species.

### A. Anharmonic Corrections

The harmonic frequencies, which correspond to atomic vibrations of infinitesimal amplitude, are functions of the harmonic potential constants, defined in equation 31. However, the anharmonic frequencies are observed experimentally. For the vibrations of  $C_{3v}$  molecules these may differ by from 1 to 5 percent from the harmonic frequencies. If the anharmonic frequencies are used to determine the quadratic potential constants, the latter will be in error by more than 5% (14). Therefore it is necessary to correct the observed frequencies for anharmonicity effects.

In principle, the anharmonicity corrections for the observed frequencies of very simple molecules such as  $CO_2$  or HCN can be determined from a study of overtones and combination bands (14). However, for  $CH_3X$  type molecules, this method is not practical because there are insufficient data available and the assignments and interpretations of overtones and combination bands are too complex to be reliable.

Three semiempirical methods have been described for estimating the anharmonicity corrections (4, 14, 27). Each of these methods have their limitations and none of them have, as yet, been applied to molecules such as methylstannane.

Dennison (14) has suggested a general procedure for estimating the anharmonicity corrections. The method is based on the Teller product rule and approximate relations between anharmonicity corrections of isotopic molecules.

If it is assumed that when an atom of a molecule is replaced by an isotopic atom of the same element the changes in the potential energy function and configuration of the molecule can be neglected, then the anharmonicity constants,  $x_i$ , can be defined by

$$\nu_i = (1-x_i)\omega_i \quad (33)$$

and

$$\nu_i' = (1-x_i')\omega_i' \quad (34)$$

where  $\nu_i$  and  $\omega_i$  are the observed and harmonic frequencies, respectively. The primed quantities refer to the isotopic species. The relationships

$$\frac{x_i}{x_i'} = \frac{\omega_i}{\omega_i'} \cong \frac{\nu_i}{\nu_i'} \quad (35)$$

have been shown to hold accurately for diatomic molecules and to be a good approximation for those polyatomic molecules, such as  $H_2O$  (14), where the anharmonicities can be determined independently.

If  $x_i/x_i' = \omega_i/\omega_i'$  is substituted into equation 34, then

$$\nu_i' = \omega_i' \left( 1 - \frac{\omega_i' x_i}{\omega_i} \right) \quad (36)$$

When  $x_i/x_i' = \nu_i/\nu_i'$  is substituted into equation 34, the ratio of equation 34 to equation 33 yields

$$\frac{\omega_i'}{\omega_i} = \frac{(1-x_i)}{\left( \frac{\nu_i}{\nu_i'} - x_i \right)} \quad (37)$$

The ratio of the product of the squares of the harmonic frequencies of the isotopic molecule to that of the unsubstituted molecule is assumed to be given by the product rule (14).

Dennison applied the procedure to methane and ammonia (14). Substitution of equation 37 into the Teller-Redlich product rule (64) gives one equation for the  $x_i$ 's. However for the triply degenerate symmetry species ( $F_2$ ) of methane and the two symmetry species of ammonia two equations are required. A second equation can be obtained for the  $F_2$  symmetry species of methane and the E symmetry species of ammonia from the analysis of vibration-rotation data (14). In the case of the  $A_1$  symmetry species of  $NH_3$  it was assumed that the differences between the harmonic and observed NH symmetric stretching frequencies was proportionately equal to the differences between the harmonic and observed NH asymmetric stretching frequencies. Thus it was possible to obtain  $x_i$  for all vibrations in methane and ammonia.

Dennison's method (14) allows an unambiguous calculation of the anharmonicity constants,  $x_i$ , when a sufficient number of relationships are available to determine the constants independently. Thus this method is limited to molecules such as methane and ammonia.

It was necessary, therefore, for Hansen and Dennison (27) to modify Dennison's method in the case of ethane. They assumed that similar vibrations in different molecules will display similar anharmonicities. This assumption made it possible to transfer some anharmonicity constants from

methane to corresponding vibrations of ethane. Other anharmonicity constants were estimated from equation 37 and the product rule. The values obtained from the methane-ethane correlation were adjusted whenever necessary to conform to the empirical rules that anharmonicity factors are generally positive and are larger for the higher frequency vibrations. This procedure was reported to give harmonic frequencies for ethane accurate to within a few wavenumbers (27).

According to Hansen and Dennison (27), "there has been no hesitation to make readjustments of the values from the ethane-methane correlation so as to conform to the empirical rules". These rules have been previously stated. This appears somewhat arbitrary since Hansen and Dennison do not describe just how these adjustments were made except for the fact that the calculated harmonic frequencies fit the product rule.

In the case of ethylene, Arnett and Crawford (4) have used an anharmonicity constant,  $x_e$ , which is defined for diatomic molecules by the equation

$$x_e = \frac{p-r}{2(p^2-r)} \quad (38)$$

where  $r = v'/v$  (38')

and  $p = \sqrt{\left(\frac{\mu}{\mu'}\right)}$  (38'')

where  $\mu$  is the reduced mass of the vibration. Arnett and Crawford (4) determined  $x_e$  for the CH stretching vibrations

but made no attempt to determine the effect of anharmonicity on the other vibrations of ethylene.

When the method of Hansen and Dennison (27) was applied to methylstannane  $x$  took on negative values for some vibrations and was unreasonably large for other vibrations for all attempts to fit the product rule. There are several factors which may account for the failure of the method of Hansen and Dennison in the case of  $\text{CH}_3\text{SnH}_3$ . First, most of the vibrational frequencies of  $\text{CH}_3\text{SnD}_3$  and some of the vibrational frequencies of  $\text{CD}_3\text{SnH}_3$  could not be studied under high resolution. Thus the location of the centers of these bands may be in error by 1-2%. This could affect the product rule ratios by as much as 5-10%. Second, equation 35 assumes that the anharmonicity constants of the different vibrations can be determined independently, and this approximation may not be valid for methylstannane. The effect of this on the calculation of anharmonicity constants is difficult to assess. Finally, in the case of the E symmetry species, bond lengths and bond angles are necessary for the calculation of the product rule ratios (Table V). Equilibrium bond lengths and bond angles are not known for methylstannane. Values for the bond angles were assumed and the bond lengths were determined by spectroscopic methods (38). These structural parameters are listed in Table VII. Those bond lengths calculated from spectroscopic measurements may differ from equilibrium bond lengths by more than  $0.01 \text{ \AA}^0$  (35). However since the structural parameters appear in both the numerator and denominator of the product rule ratio they probably have

negligible effects on the calculations. It will be shown at the end of this section that the errors in locating the band centers of the isotopic species is probably the main reason why Hansen and Dennison's method does not work for methylstannane.

When equation 37 is substituted into equation 38 for  $r = \nu'/\nu$ ,  $x$  is found to be related to  $x_e$  by the equation

$$x = \frac{(1-pq) + (2p^2q-2)x_e}{(p-pq) - (2p^2-2p^2q)x_e} \quad (39)$$

or

$$x = K/(L-Nx_e) + Mx_e/(L-Nx_e) \quad (39')$$

where  $K = (1-pq)$

$L = (p-pq)$

$M = (2p^2q-2)$

$N = (2p^2-2p^2q)$

and  $q = \omega/\omega'$

Within the limits of the uncertainty in the calculations of anharmonicity constants,  $Nx_e \ll L$  and thus  $Nx_e$  may be neglected. The equation

$$x = \frac{K}{L} + \frac{Mx_e}{L} \quad (40)$$

indicates that an approximate linear relationship should exist between  $x$  and  $x_e$ .

If it is assumed that the CH stretching vibration can be separated from the other vibrations of a symmetry species, then

$$p = \sqrt{(\mu/\mu')} \cong (\omega'/\omega) = \frac{1}{q}$$

When this approximation is made equation 39 becomes

$$x = \frac{2 x_e}{1-2px_e} \quad (41)$$

For small ranges of  $x_e$ , a plot of  $x$  vs.  $x_e$  should give a straight line for the CH stretching vibration.

In this study, it has been found empirically that  $x$ , calculated from equation 37, and  $x_e$ , calculated from equation 38 show similar trends for the CH asymmetric stretching and  $\text{CH}_3$  symmetric deformation vibrations of the methyl halides (2) and methane (20). Thus, it appears that  $x$  and  $x_e$  for each of these vibrations differ by some common factor. These trends are described below.

Applying equation 38 and assuming that the reduced mass,  $\mu$ , is approximately given by  $1/m_H$ , a linear relationship was obtained between  $x$  and  $x_e$  for the CH asymmetric stretching vibration of methane (20) and of the methyl halides (2). This is shown in Figure 14 and given by the equation

$$x = 1.24 x_e + 0.0008 \quad (42)$$

This equation is of the same form as equation 41. The difference in the slopes is due to the approximation made in determining the reduced mass of the vibration.

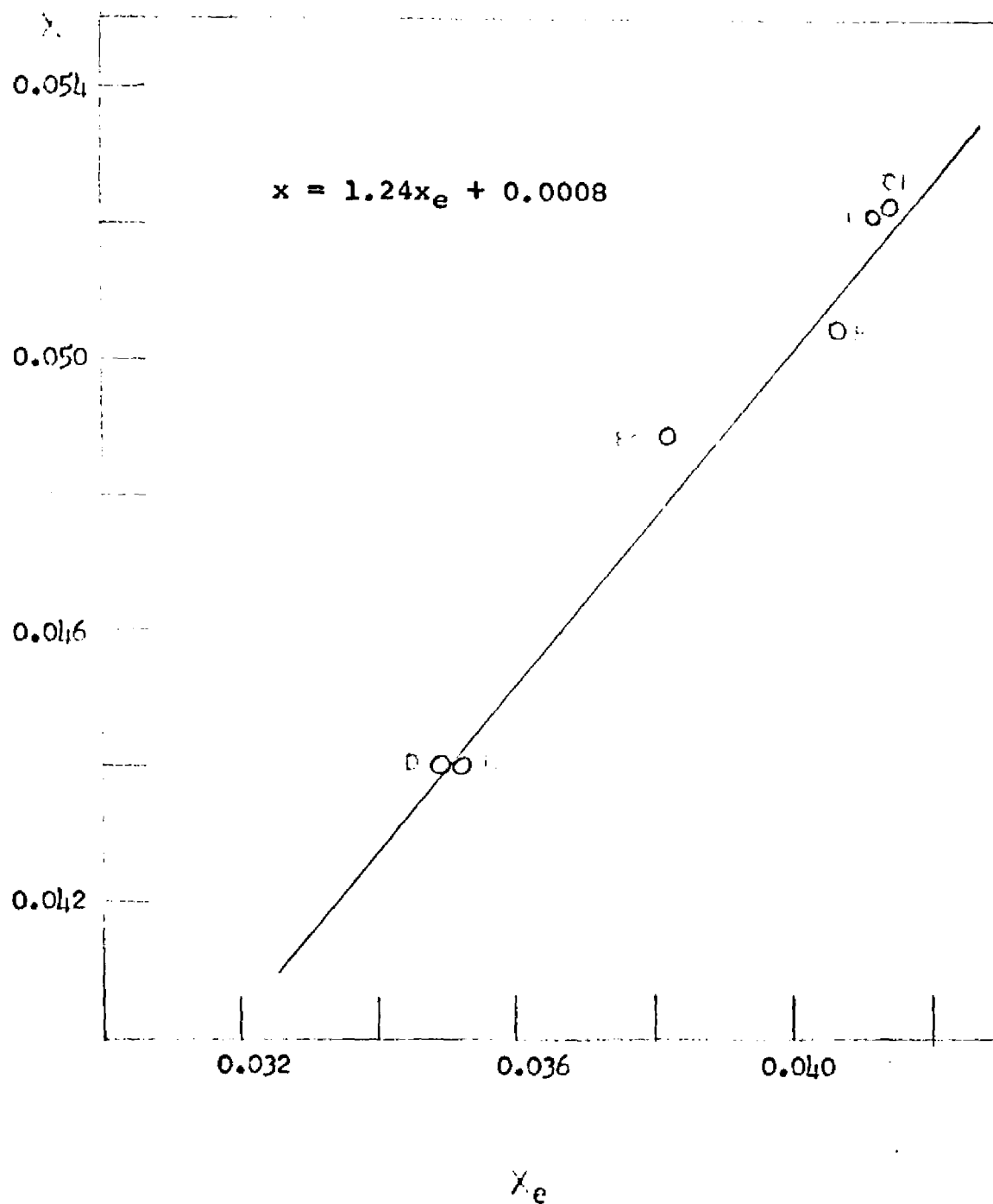


Figure 14.  $x_e$  vs.  $x$  for the CH Asymmetric Stretching Vibration of  $\text{CH}_3\text{X}$  Molecules ( $\text{X} = \text{H}, \text{D}, \text{F}, \text{Cl}, \text{Br}, \text{I}$ ).

The reduced mass,  $\mu$ , for the symmetric deformation vibration is approximately given by

$$\left[ m_H / (1 + (3m_H/m_X) \sin^2 \theta) \right]$$

where  $\theta$  is the angle between the CH bond and the axis at the molecule. Using equation 38 values of  $x_e$  were calculated for the  $\text{CH}_3$  symmetric deformation vibration of methane (20) and of the methyl halides (2). In Figure 15, these values of  $x_e$  are plotted against the values of  $x$  (2, 20) calculated by equation 37. A linear relationship

$$x = -0.471 x_e + 0.073 \quad (43)$$

is found. In the calculation of  $x_e$  from equation 38  $\mu$  is assumed to be approximately equal to  $m_H / (1 + 3 m_H/m_X)$ , where  $m_X$  is the mass of the CX group ( $X = \text{H}, \text{D}, \text{F}, \text{Cl}, \text{Br}, \text{I}$ ). Within the uncertainty of the calculated anharmonicity constants,  $\sin^2 \theta$  may be considered to be X constant for these molecules. Since  $x$  and  $x_e$  are related by an equation which is obtained by graphical methods and since the angle is assumed to be constant, the values of  $x$  obtained from equation 42 should be approximately independent of  $\sin^2 \theta$ . In equation 40, the parameters M and L represent small differences between approximate quantities, thus the forms of equations 40 and 43 are similar but the slopes may differ.

The quantity  $x_e$  for the CH asymmetric stretching and  $\text{CH}_3$  symmetric deformation vibrations in  $\text{CH}_3\text{SnH}_3$  was calculated from equation 38. Then equations 42 and 43 were applied to obtain values corresponding to the anharmonicity constants,  $x$ .

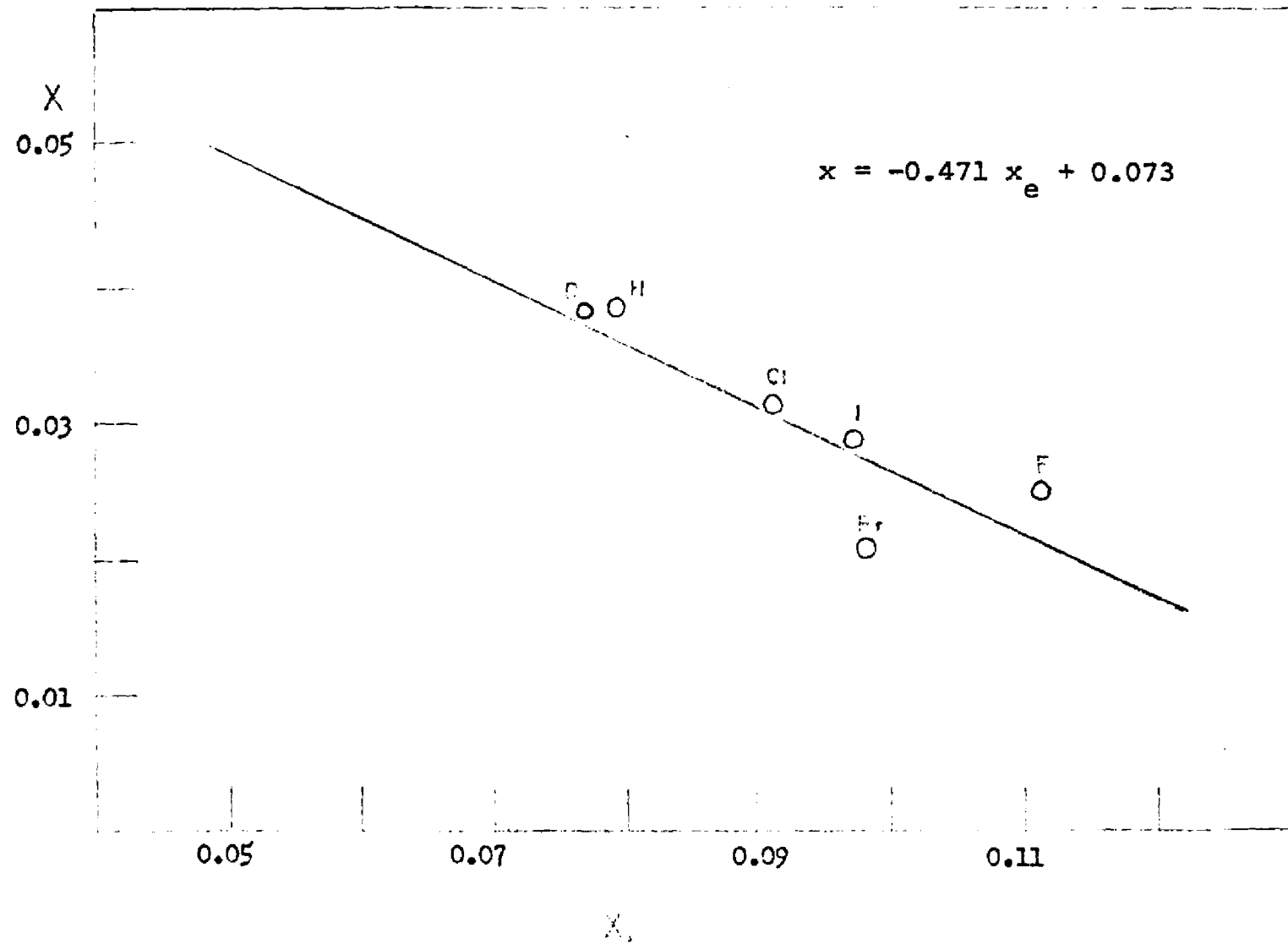


Figure 15.  $x_e$  vs.  $x$  For the  $\text{CH}_3$  Symmetric Deformation Vibration of  $\text{CH}_3\text{X}$  Molecules (X=H, D, F, Cl, Br, I)

In Figure 16, the anharmonicity constants for the  $\text{CH}_3$  rocking mode,  $x_R$ , of methane (20) and the methyl halides (2) are plotted against the corresponding  $\text{CH}_3$  symmetric deformation anharmonicity constants,  $x_{SD}$ . A linear relationship was obtained which is given by the expression,

$$x_R = 0.923 x_{SD} + 0.0030 \quad (44)$$

Applying this to the case of  $\text{CH}_3\text{SnH}_3$ ,  $x$  for the  $\text{CH}_3$  symmetric deformation vibration was calculated from equation 43, and  $x_R$  was then determined from equation 44.

The anharmonicity constants for the CH symmetric stretching mode of the methyl halides (2) are approximately the same. Thus the average value of  $x$  for this series was assumed for the corresponding vibration in  $\text{CH}_3\text{SnH}_3$ . The same approximation was made for the  $\text{CH}_3$  asymmetric deformation mode. In this case, however,  $x$  for  $\text{CH}_3\text{F}$  was ignored since it was significantly different from that of the other halides (2).

The anharmonicity constant for the  $\text{SnH}_3$  rocking vibration was calculated by means of equation 44. Although there is a difference in the bonding in the  $\text{CH}_3$  and  $\text{SnH}_3$  groups, the forms of the vibrations should be approximately the same for the two groups. Since the anharmonicity constant of a  $\text{XH}_3$  rocking vibration is being determined from the symmetric deformation vibration of the same  $\text{XH}_3$  group, equation 43 should hold approximately for either group in  $\text{CH}_3\text{SnH}_3$ . The constants for the remaining vibrations of the stannyl group were transferred from stannane (36). The  $\text{snC}$  stretching vibration was assumed to be harmonic.

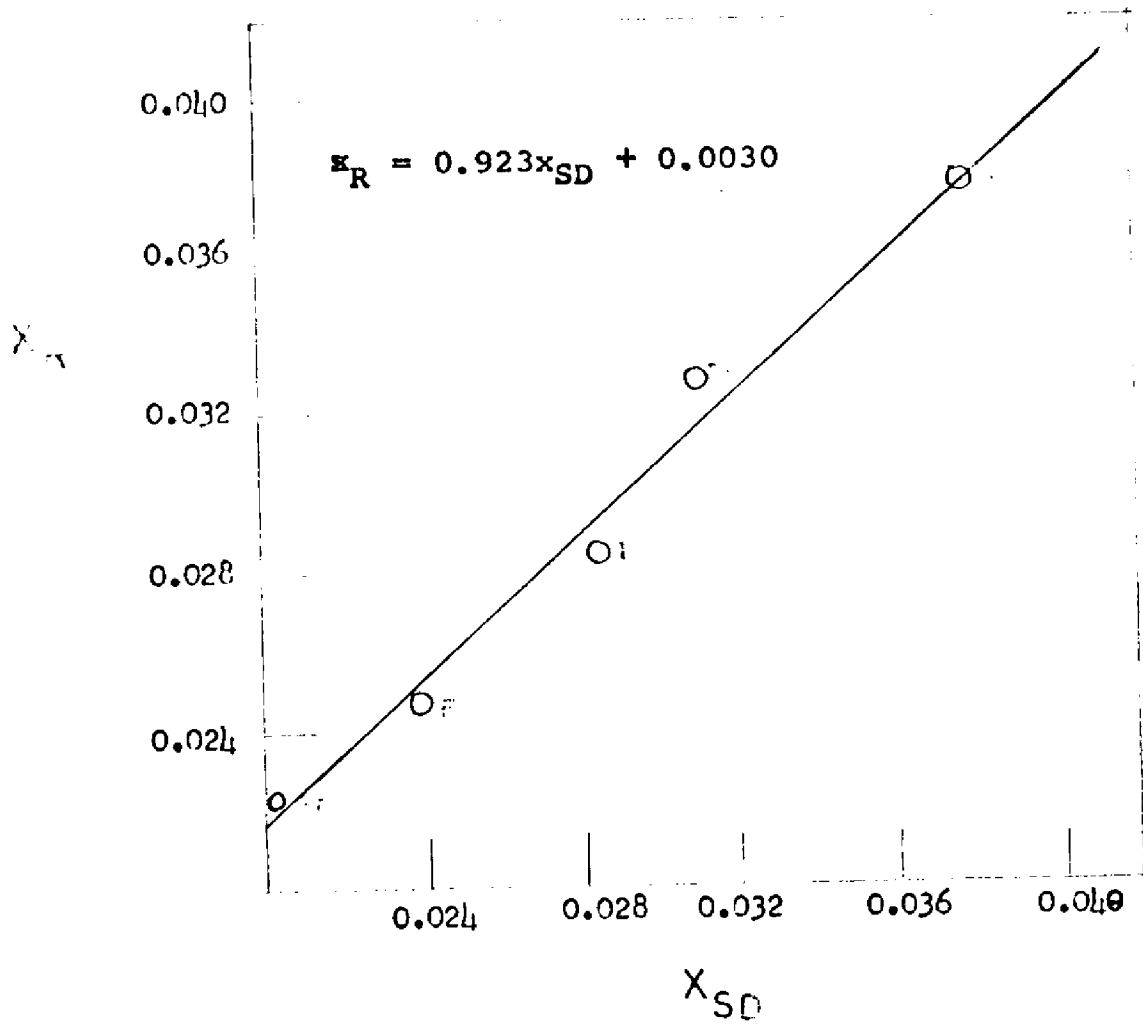


Figure 16.  $x_{SD}$  vs.  $x_R$  of  $CH_3X$  Molecules ( $X=H, F, Cl, Br, I$ ).

The anharmonic frequencies,  $\nu$ , the harmonic frequencies,  $\omega$ , and the anharmonicity constants,  $x$ , calculated in this study are listed in Table XV. The product rule ratios, calculated from the harmonic frequencies, are shown in Table XVI. It is seen that the product rule ratios are in agreement for  $\text{CD}_3\text{SnH}_3/\text{CH}_3\text{SnH}_3$  but do not agree exactly for  $\text{CH}_3\text{SnD}_3/\text{CH}_3\text{SnH}_3$ . Since high resolution could not be used to locate most of the band centers in  $\text{CH}_3\text{SnD}_3$ , it appears that the errors in locating the band centers are causing the differences in the product rule ratios of  $\text{CH}_3\text{SnD}_3$ . Also, this was probably the main reason why the method of Hansen and Dennison did not work. The effect of these errors on the force constants to be calculated is probably about 1%.

TABLE XV

Anharmonicity Constants, Anharmonic and Harmonic Frequencies ( $\text{cm}^{-1}$ ) for the Methylstannanes

Description	$\text{CH}_3\text{SnH}_3$			$\text{CH}_3\text{SnD}_3$			$\text{CD}_3\text{SnH}_3$		
	$\nu$	$x$	$\omega$	$\nu$	$x$	$\omega$	$\nu$	$x$	$\omega$
A <sub>1</sub> Species									
<sup>a</sup> CH sym. str.	2932.5	0.0409	3057.6	2930.0	0.0409	3054.9	2144.3	0.0299	2210.4
<sup>b</sup> SnH sym. str.	1874.5	0.0310	1934.5	1352.0	0.0224	1383.0	1889.0	0.0312	1949.8
<sup>c</sup> CH <sub>3</sub> sym. deform.	1209.3	0.0263	1242.0	1204.5	0.0262	1236.9	920.2	0.0200	939.0
<sup>b</sup> SnH <sub>3</sub> sym. deform.	694.5	0.0301	716.1	493.0	0.0214	503.8	703.5	0.0305	725.6
CSn str.	526.9	0	526.9	509.1	0	509.1	478.0	0	478.0
E Species									
<sup>c</sup> CH asym. str.	3005.4	0.0480	3156.9	3000.0	0.0479	3150.9	2254.5	0.0360	2338.7
<sup>b</sup> SnH asym. str.	1874.5	0.0310	1934.5	1352.0	0.0224	1383.0	1889.0	0.0312	1949.8
<sup>a</sup> CH <sub>3</sub> asym. deform.	1417.0	0.0426	1480.9	1400.0	0.0421	1461.5	1017.1	0.0306	1049.2
<sup>c</sup> CH <sub>3</sub> rock	774.1	0.0273	795.8	765.0	0.0270	786.2	628.4	0.0222	642.7
<sup>b</sup> SnH <sub>3</sub> asym. deform.	741.3	0.0176	754.6	502.5	0.0119	508.6	738.1	0.0175	751.2
<sup>c</sup> SnH <sub>3</sub> rock	416.3	0.0308	429.5	316.6	0.0234	324.2	392.4	0.0290	404.1

<sup>a</sup> Transferred from methyl halides (2)

<sup>b</sup> Transferred from stannane (36)

<sup>c</sup> Calculated from equations 42-44

TABLE XVI

Product Rule Ratios for Harmonic Frequencies

Calculated From	<u>CD<sub>3</sub>SnH<sub>3</sub>/CH<sub>3</sub>SnH<sub>3</sub></u>		<u>CH<sub>3</sub>SnD<sub>3</sub>/CH<sub>3</sub>SnH<sub>3</sub></u>	
	<u>A<sub>1</sub></u>	<u>E</u>	<u>A<sub>1</sub></u>	<u>E</u>
Structural Parameters	0.5055	0.3980	0.5055	0.3740
Harmonic Frequencies	0.5064	0.4001	0.4835	0.3540

## B. Model Force Fields

The force constants,  $F_{ij}$ , of equation 31, define the harmonic force field. In this work, the potential energy function is described in terms of the Harmonic Hybrid-Orbital Force Field (HOFF). The choice was made after considering several alternatives as discussed below. The choice of the assumed force field was dictated by the following considerations: (1) choice of suitable coordinates; (2) availability of sufficient data to uniquely determine the force constants of the field; (3) comparisons between observed and calculated data; and (4) physical significance of the force field.

The General Force Field (GFF) in which all possible interactions between all vibrations are included, would be the most rigorous treatment of the problem. However, in most cases, there is insufficient data to fix the General Force Field, because for unsymmetrical molecules of  $N$  atoms there are  $\frac{1}{2} (3N-6)(3N-5)$  independent harmonic force constants. For an eight atom molecule, in the absence of symmetry, there are 171 force constants. The number of independent harmonic force constants is greatly reduced for molecules in which some symmetry exists. Thus for a given symmetry species containing  $n$  vibrations, there will be  $\frac{1}{2} n (n + 1)$  independent harmonic force constants.

In the case of methylstannane the  $A_1$  symmetry species, which contains 5 vibrations will have 15 independent harmonic force constants, and the  $E$  symmetry species, which contains 6 vibrations, will have 21 independent harmonic force constants. A listing of the symbols of

the 36 independent force constants for  $\text{CH}_3\text{SnH}_3$  is given in Table XVIIIA. For general discussions of the  $\text{CH}_3\text{XH}_3$  molecules, where it is not necessary to distinguish between the force constants of the  $\text{CH}_3$  group and those of the  $\text{XH}_3$  group, the symbols in Table XVIIB will be used.

Difficulties arising from lack of sufficient data may be circumvented by using data on several isotopic molecules supplemented by assumptions about transferability of force constants from one molecule to another and by assuming that certain interaction constants,  $F_{ij}$ , are zero. Since the  $\text{CH}_3$  and  $\text{SnH}_3$  groups of  $\text{CH}_3\text{SnH}_3$  are separated by a C-Sn bond, it is reasonable to assume that all interaction terms involving a  $\text{CH}_3$  vibration and a  $\text{SnH}_3$  vibration are zero except for  $F_{1012}$  where the two rocking vibrations involve the common C-Sn bond. Thus  $F_{12}$ ,  $F_{14}$ ,  $F_{23}$ ,  $F_{34}$ ,  $F_{78}$ ,  $F_{711}$ ,  $F_{712}$ ,  $F_{89}$ ,  $F_{810}$ ,  $F_{911}$ ,  $F_{912}$ , and  $F_{1011}$  were set equal to zero. Hence the number of independent force constants still to be determined for  $\text{CH}_3\text{SnH}_3$  was reduced to 24.

Even when sufficient data are available to resolve the problem the vibrational frequencies of the several isotopic molecules may be insensitive to the assumed values of the interaction constants. Unless the difference in mass between isotopic nuclei is very large, the forms of the normal coordinates are altered only to a negligible extent.

As an alternative to the GFF, other interaction constants of the potential field can be set equal to zero by assuming a simplified physical model of the molecule.

TABLE XVIIIA

Symbols for the Independent Force Constants for the  $\text{CH}_3\text{XH}_3$   
Molecule for Both the  $\text{CH}_3$  and  $\text{XH}_3$  Groups

$A_1$  Species

<u>Description</u>	<u>Symbol</u>
CH sym. str.	$F_{11}$
XH sym. str.	$F_{22}$
$\text{CH}_3$ sym. deform.	$F_{33}$
$\text{XH}_3$ sym. deform.	$F_{44}$
XC str.	$F_{55}$
CH sym. str.-XH sym. str.	$F_{12}$
CH sym. str.- $\text{CH}_3$ sym. deform.	$F_{13}$
CH sym. str.- $\text{XH}_3$ sym. deform.	$F_{14}$
CH sym. str.-XC str.	$F_{15}$
XH sym. str.- $\text{CH}_3$ sym. deform.	$F_{23}$
XH sym. str.- $\text{XH}_3$ sym. deform.	$F_{24}$
XH sym. str.-XC str.	$F_{25}$
$\text{CH}_3$ sym. deform.- $\text{XH}_3$ sym. deform.	$F_{34}$
$\text{CH}_3$ sym. deform.-XC str.	$F_{35}$
$\text{XH}_3$ sym. deform.-XC str.	$F_{45}$

TABLE XVIIIA - Cont.

E Species

<u>Description</u>	<u>Symbol</u>
CH asym. str.	F77
XH asym. str.	F88
CH <sub>3</sub> asym. deform.	F99
CH <sub>3</sub> rock	F1010
XH <sub>3</sub> asym. deform.	F1111
XH <sub>3</sub> rock	F1212
CH asym. str.-XH asym. str.	F78
CH asym. str.-CH <sub>3</sub> asym. deform.	F79
CH <sub>3</sub> asym. str.-CH <sub>3</sub> rock	F710
CH asym. str.-XH <sub>3</sub> asym. deform.	F711
CH asym. str.-XH <sub>3</sub> rock	F712
XH asym. str.-CH <sub>3</sub> asym. deform.	F89
XH asym. str.-CH <sub>3</sub> rock	F810
XH asym. str.-XH <sub>3</sub> asym. deform.	F811
XH asym. str.-XH <sub>3</sub> rock	F812
CH <sub>3</sub> asym. deform.-CH <sub>3</sub> rock	F910
CH <sub>3</sub> asym. deform.-XH <sub>3</sub> asym. deform.	F911
CH <sub>3</sub> asym. deform.-XH <sub>3</sub> rock	F912
CH <sub>3</sub> rock-XH <sub>3</sub> asym. deform.	F1011
CH <sub>3</sub> rock-XH <sub>3</sub> rock	F1012
XH <sub>3</sub> asym. deform.-XH <sub>3</sub> rock	F1112

TABLE XVIIB

Symbols for the Independent Force Constants for  $\text{CH}_3\text{XH}_3$

Type Molecules

A<sub>1</sub> Species

<u>Description</u>	<u>Symbol</u>
XH sym. str.	F <sub>SS</sub>
XH <sub>3</sub> sym. deform.	F <sub>SD</sub>
CX str.	F <sub>St</sub>
XH sym. str.-XH <sub>3</sub> sym. deform.	F <sub>SS-SD</sub>
XH sym. str. -CX str.	F <sub>SS-St</sub>
XH <sub>3</sub> sym. deform-CX str.	F <sub>SD-St</sub>

E Species

<u>Description</u>	<u>Symbol</u>
XH asym. str.	F <sub>AS</sub>
XH <sub>3</sub> asym. deform.	F <sub>AD</sub>
XH <sub>3</sub> rock	F <sub>R</sub>
XH asym. str.-XH <sub>3</sub> asym. deform.	F <sub>AS-AD</sub>
XH asym. str.-XH <sub>3</sub> rock	F <sub>AS-R</sub>
XH <sub>3</sub> asym. deform-XH <sub>3</sub> rock	F <sub>AD-R</sub>
CH <sub>3</sub> rock -XH <sub>3</sub> rock	F <sub>R-R</sub>

The simplest model used is the Valence Force Field (VFF) in which it is assumed that the force field is diagonal; i.e., all interaction constants are zero. Although it is found that most interaction terms are small compared to the diagonal terms,  $F_{ii}$ , it has been shown that small but definite interactions do occur between neighboring bond-stretch and angle-bend coordinates (39). Therefore extra interaction terms must be introduced into the VFF model, either empirically, or according to some theoretical model of interactions between coordinates. Hence the unmodified VFF was considered unsatisfactory.

One example of an empirical modification of the VFF is the Modified Valence Force Field (MVFF) (39). In the MVFF it is assumed that certain off-diagonal terms are zero, the others being given non-zero values which are adjusted to fit the data. The number of non-zero interaction constants is also chosen to be sufficient to fit the available data. The choice of interaction constants is not based on any definite model of the valence forces, and the constants have no theoretical significance. Thus the MVFF was not used in this study.

The Urey-Bradley Force Field (UBFF) is an alternate model field which, in addition to valence forces, takes into account the Van der Waals repulsive forces between nonbonded atoms (57, 60). For  $\text{CH}_3\text{X}$  molecules the model interprets molecular vibrations in terms of force constants related to changes in bond lengths, and bond angles, and repulsive force constants between nonbonded atoms. Duncan (19) has shown that for many types of molecules a satisfactory fit to observed data can be obtained only if the UBFF is modified by introducing empirical non-Urey-Bradley inter-

action constants. Aldous and Mills (2) found that the Urey-Bradley model did not adequately reproduce the observed data for the methyl halides. Long et al. (42) found that the UBFF derived for fluoroform was unacceptable because negative values were obtained for the bending force constants. Therefore the UBFF was not used in this study.

Heath and Linnett (28) have developed the Orbital Valency Force Field (OVFF), based on Pauling's theory of directed valency. This field interprets the valency force constants in terms of changes in the overlap of the atomic orbitals that make up the bonds. The OVFF was found to reproduce data much better than the MVFF but not in a completely satisfactory manner (29). In principle, the OVFF is a suitable field because it is based on a definite model of the valence forces.

Linnett and Wheatley (40) modified the OVFF by incorporating the effects of orbital following due to a change in hybridization. According to this modification, the orbitals of the central atom, by changing their hybridization ratios, alter the angles they make with one another in such a way as to follow the movement of the surrounding atoms during a vibration. Thus the angular displacements are described by a combination of two force constants, a bending force constant,  $k_H$ , which allows for departure from maximum overlap of the hydrogen atoms and an orbital following force constant,  $k_f$ . For example, in the  $CH_3$  deformation vibration of a  $CH_3X$  type molecule, the hydrogen atoms tend to move in a direction at right angles to the CH bond. For this motion there will be a

restoring force proportional to the displacement, which can be represented by the bending force constant,  $k_H$ , that tends to return the hydrogen atom to its equilibrium position of maximum overlap with the carbon atom bonding orbital. However, there is also the possibility that as the vibration occurs, the orbitals of the carbon atom, by changing their hybridization ratios might alter the angles they make with one another in such a way as to follow the movements of the hydrogen atoms. The resistance to orbital following due to a change of hybridization is measured by the orbital following force constant,  $k_f$ .

If  $k_f$  is infinite there is no orbital following and the deformation vibration is governed by the bending force constant,  $k_H$ . However, if  $k_f$  is finite there is orbital following, and the actual magnitude of  $k_H$  is less than it would be without orbital following. This modified OVFF gave very satisfactory predictions of the vibrational frequencies of methane and its deuterated derivatives. However, the direct calculation of these force constants for methylstannane would be very difficult.

Mills (47) has proposed a Hybrid Orbital Force Field (HOFF) by considering that changing the bond hybridization also changes the bond length (11B). Hence changing the hybridization ratios during a bending vibration should create a secondary interaction with the bond stretching vibration. For example, increasing the s orbital content of a hybrid orbital tends to shorten the bond while increasing the p orbital content tends to lengthen it. Since the angles of the  $XH_3$  groups are close to tetrahedral both  $sp^3$  and  $sd^3$  hybridization should be important in  $CH_3XH_3$  molecules (X = Si, Ge, Sn). However, since both hybrids have the same

tetrahedral symmetry, it appears reasonable to assume that the results of the HOFF are applicable to the  $\text{CH}_3\text{XH}_3$  molecules. Both the OVFF and the HOFF are based on re-hybridization arguments. The HOFF gives a satisfactory fit to the observed data for the methyl halides (2), silyl halides (18), and other methyl (17) and silyl (18) compounds.

Applied to  $\text{CH}_3\text{X}$  molecules (47), the HOFF provides the following relationships between stretch-bend interaction constants and the corresponding diagonal stretching constants. For the nondegenerate symmetry species ( $A_1$ ):

$$F_{\text{SS-SD}} = \sqrt{3} \left( \frac{\partial r}{\partial \lambda} \right)_{\text{CH}} \cdot F_{\text{SS}} \quad (45)$$

and

$$F_{\text{SD-St}} = -3 \left( \frac{\partial R}{\partial \lambda} \right)_{\text{CX}} \cdot F_{\text{St}} \quad (46)$$

For the degenerate symmetry species (E):

$$- F_{\text{AS-R}} = F_{\text{AS-AD}} = -\sqrt{6} \left( \frac{\partial r}{\partial \lambda} \right)_{\text{CH}} \cdot F_{\text{AS}} \quad (47)$$

where  $\lambda$  is a hybridization parameter defining the s-p hybridization of the central atom orbital. The hybridization parameter,  $\lambda$ , is defined by the equation (11A):

$$\varphi = \frac{s + \lambda p}{\sqrt{1 + \lambda^2}} \quad (48)$$

where  $\phi$  is the wavefunction of the s-p atomic hybrid on the central atom, and s and p denote atomic orbital functions.

The results of the force constant calculations for the methyl halides (2) and other methyl compounds (17) indicate that the  $F_{AD-R}$ 's are negative for groups whose HCH bond angle is greater than the tetrahedral value and positive for groups whose HCH bond angle is equal to or less than tetrahedral. The same kind of results are observed for the silyl compounds (18) indicating that this empirical relationship could hold for the other group IVA elements. In this study, when the HXH bond angle,  $\gamma$ , for group IVA elements (greater than the tetrahedral value) was plotted against the corresponding  $F_{AD-R}$  with negative values an approximate linear relationship was obtained (Figure 17). This is given by the expression

$$F_{AD-R} = 0.00213 \gamma - 0.2407 \quad (49)$$

On the other hand when the HXH bond angle is equal to or less than the tetrahedral value, the interaction force constants have values ranging from 0.010 to 0.030 with no angular dependence (17, 18). Thus, it is possible to estimate negative values of this force constant from equation 49 while the range of possible positive values is  $0.02 \pm 0.01$ .

### C. The Vibrational Secular Equation

The Hybrid Orbital force constants were calculated following the procedures outlined by Wilson, Decius and Cross (64), and by Herzberg (32). These procedures are summarized below.

The potential, and kinetic energies,  $V$  and  $T$ , respectively, for the vibrating molecule may be written as

$$2V = \sum_i \sum_j F_{ij} R_i R_j \quad (50')$$

and

$$2T = \sum_i \sum_j G_{ij} \dot{R}_i \dot{R}_j \quad (51')$$

or using matrix notation

$$2V = R'FR \quad (50)$$

and

$$2T = \dot{R}'G^{-1}\dot{R} \quad (51)$$

where  $F$  is the matrix of force constants defined in equation 31 and the elements of the  $G^{-1}$  matrix are functions of the atomic masses and equilibrium geometry of the molecule. The values of the elements of the  $F$  and  $G^{-1}$  matrixes depend on the choice of coordinates and in general there will be non-zero off-diagonal terms in the expressions for both  $V$  and  $T$ . The primes in equations 50 and 51 denote the transpose of a matrix and

$\dot{R}_i = (\partial R_i / \partial t)$  in equation 51 where  $t$  represents time.

To derive equations for the frequencies of the normal vibrations it is convenient to define a column matrix of normal coordinates,  $Q$ , by the equation

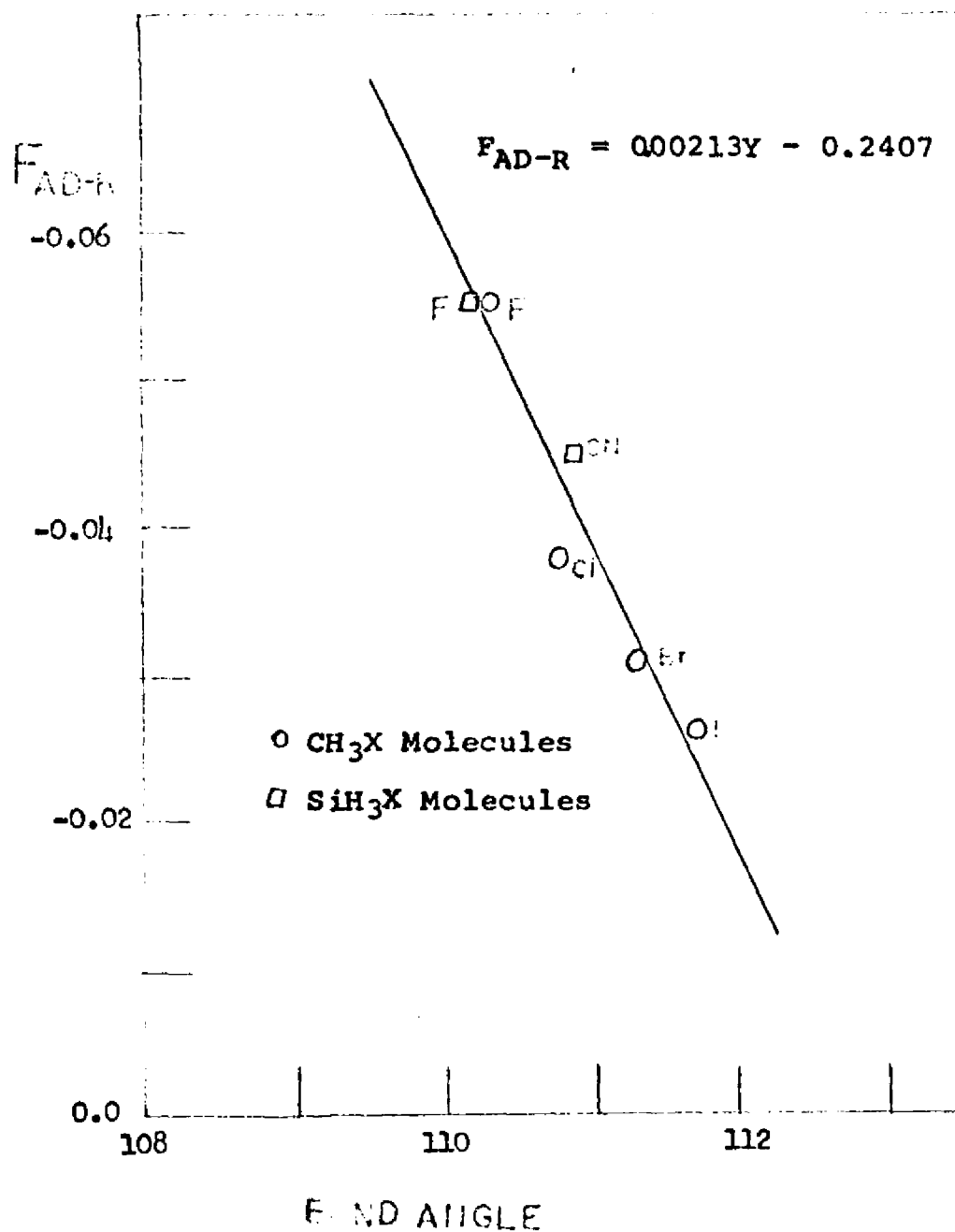


Figure 17. Angular Dependence of  $F_{AD-R}$  with Negative Values.

$$R = L Q \quad (52)$$

where L is the transformation matrix from internal coordinates, R, to the normal coordinates, Q, i.e.,

$$Q_j = \sum_i L_{ij} R_i \quad (53)$$

The transformation matrix is chosen in such a way that V and T can take the form

$$2V = Q' \Lambda Q \quad (54)$$

and

$$2T = \dot{Q}' E \dot{Q} \quad (55)$$

where E is the identity matrix and  $\Lambda$  is a diagonal matrix of the frequency parameters,  $\lambda_k = 4 \pi^2 \nu^2$ . In terms of the normal coordinates, the expressions for both V and T have zero coefficients for all the cross terms and the coefficients of the diagonal terms in equation 55 are chosen to be unity.

Using equation 52 to substitute for R in equations 50 and 51, and comparing the results with equations 54 and 55, one finds:

$$L' F L = \Lambda \quad (56)$$

and

$$L' G^{-1} L = E \quad (57)$$

Combining these two equations gives:

$$F L = G^{-1} \Lambda \quad (58)$$

or

$$G F L = \Lambda \quad (59)$$

Consider a single column of the L matrix denoted by  $L_i$  and let the corresponding frequency parameter be  $\lambda_i$ . Equation 59 can now be written in the form

$$(GF - \lambda_i E) L_i = 0 \quad (60)$$

where

$GF = (GF)_{ji} = \sum_k G_{jk} F_{ki}$ . A necessary and sufficient condition that non-trivial solutions for equation 60 can be found (i.e.,  $L_i \neq 0$ ) is that

$$|GF - \lambda E| = 0 \quad (61)$$

Expansion of the vibrational secular equation (equation 61) leads to a polynomial equation in  $\lambda$  which can be solved if the elements of the G and F matrices are known.<sup>1</sup> Then by substitution of the  $\lambda_i$ 's back into equation 60 sets of homogeneous linear equations are obtained, one for each column of L, from which the  $L_i$ 's may be determined.

---

<sup>1</sup> The secular equation (equation 61) factorizes in terms of symmetry coordinates so that the cross terms of the F and G matrices between coordinates of different species are always zero. Thus, the problem of solving the original (3N-6) square secular equations reduces to several smaller problems which are correspondingly simpler. Also, in molecules containing necessarily degenerate vibrations, the block of the secular equation corresponding to the degenerate species can be further factorized into d identical sub-blocks, where d is the degeneracy. In the case of  $\text{CH}_3\text{SnH}_3$  the 18 x 18 secular equation becomes one 5 x 5, one 1 x 1, and two 6 x 6 matrices. And since the two 6 x 6 matrices are degenerate, only one of them need be considered.

#### D. The Force Constant Refinement

Using equations 60 and 61, normal coordinate calculations may be conveniently performed by starting with assumed force constants to obtain the vibrational frequencies and normal coordinates. However, in practice, it is the vibrational frequencies that are observed and the force constants and normal coordinates are obtained from the frequencies.

Wilson, Decius and Cross (64) have employed the procedures of perturbation theory to the solution of equation 61. In this procedure, an initial set of force constants,  $F^{\circ}$ , was used to calculate the frequency parameter,  $\lambda$ , and transformation matrix,  $L$ . The force constants were then adjusted to obtain better values for  $\lambda_i^{\circ}$ . The corresponding change in the frequency parameters were shown to be (64)

$$\Delta \lambda_i = \sum_{j,k} L_{ji} L_{ki} \Delta F_{jk} \quad (62)$$

where  $L_{ji}$  and  $L_{ki}$  are the transformation coefficients defined in equation 53. This gives a linear relation between the change in force constants and the change in the frequency parameters, which can be written in matrix notation as

$$\Delta \Lambda = J \Delta F \quad (63)$$

where  $\Delta \Lambda$  is a column matrix of  $\Delta \lambda_i$ ,  $F$  is a column matrix of the elements  $\Delta F_{jk}$  and  $J$  is the Jacobian matrix whose elements are the products  $L_{ji} L_{ki}$  of equation 62.

Equation 63 forms the basis for an iterative method for refining a set of force constants to give the best fit to the observed frequencies. Such force constant refinement procedures have been developed by Aldous and Mills (1, 2), and by Overend and Scherer (52). A computer program has been developed by W. T. Thompson and C. S. Shoup for performing this force constant refinement on the IBM 7090 computer<sup>1</sup>. This program, modified in this study to fit the IBM 7040 computer<sup>2</sup>, is listed in Appendix III. Using the notation of Aldous and Mills (2) their force constant refinement procedure, as it was performed by the computer, is summarized below.

The symmetry coordinates obtained for methylsilane (18) were adopted in this study for methylstannane and are defined in Table XVIII. Internal valence coordinates for  $\text{CH}_3\text{SnH}_3$  are shown in Figure 18. Geometric and atomic parameters used in calculating the G matrices are given in Table VII (Chapter IV). The HOFF was assumed to be the model force field and an initial set of force constants was estimated. For  $\text{CH}_3\text{SnH}_3$ , the force constants,  $F_0$ , of the  $\text{CH}_3$  group, the  $\text{SnH}_3$  group, and the  $\text{CSn}$  force constant were taken from  $\text{CH}_3\text{SiH}_3$  (18),  $\text{SnH}_4$  (36), and  $\text{CH}_3\text{SnCl}_3$  (48), respectively.

---

<sup>1</sup> The kindness of Professor W. A. Fletcher of the University of Tennessee in making available the force constant refinement program of W. T. Thompson and C. S. Shoup is gratefully acknowledged.

<sup>2</sup> The contributions of Professor M. Pei of the City College of New York Computation Center for time on the IBM 7040 computer, and Mrs. Ann File and other members of the City College of New York Computation Center staff toward modifying the program to fit the IBM 7040 computer are gratefully acknowledged.

TABLE XVIII

Symmetry Coordinates for Methylstannane  
In Terms of Internal Coordinates

A<sub>1</sub> Species:

$$S_1 = (\Delta A_1 + \Delta A_2 + \Delta A_3) / (3)^{\frac{1}{2}}$$

$$S_2 = (\Delta B_1 + \Delta B_2 + \Delta B_3) / (3)^{\frac{1}{2}}$$

$$*S_3 = -\left[ K(\Delta a_1 + \Delta a_2 + \Delta a_3) + (\Delta a'_1 + \Delta a'_2 + \Delta a'_3) \right] / \left[ 3(1 + K^2) \right]^{\frac{1}{2}}$$

$$**S_4 = -\left[ K'(\Delta b_1 + \Delta b_2 + \Delta b_3) + (\Delta b'_1 + \Delta b'_2 + \Delta b'_3) \right] / \left[ 3(1 + K'^2) \right]^{\frac{1}{2}}$$

$$S = \Delta R$$

E Species:

$$S_{7a} = (2 \Delta A_1 - \Delta A_2 - \Delta A_3) / (6)^{\frac{1}{2}}$$

$$S_{8a} = (2 \Delta B_1 - \Delta B_2 - \Delta B_3) / (6)^{\frac{1}{2}}$$

$$S_{9a} = (2 \Delta a_1 - \Delta a_2 - \Delta a_3) / (6)^{\frac{1}{2}}$$

$$S_{10a} = (2 \Delta a'_1 - \Delta a'_2 - \Delta a'_3) / (6)^{\frac{1}{2}}$$

$$S_{11a} = (2 \Delta b_1 - \Delta b_2 - \Delta b_3) / (6)^{\frac{1}{2}}$$

$$S_{12a} = (2 \Delta b'_1 - \Delta b'_2 - \Delta b'_3) / (6)^{\frac{1}{2}}$$

$$*K = 3 (\sin a') (\cos a') / \sin a$$

$$**K = 3 (\sin b') (\cos b') / \sin b$$

where A and B represent the CH and SnH bond lengths,  
respectively;

a and b represent the HCH and HS<sub>n</sub>H bond angles,  
respectively;

a' and b' represent the HCS<sub>n</sub> and HS<sub>n</sub>C bond angles,  
respectively;

and R represents the CS<sub>n</sub> bond length

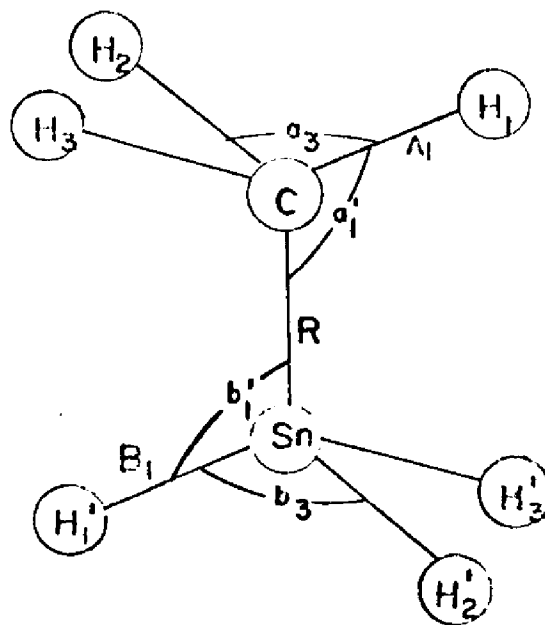


Figure 18. Valence Coordinates for Methylstannane.

For a given set of harmonic frequency parameters,  $\lambda$ , an assumed F matrix,  $F^{\circ}$ , was used to obtain a set of calculated frequency parameters,  $\lambda^{\circ}$ , from equation 61, and a set of calculated transformation coefficients,  $L^{\circ}$  from equation 59. Let  $\Delta \lambda_i = \lambda_i - \lambda_i^{\circ}$  in equation 63, where the matrix J is computed from the  $L^{\circ}$ 's. It might not be possible to find a  $\Delta F$  which satisfies equation 63 exactly. Thus it is necessary to compute the correction to  $F^{\circ}$  so that the differences between the observed and calculated frequency parameters,  $\Delta \lambda$ , are minimized. Let

$$r = J \Delta F - \Delta \lambda \quad (64)$$

where r represents the errors in the solution of equation 63 for each correction to  $F^{\circ}$ ,  $\Delta F$ . The solution,  $\Delta F$ , was obtained by the method of least squares. If the weighted square error, S, in the solution of equation 63 is defined as

$$S = r'Wr \quad (65)$$

where the matrix W is a diagonal matrix of the weights  $w_i = 1/\lambda_i^2$ , then the solution  $\Delta F$  that minimizes S can be determined by forming the equations

$$J'WJ\Delta F = J'W\Delta \lambda \quad (66)$$

The solution for equation 66 is

$$\Delta F = (J'WJ)^{-1} J'W\Delta \lambda \quad (67)$$

The  $\Delta F$ 's were used to form a new set of force constants

$$F \text{ (new)} = F \text{ (old)} + \Delta F \quad (68)$$

The calculations were returned to the beginning of the cycle by calculating a new set of frequency parameters and transformation coefficients from equations 61 and 59, and then returning to equation 63. The procedure was continued until  $\Delta F = 0$ , or was negligibly small.

The dispersion of each refined force constant was evaluated by the relation:

$$\sigma^2(F) = (J' W J)^{-1} \sigma^2 \quad (69)$$

where

$$\sigma^2 = (\Delta \Lambda') W (\Delta \Lambda) / (N - P) \quad (70)$$

N is the number of fundamental frequencies used in the calculations and P is the number of refined force constants. The diagonal elements of  $\sigma^2(F)$  give the uncertainties in the calculated force constants. The uncertainties obtained by equation 69 have meaning when a large number of independently observed frequencies are being used to determine a small number of force constants, i.e., (N-P) is not too small a number and when the linear relationship between  $\Delta F$  and  $\Delta \Lambda$  expressed in equation 63 is valid.

Using the HOFF, (N-P) is 15-9=6 for the  $A_1$  species and 18-11=7 for the E species of  $CH_3SnH_3$ . As it will be seen shortly, additional constraints were necessary to perform the calculations. Thus (N-P) became 15-7=8 for the  $A_1$  species and 18-7=11 for the E species of  $CH_3SnH_3$ .

In many force constant calculations, equation 66 may yield a whole family of solutions rather than a unique solution for  $\Delta F$ . In such a situation, different solutions to the force field may be obtained by starting the calculation with different initial F matrices. In several cases a

solution may be unacceptable because the force constants are physically unreasonable, e.g., negative principal force constants or interaction force constants which are much larger than the principal force constants. However, in some cases, there will be no method of deciding which is the best solution without some additional data.

If the number of frequencies is greater than the number of force constants, the matrix  $(J'WJ)$  should be nonsingular and unique solutions for  $\Delta F$  could be obtained which will minimize  $S$ . A simple test for singularity is obtained by comparing the product of the diagonal elements with the determinant of the matrix. These should be of a similar magnitude. Thus if

$$|J'WJ| / \prod_i^N (J'WJ)_{ii} \ll 1 \quad (71)$$

the matrix is close to being singular. However, as has already been pointed out, in most cases, the number of data is not sufficient to determine all of the force constants. This occurs even though the number of frequencies is greater than the number of parameters in the force field. Consequently the matrix  $(J'WJ)$  will be singular or nearly singular and a unique solution for  $\Delta F$  is not obtained.

The criterion  $|J'WJ| / \prod_i^N (J'WJ)_{ii}$  was set to equal 0.001 in this work to indicate whether or not the matrix  $(J'WJ)$  was singular. Duncan (17) set the criterion equal to 0.0001 with apparent success. If the singularity criterion gave a value greater than 0.001, the matrix to be inverted was nonsingular and a unique solution of equation 66 was possible.

The value of  $|J'WJ|/\sum_1^N (J'WJ)_{ii}$  gave values of 0.13 for the  $A_1$  species and 0.15 for the E species of  $CH_3SnH_3$  in this work, indicating that unique solutions for equation 66 were obtained.

The force constant refinement for each symmetry species of  $CH_3SnH_3$  was performed separately. Initial calculations for the  $A_1$  species using nine independent parameters were terminated before convergence was reached because a value of 0.00012 was obtained for the singularity criterion. A further restriction was imposed on the field by constraining to zero the two  $F_{SS-SD}$  constants. The methyl halide calculations using the HOFF were performed in this manner (2). Convergence was achieved after eight iterations. Equation 45 was then used to calculate  $F_{SS-SD}$  for both the  $CH_3$  and  $SnH_3$  groups. Values of 0.010 and 0.0082 were obtained for  $(\partial r/\partial \lambda)$  for the CH and SnH bonds, from the general harmonic force constants of the corresponding tetrahedral molecules,  $CH_4$  (20) and  $SnH_4$  (36), respectively. These quantities and the corresponding principal stretching force constants were substituted into equation 45 to obtain approximate values of  $F_{SS-SD}$ . The latter interaction constants were then incorporated into the converged calculation. Changes of less than 0.1% were observed in the calculated frequencies. The force constants, their dispersions, and the calculated and corrected harmonic frequencies obtained from this calculation are shown in Table XIX.

Initial calculations for the E species using eleven independent parameters in the HOFF were terminated before convergence was reached because a value of  $9.7 \times 10^{-11}$  resulted from the singularity test. The field was constrained

TABLE XIX

Harmonic Force Constants, m dyn/A, and Calculated and Observed Frequencies  $\text{cm}^{-1}$

$A_1$  Symmetry Species

Description	Force Constants			Frequencies						
		F	$\sigma(F)$	$\text{CH}_3\text{SnH}_3$		$\text{CH}_3\text{SnD}_3$		$\text{CD}_3\text{SnH}_3$		
				obs.	calc.	obs.	calc.	obs.	calc.	
CH sym. str.	$F_{11}$	5.391	0.091	$\nu_1$	3057.6	3061.5	3054.9	3061.5	2210.4	2202.6
SnH sym. str.	$F_{22}$	2.241	0.038	$\nu_2$	1934.5	1945.4	1383.0	1378.1	1949.8	1945.4
$\text{CH}_3$ sym. deform.	$F_{33}$	0.386	0.015	$\nu_3$	1242.0	1238.3	1236.9	1238.2	939.0	941.0
$\text{SnH}_3$ sym. deform.	$F_{44}$	0.149	0.003	$\nu_4$	716.1	715.5	503.8	507.8	725.6	715.4
CSn str.	$F_{55}$	2.124	0.044	$\nu_5$	526.9	516.8	509.1	519.9	478.0	478.3
	$*F_{13}$	0.093								
	$*F_{24}$	0.032								
	$F_{35}$	-0.236	0.078							
	$F_{45}$	-0.026	0.013							
	$F_{12} = F_{14} = F_{15} = F_{23} = F_{25} = F_{34} = 0$									

\* Calculated from equation 57

by using fixed values for  $F_{AS-AD}$  and  $F_{AS-R}$  for the  $CH_3$  and  $SnH_3$  groups. These interaction force constants were determined from equation 47 and assuming that  $F_{AS-AD}$  is approximately equal to  $-\sqrt{2} F_{SS-SD}$ . With this constraint a value of  $3.4 \times 10^{-6}$  resulted from the singularity test and the calculation was terminated.

To further restrict the field,  $F_{AD-R}$  for the  $CH_3$  and  $SnH_3$  groups were estimated from equation 49. These force constants were then fixed as a further constraint on the force field. The resulting force field containing seven independent parameters converged after six iterations. The force constants, their dispersions, and the calculated and corrected harmonic frequencies obtained from this calculation are shown in Table XX.

The force constant refinements also yielded the normal coordinates. These are shown in Table XXI and XXII for  $CH_3SnH_3$ ,  $CH_3SnD_3$ , and  $CD_3SnH_3$ .

The force constant refinement procedure was applied to the following molecules:  $CH_3CH_3$ ,  $CH_3SiH_3$ , and  $CH_3GeH_3$  to obtain corrected force constants. The frequencies and structural parameters for ethane (27), methylsilane (18, 63) and methylgermane (26) have been reported in the literature. Harmonic frequencies for ethane have been calculated (27). The observed frequencies for the isotopic molecules of methylsilane and methylgermane were corrected for anharmonicity effects by the methods previously described for methylstannane. Since frequency data for only two molecules of methylsilane were available, the refinement procedure for the degenerate species of  $CH_3SiH_3$  was modified.

TABLE XX

Harmonic Force Constants m dyn/A, Calculated and Observed Frequencies,  $\text{cm}^{-1}$   
E Symmetry Species

Description	Force Constants			Frequencies						
		F	$\sigma(F)$	$\text{CH}_3\text{SnH}_3$		$\text{CH}_3\text{SnD}_3$		$\text{CD}_3\text{SnH}_3$		
				obs.	calc.	obs.	calc.	obs.	calc.	
CH asym. str.	$F_{77}$	5.366	0.165	$\nu_7$	3156.9	3155.3	3150.9	3155.3	2338.7	2335.3
SnH asym. str.	$F_{88}$	2.217	0.069	$\nu_8$	1934.5	1943.5	1383.0	1381.7	1949.8	1934.5
$\text{CH}_3$ asym. deform.	$F_{99}$	0.470	0.015	$\nu_9$	1480.9	1472.0	1461.5	1472.0	1049.2	1064.6
$\text{CH}_3$ rock	$F_{1010}$	0.352	0.019	$\nu_{10}$	795.8	809.4	786.2	785.3	642.7	605.4
$\text{SnH}_3$ asym. deform.	$F_{1111}$	0.115	0.005	$\nu_{11}$	754.6	723.4	508.6	524.8	751.2	753.4
$\text{SnH}_3$ rock	$F_{1212}$	0.141	0.012	$\nu_{12}$	429.5	428.2	324.2	319.0	404.1	408.7
	$^1F_{79} = -F_{710}$	-0.132								
	$^1F_{811} = -F_{812}$	-0.044								
	$^2F_{910}$	0.012								
	$^2F_{1112}$	0.010								
	$F_{1012}$	0.047	0.017							
	$F_{711} = F_{712} = F_{89} = F_{810} = F_{78} = F_{911} = F_{912} = F_{1011} = 0$									

<sup>1</sup>Calculated from equation 47 and assumption  $F_{\text{AS-AD}} = -\sqrt{2} F_{\text{SS-SD}}$

<sup>2</sup>Calculated from equation 49

Table XXI. L-Matrices of the Methylstannanes.  $A_1$  Symmetry Species.

	Q/S	1	2	3	4	5
$\text{CH}_3\text{SnH}_3$	1	1.011	-0.000	0.013	-0.000	0.005
	2	0.000	0.997	-0.001	0.001	0.001
	3	-0.138	0.001	1.575	0.014	0.069
	4	0.000	-0.013	-0.014	1.424	0.026
	5	-0.052	-0.005	0.107	0.010	0.278
$\text{CH}_3\text{SnD}_3$	1	1.011	-0.000	0.013	0.004	-0.003
	2	0.000	0.707	-0.004	0.003	-0.000
	3	-0.138	0.008	1.576	0.063	-0.029
	4	-0.000	-0.019	-0.008	0.575	0.841
	5	-0.052	-0.008	0.107	0.241	-0.141
$\text{CD}_3\text{SnH}_3$	1	0.725	-0.001	0.023	0.000	0.007
	2	0.001	0.997	0.000	0.001	0.001
	3	-0.200	0.000	1.200	0.029	-0.029
	4	0.001	-0.013	-0.034	1.424	0.017
	5	-0.077	-0.005	0.155	0.014	0.248

Table XXII. L-Matrices of the Methylstannanes. E Symmetry Species.

	Q/S	7	8	9	10	11	12
CH <sub>3</sub> SnH <sub>3</sub>	7	1.049	0.001	0.018	-0.015	-0.009	0.005
	8	-0.001	1.001	0.002	0.004	-0.023	-0.026
	9	0.117	-0.003	1.625	0.005	0.005	-0.007
	10	-0.082	-0.009	0.231	0.888	0.442	-0.207
	11	-0.002	0.029	0.001	0.591	-1.409	-0.408
	12	-0.056	-0.003	-0.044	0.490	-0.375	0.837
CH <sub>3</sub> SnD <sub>3</sub>	7	1.049	0.018	0.001	-0.017	0.003	0.004
	8	-0.000	-0.008	0.712	0.001	0.015	-0.019
	9	0.117	1.625	0.018	0.007	-0.002	-0.005
	10	-0.082	0.231	-0.013	0.998	-0.117	-0.130
	11	-0.001	0.001	-0.001	0.071	1.076	-0.316
	12	-0.055	-0.046	-0.011	0.223	0.382	0.625
CD <sub>3</sub> SnH <sub>3</sub>	7	-0.778	0.003	-0.001	0.001	-0.006	-0.006
	8	0.004	1.001	0.002	0.019	-0.017	0.023
	9	-0.198	-0.001	1.180	0.025	0.044	0.010
	10	0.121	-0.009	0.089	0.177	0.670	0.298
	11	0.004	-0.029	-0.012	1.441	-0.553	0.344
	12	0.081	-0.003	-0.075	0.630	0.304	-0.765

In this case, the  $\text{CH}_3$  rock-SiH<sub>3</sub> rock interaction force constant was assumed to be independent of anharmonicity effects and this force constant was constrained to the value obtained by Duncan (18). The results of the force constant calculations for the four molecules are summarized in Table XXIII.

#### E. The Calculation of the Potential Energy Distributions and Coriolis Constants.

##### 1. The Potential Energy Distributions

From equation 62, the relation

$$\lambda_i = \sum_{j,k} L_{ji} L_{ki} F_{jk} \quad (72)$$

can be obtained. The frequency parameter,  $\lambda_i$ , gives the potential energy for a unit displacement of the normal mode,  $Q_i$ , since according to equation 54

$$2V = \sum_i \lambda_i Q_i^2 \quad (73)$$

The potential energy distribution whose columns are made up of fractional contributions for a given mode, is given by

$$\text{P.E.D.} = \mathbf{JFA}^{-1} \quad (74)$$

The fractional contribution to  $\lambda_i$  from the principal force constants,  $F_{jj}$  is given by  $L_{ji}^2 F_{jj} / \lambda_i$ .

The results of the P.E.D. calculations are given in Tables XXIV and XXV. The interaction force constants were neglected in the P.E.D. calculations.

Table XXIII. Force Constants of the  $\text{CH}_3\text{XH}_3$  Series of Molecules, in Mdyn/A.

Description		$\text{CH}_3\text{CH}_3$	$\text{CH}_3\text{SiH}_3$	$\text{CH}_3\text{GeH}_3$	$\text{CH}_3\text{SnH}_3$
CH sym. str.	$F_{11}$	5.304	5.360	5.263	5.391
XH sym. str.	$F_{22}$		2.968	2.763	2.241
$\text{CH}_3$ sym. deform.	$F_{33}$	0.644	0.416	0.392	0.386
$\text{XH}_3$ sym. deform.	$F_{44}$		0.253	0.219	0.149
CX str.	$F_{55}$	4.482	2.954	2.760	2.124
CH asym. str.	$F_{77}$	5.156	5.300	5.332	5.366
XH asym. str.	$F_{88}$		2.863	2.721	2.217
$\text{CH}_3$ asym. deform.	$F_{99}$	0.596	0.463	0.467	0.470
$\text{CH}_3$ rock	$F_{1010}$	0.725	0.366	0.394	0.352
$\text{XH}_3$ asym. deform.	$F_{1111}$		0.216	0.187	0.115
$\text{XH}_3$ rock	$F_{1212}$		0.252	0.217	0.141
	$F_{13}$	0.055	0.075	0.091	0.093
	$F_{24}$		0.032	0.040	0.032
	$F_{35}$	-0.352	-0.302	-0.183	-0.236
	$F_{45}$		-0.090	-0.131	-0.026
	$F_{79} = -F_{710}$	-0.085	-0.106	-0.129	-0.132
	$F_{811} = -F_{812}$		-0.045	-0.057	-0.044
	$F_{910}$	0.007	0.020	0.010	0.012
	$F_{1112}$		-0.023	0.010	0.010
	$F_{1012}$		0.090	0.080	0.047

TABLE XXIV

Potential Energy Distributions.  $A_1$  Symmetry Species

HARMONIC FREQUENCIES		FORCE CONSTANTS				
		CH str.	SnH str.	CH <sub>3</sub> deform.	SnH <sub>3</sub> deform.	CSn str.
<b>CH<sub>3</sub>SnH<sub>3</sub></b>						
$\nu_1$	3057.6	99.70	0.00	0.13	0.00	0.11
$\nu_2$	1934.5	0.00	100.00	0.00	0.00	0.00
$\nu_3$	1242.0	0.09	0.00	90.17	0.00	2.27
$\nu_4$	716.1	0.00	0.00	0.03	99.65	0.07
$\nu_5$	526.9	0.06	0.00	1.04	0.06	93.49
<b>CH<sub>3</sub>SnD<sub>3</sub></b>						
$\nu_1$	3054.9	99.70	0.00	0.13	0.00	0.11
$\nu_2$	1383.0	0.00	99.98	0.00	0.01	0.01
$\nu_3$	1236.9	0.09	0.00	90.17	0.00	2.27
$\nu_4$	503.8	0.02	0.00	0.21	67.62	26.92
$\nu_5$	509.1	0.04	0.01	0.82	26.15	65.29
<b>CD<sub>3</sub>SnH<sub>3</sub></b>						
$\nu_1$	2210.4	98.78	0.00	0.54	0.00	0.43
$\nu_2$	1949.8	0.00	100.00	0.00	0.00	0.00
$\nu_3$	939.0	0.40	0.00	79.64	0.02	7.32
$\nu_4$	725.6	0.00	0.00	0.11	99.34	0.14
$\nu_5$	478.0	0.19	0.00	0.24	0.03	96.85

TABLE XXV

Potential Energy Distributions. E Symmetry Species

	HARMONIC FREQUENCIES	FORCE CONSTANTS					
		CH str.	SnH str.	CH <sub>3</sub> deform.	CH <sub>3</sub> rock	SnH <sub>3</sub> deform.	SnH <sub>3</sub> rock
					CH <sub>3</sub> SnH <sub>3</sub>		
v <sub>7</sub>	3156.9	98.93	0.00	0.11	0.04	0.00	0.01
v <sub>8</sub>	1934.5	0.00	99.89	0.00	0.00	0.00	0.00
v <sub>9</sub>	1480.9	0.13	0.00	94.84	1.39	0.00	0.02
v <sub>10</sub>	795.8	0.30	0.01	0.00	70.03	10.19	8.57
v <sub>11</sub>	754.6	0.12	0.33	0.00	20.12	66.92	5.80
v <sub>12</sub>	429.5	0.09	0.90	0.01	9.34	11.87	61.34
					CH <sub>3</sub> SnD <sub>3</sub>		
v <sub>7</sub>	3150.9	98.93	0.00	0.11	0.04	0.00	0.01
v <sub>8</sub>	1383.0	0.00	99.96	0.01	0.01	0.00	0.00
v <sub>9</sub>	1461.5	0.13	0.01	94.83	1.39	0.00	0.02
v <sub>10</sub>	786.2	0.42	0.00	0.01	90.85	0.15	1.81
v <sub>11</sub>	508.6	0.03	0.29	0.00	2.80	78.16	12.04
v <sub>12</sub>	324.2	0.08	0.90	0.01	6.83	13.27	63.48
					CD <sub>3</sub> SnH <sub>3</sub>		
v <sub>7</sub>	2338.7	97.34	0.00	0.57	0.15	0.00	0.03
v <sub>8</sub>	1949.8	0.00	99.89	0.00	0.00	0.00	0.00
v <sub>9</sub>	1049.2	0.00	0.00	97.78	0.40	0.00	0.12
v <sub>10</sub>	642.7	0.09	0.27	0.39	66.80	14.93	5.53
v <sub>11</sub>	751.2	0.00	0.24	0.09	3.29	71.60	16.74
v <sub>12</sub>	404.1	0.14	0.73	0.03	19.61	8.60	52.02

The distribution of potential energy among the force constants, given in Table XXIV, shows that except for the  $\text{SnH}_3$  deformation and  $\text{CSn}$  stretching modes the concept of characteristic group frequencies can be applied to the  $A_1$  symmetry species of the methylstannanes. The frequencies at  $716.1 \text{ cm}^{-1}$  for  $\text{CH}_3\text{SnH}_3$  and  $725.6 \text{ cm}^{-1}$  for  $\text{CD}_3\text{SnH}_3$  are almost pure  $\text{SnH}_3$  angle bending, and the frequencies at  $526.9 \text{ cm}^{-1}$  for  $\text{CH}_3\text{SnH}_3$  and  $478 \text{ cm}^{-1}$  for  $\text{CD}_3\text{SnH}_3$  are almost pure  $\text{CSn}$  stretching modes. However, in  $\text{CH}_3\text{SnD}_3$  there is a large amount of mixing between the modes.

From Table XXV, it is seen that the  $\text{CH}_3$  rocking,  $\text{SnH}_3$  deformation, and  $\text{SnH}_3$  rocking modes show a significant amount of mixing for  $\text{CH}_3\text{SnH}_3$  and  $\text{CD}_3\text{SnH}_3$  whereas the  $\text{CH}_3$  rocking vibration becomes a pure mode in  $\text{CH}_3\text{SnD}_3$ . Examination of the results of the normal coordinate treatments of  $\text{CH}_3\text{SiH}_3$  and  $\text{CH}_3\text{GeH}_3$  (Table XXVI.) show that the amount of localization of this mode increases by about 20% on deuteration of the  $\text{GeH}_3$  group and about 10% on deuteration of the  $\text{SiH}_3$  group. These results indicate that if the hydrogen atom on the  $\text{XH}_3$  group of a  $\text{CH}_3\text{XH}_3$  molecule is replaced by heavier atoms the  $\text{CH}_3$  rocking mode changes from a noncharacteristic group vibration to one which will be approximately independent of the molecular framework to which the group is bonded and the  $\text{CH}_3$  rocking mode will behave as a characteristic group vibration. As a result, the  $\text{CH}_3$  rocking frequency for the  $(\text{CH}_3)_n\text{SnCl}_{(4-n)}$  or the  $(\text{CH}_3)_n\text{GeCl}_{(4-n)}$  series of molecules, for example, would be expected to be independent of the molecular framework and constant for the series.

TABLE XXVI

P.E.D. Among the  $\text{CH}_3$  Rocking,  $\text{XH}_3$  Asymmetric Deformation,  
and  $\text{XH}_3$  Rocking Modes of  $\text{CH}_3\text{SiH}_3$  and  $\text{CH}_3\text{GeH}_3$

	<u><math>\text{CH}_3</math> Rock</u>	<u><math>\text{XH}_3</math> Asymmetric Deformation</u>	<u><math>\text{XH}_3</math> Rock</u>
$\text{CH}_3\text{SiH}_3$	83.15	52.44	47.79
$\text{CH}_3\text{SiD}_3$	92.56	73.40	59.51
$\text{CH}_3\text{GeH}_3$	59.66	59.14	54.36
$\text{CH}_3\text{GeD}_3$	82.01	77.00	60.52

Ward (62) has found that for the  $(\text{CH}_3)_n \text{SnCl}_{(4-n)}$  the  $\text{CH}_3$  group does indeed behave as if it were attached to a heavy point mass. For the  $(\text{CH}_3)_n \text{GeCl}_{(4-n)}$  series the  $\text{CH}_3$  rocking frequency only varies from 838 to 824  $\text{cm}^{-1}$  (45). These results confirm the conclusions that in  $\text{CH}_3\text{XY}_3$  molecules, where Y is a heavy atom, the  $\text{CH}_3$  rocking mode does become a characteristic group vibration.

#### 1. Coriolis Constants.

Since the Coriolis constants are sensitive to the form of the normal coordinates, they were used to verify the results of the force constant calculations. The Coriolis constants were obtained from the transformation matrix, L, by the method of Meal and Polo (46), using the relationship

$$\zeta = L^{-1}C(L^{-1})' \quad (75)$$

where C is a matrix, the elements of which are determined from the known molecular geometry by the methods described by Meal and Polo (46). A tabulation of the elements of the C matrix for  $\text{CH}_3\text{XH}_3$  molecules has been reported by Randic (55). The computer program used to calculate the Coriolis constants is given in Appendix III. The calculated and observed constants for the methylstannanes are shown in Table XXVII. The agreement between the observed and the calculated Coriolis constants confirm the results of the normal coordinate analysis.

The algebraic signs and relative magnitudes of the Coriolis constants are of interest. The Coriolis interaction has been defined in Chapter IV as the interaction between the angular momentum of vibration and the angular momentum of rotation. If the Coriolis constant is negative,

TABLE XXVII

Coriolis Constants of Methylstannane (dimensionless)

Description		$\text{CH}_3\text{SnH}_3$	
		Observed	Calculated
CH asym. str.	$\zeta_7$	$0.0153 \pm 0.056$	0.0548
SnH asym. str.	$\zeta_8$	$-0.0574 \pm 0.030$	-0.0514
CH <sub>3</sub> asym. deform.	$\zeta_9$	$-0.129 \pm 0.081$	-0.234
CH <sub>3</sub> rock	$\zeta_{10}$	$0.112 \pm 0.077$	0.129
SnH <sub>3</sub> asym. deform.	$\zeta_{11}$	$-0.098 \pm 0.084$	-0.114
SnH <sub>3</sub> rock	$\zeta_{12}$	$0.260 \pm 0.021$	0.294
		$\text{CD}_3\text{SnH}_3$	
	$\zeta_8$	$-0.0299 \pm 0.011$	-0.0515
	$\zeta_{10}$	$0.242 \pm 0.031$	0.276
	$\zeta_{11}$	$-0.131 \pm 0.049$	-0.251

then the angular momentum of vibration produces an increase in the angular velocity of rotation of the molecule about the molecular axis (43). If the constant is positive, then the velocity of rotation about the molecular axis is less than it would be if no angular momentum of vibration were present (43). It is seen from Table XXVIII that the Coriolis constant for the  $\text{XH}_3$  asymmetric deformation vibration is negative for all the molecules of the  $\text{CH}_3\text{XH}_3$  series whereas the constant for the  $\text{XH}_3$  rocking vibration is positive. This is also true for the  $\text{CH}_3$  asymmetric deformation and  $\text{CH}_3$  rocking vibrations. This means that there is a significant increase in the velocity of rotation during the  $\text{XH}_3$  asymmetric deformation vibration and a significant decrease in the velocity of rotation during the  $\text{XH}_3$  rocking vibration.

These results are consistent with the forms of the normal modes of vibrations involved. If the  $\text{CH}_3$  group is considered to be rotating about a fixed axis the velocity of rotation would be increased if one or more of the CH bonds were bent toward the fixed axis. In the case of the  $\text{CH}_3$  asymmetric deformation vibration there is an alternating bending of two hydrogen atoms with one hydrogen atom toward and away from the molecular axis. The  $\text{CH}_3$  rocking vibration is essentially a bending of the  $\text{H}_3\text{C-X}$  bond and the shift of this group off of the molecular axis should slow down the velocity of the molecular rotation relative to that of the fixed rigid rotating molecule.

**TABLE XXVIII**

Coriolis Constants for the  $\text{CH}_3\text{XH}_3$  Molecules (dimensionless)

Description		1	2	3	4
		$\text{CH}_3\text{CH}_3$	$\text{CH}_3\text{SiH}_3$	$\text{CH}_3\text{GeH}_3$	$\text{CH}_3\text{SnH}_3$
CH asym. str.	$\zeta_7$	0.10	0.06	0.043	0.0153
XH asym. str.	$\zeta_8$	0.256	0.01	-0.035	-0.0515
$\text{CH}_3$ asym. deform	$\zeta_9$	-0.33	-0.33	-0.303	-0.129
$\text{CH}_3$ rock	$\zeta_{10}$	0.24	0.35	0.342	0.112
$\text{XH}_3$ asym. deform	$\zeta_{11}$	-0.36	-0.26	-0.227	-0.098
$\text{XH}_3$ rock	$\zeta_{12}$	0.36	0.24	0.26	0.260

<sup>1</sup>Ref. 27

<sup>2</sup>Ref. 54

<sup>3</sup>Ref. 26

<sup>4</sup>This work

## CHAPTER VI

### FORCE CONSTANT CORRELATIONS

Several empirical correlations have been made relating the vibrational frequencies of series of molecules to structural parameters. These include the  $(\text{CH}_3)_n\text{SnCl}_{(4-n)}$  series (62), the  $(\text{CH}_3)_n\text{SnH}_{(4-n)}$  series (16), the  $(\text{C}_2\text{H}_5)_n\text{Sn}(\text{CH}_3)_{(4-n)}$  series (15), the  $(\text{CH}_3)_n\text{GeCl}_{(4-n)}$  series (45), the  $(\text{CH}_3)_n\text{SiCl}_{(4-n)}$  series (59), and the  $(\text{CH}_3)_n\text{CCl}_{(4-n)}$  series (59). However, such correlations do not provide methods for predicting vibrational frequencies of other molecules because of the several factors contributing to the magnitude of the observed frequencies. These factors include: (1) the atomic masses and geometrical arrangement of the atoms in the molecule; and (2) the molecular force field. On the other hand, the force constants depend on the nature of the bonding in the molecule. Comparisons of analogous force constants for a series of molecules should give useful relationships for determining force constants for molecules not in the series.

Linnett (39) has discussed the empirical relationships between force constants and bond lengths, bond orders, the number of valence electrons, and electronegativity, which have been developed by Badger, Gordy, and others. On the assumption that the variation of bond lengths within the series of  $\text{CH}_3\text{XH}_3$  molecules reflect the effects of other factors such as electronegativity and changes in bond hybridization, an attempt has been made in this investigation to relate the

calculated force constants to bond lengths empirically. The relevant bond lengths, determined from spectroscopic measurements, are given in Table XXIX. These bond lengths usually differ from equilibrium bond lengths by about 0.01 Å (35). The Hybrid Orbital Force Constants for  $\text{CH}_3\text{XH}_3$  molecules ( $\text{X} = \text{C}, \text{Si}, \text{Ge}, \text{Sn}$ ), listed in Table XXIII, were determined in this investigation from the vibration frequencies.

Table XXIX. Bond Lengths (Å) for  $\text{CH}_3\text{XH}_3$  Molecules.

<u>Molecule</u>	<u>Ref.</u>	<u>CH Bond</u>	<u>XH Bond</u>	<u>CX Bond</u>
$\text{CH}_3\text{CH}_3$	27	1.093		1.534
$\text{CH}_3\text{SiH}_3$	63	1.092	1.484	1.867
$\text{CH}_3\text{GeH}_3$	26	1.083	1.529	1.945
$\text{CH}_3\text{SnH}_3$	38	1.083	1.700	2.143

The case of ethane deserves special mention. It can be seen in Table XXIII that, despite similar CH bond distances, the two  $\text{CH}_3$  bending force constants and the  $\text{CH}_3$  rocking force constant for ethane are significantly larger than the corresponding  $\text{CH}_3$  force constants in the other  $\text{CH}_3\text{XH}_3$  molecules. Except for ethane, it is assumed that the mass of the  $\text{XH}_3$  group is sufficiently heavy so that vibration frequencies of the  $\text{XH}_3$  group are too low to interact appreciably with the frequencies of the rest of the molecule. Or equivalently (except for the interaction between the  $\text{CH}_3$  rocking and  $\text{XH}_3$  rocking vibrations) the interaction force constants between the  $\text{CH}_3$  and  $\text{XH}_3$  groups of  $\text{CH}_3\text{XH}_3$  molecules may be set equal to zero. However, it has been shown by Hansen and Dennison (27)

that some of the interaction force constants between the two  $\text{CH}_3$  groups of ethane are appreciably different from zero. Hence in this work, ethane was not considered in the correlation of force constants with bond lengths. In support of this decision, it is pointed out that in methane, where there is no interaction with another  $\text{CH}_3$  group, the doubly degenerate bending force constant has a value of 0.469 mdyn/A (20) which is in agreement with the corresponding force constants of the  $\text{CH}_3$  group observed in  $\text{CH}_3\text{SiH}_3$ ,  $\text{CH}_3\text{GeH}_3$ , and  $\text{CH}_3\text{SnH}_3$ .

#### A. Relationships Between the Force Constants and Bond Lengths

In principle, the existence of such relationships could be established theoretically. Even the functional form of such a relationship would be quite useful. The attempts in this study to establish a theoretical relationship based on force constant expressions derived from the Hellmann-Feynman theorem (34a, 56) were not successful.

Instead, empirical relationships between the  $\text{XH}_3$  group force constants and the  $\text{XH}$  bond lengths for  $\text{CH}_3\text{XH}_3$  molecules were determined. Previous investigations of empirical relationships between the stretching force constants and bond lengths have shown that these force constants are proportional to  $1/r^n$  where  $n$  has values between 1.5 and 3.0. It was found in this study that plots of  $F_{\text{SS}}$  and  $F_{\text{AS}}$  vs.  $1/r^2$  gave linear relationships.

These relationships are considered linear if the standard errors of the force constants calculated from the empirical equations are within the standard deviations of the force

constants (e.g., Tables XIX and XX) used for determining the relationships. The standard errors for the equations relating  $F_{SS}$  with  $1/r^2$  and  $F_{AS}$  with  $1/r^2$  were 0.064 and 0.053, respectively, compared to 0.091 and 0.165 for  $F_{SS}$  and  $F_{AS}$ .

Linear relationships between the bending force constants and  $1/r^2$  had standard errors of 0.041, 0.022 and 0.049 for  $F_{SD}$ ,  $F_{AD}$ , and  $F_R$ , respectively. These linear relationships were rejected because their standard errors were larger than the standard deviations of  $F_{SD}$ ,  $F_{AD}$ , and  $F_R$ , which were 0.015, 0.015, and 0.019, respectively. Plots of these force constants against  $r$  directly are shown in Figures 19-21. When  $F_{SD}$ ,  $F_{AD}$ , and  $F_R$  were linearly related to  $r$ , standard errors of 0.019, 0.020, and 0.025 were obtained, respectively. These standard errors were also larger than the standard deviations of the bending force constants. On the other hand, quadratic equations did satisfy the standard deviation criterion. These equations had standard errors of 0.010, 0.005, and 0.016 for  $F_{SD}$ ,  $F_{AD}$ , and  $F_R$ , respectively.

In Figures 19-21, the points corresponding to the  $CH_3$  moieties are the average values of the force constants for the  $CH_3$  group attached to the  $XH_3$  group for the  $CH_3XH_3$  molecules in which X is Si, Ge, or Sn. The equations described below were obtained by a least squares polynomial curve fitting library computer program (33).

For  $F_{AS}$  and  $F_{SS}$ , the result was

$$F_{AS} = (6.51/r^2) - 0.0600 \quad (79)$$

$$F_{SS} = (6.31/r^2) + 0.0927 \quad (80)$$

A smooth curve was obtained when the  $\text{XH}_3$  symmetric deformation force constants,  $F_{\text{SD}}$ , were plotted against the XH bond length,  $r$  (Fig. 19). The relationship between  $F_{\text{SD}}$  and  $r$  obtained is

$$F_{\text{SD}} = -0.1704 r^2 + 0.08788 r + 0.4910 \quad (81)$$

Similar relationships were obtained for the  $\text{XH}_3$  asymmetric deformation and  $\text{XH}_3$  rocking force constants. These are shown in Figures 20 and 21 and are given by the expressions

$$F_{\text{AD}} = 0.2955 r^2 - 1.401 r + 1.641 \quad (82)$$

and 
$$F_{\text{R}} = -0.2718 r^2 + 0.2790 + 0.3802 r \quad (83)$$

In order to calculate the frequencies of the  $\text{CH}_3\text{XH}_3$  type molecules, a relationship is also necessary for the CX stretching force constant,  $F_{\text{X-Y}}$ . A plot of  $F_{\text{X-Y}}$  vs.  $1/r_{\text{X-Y}}^2$  yielded a linear relationship given by the equation

$$F_{\text{X-Y}} = 10.16/r_{\text{X-Y}}^2 \quad (85)$$

The above equations reproduce the principal force constants to within their standard deviations. However, two questions remain: Do these equations have physical significance, i.e., do the force constants in the  $\text{CH}_3\text{XH}_3$  series really depend only upon the bond length? If they do, then how reliably can these equations be expected to predict new force constants within the  $\text{CH}_3\text{XH}_3$  series? The fact that only four experimental points determine each equation precludes definite answers. Only further experimental or theoretical work might give such answers. Assuming that the force constants do depend only on the bond lengths, some idea of the reliability of these equations, however, can be obtained by considering in detail

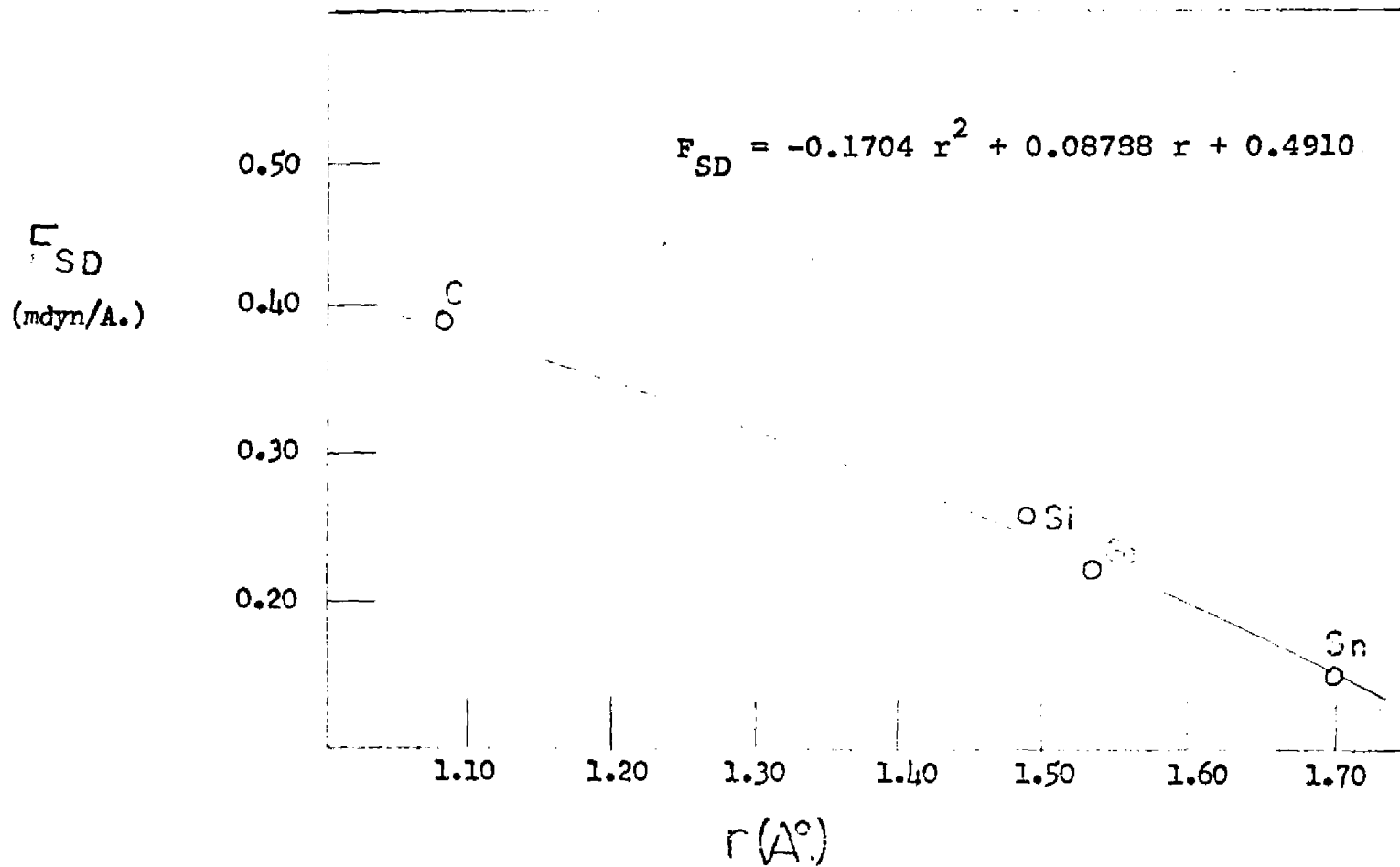


Figure 19. XH Bond Lengths vs.  $XH_3$  Symmetric Deformation Force Constants of  $CH_3XH_3$  Molecules (X = Si, Ge, Sn)

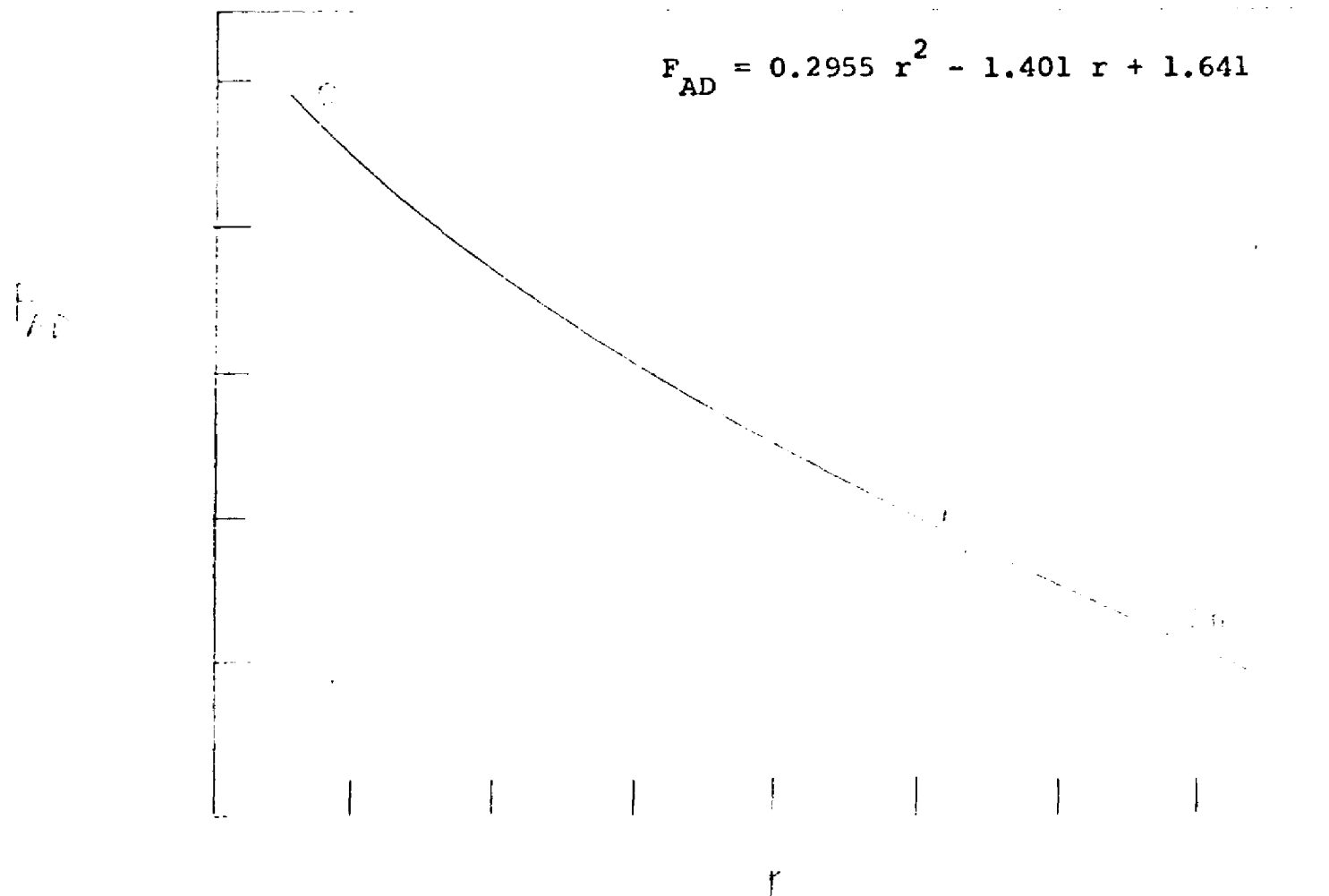


Figure 20. Plot of  $F_{AD}$  (mdyn/A) vs.  $r$  (A) for  $CH_3XH_3$  Molecules (X = Si, Ge, Sn).

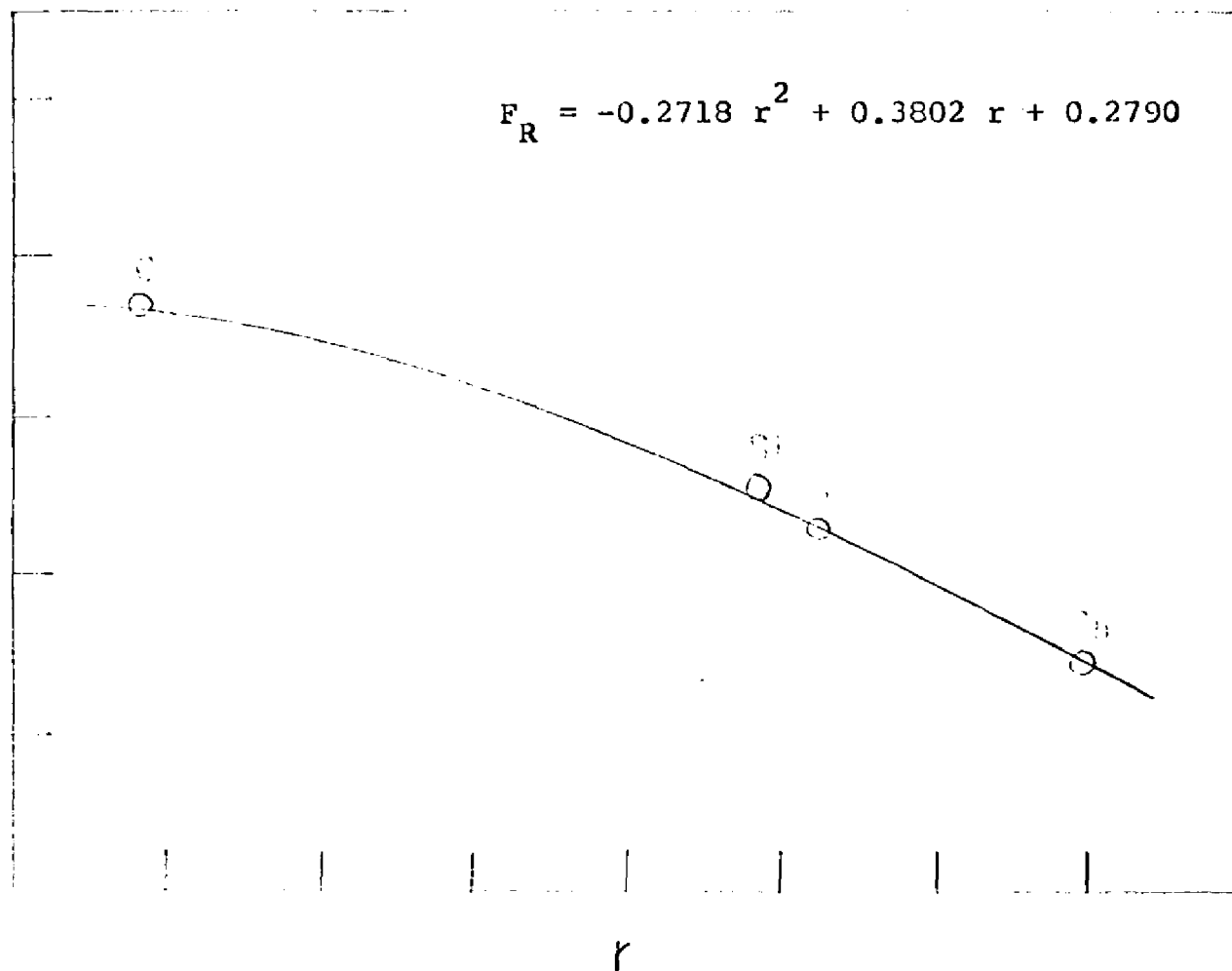


Figure 21. Plot of  $F_R$  (mdyn/A) vs.  $r$  (A) for  $\text{CH}_3\text{XH}_3$  Molecules (X = Si, Ge, Sn).

the number of experimental points in relation to the number of parameters to be determined in a given equation. It can be said at the outset that all parameters in these equations are unreliable. However, the parameters of equations 79 and 80 should be more reliable than those of equations 81 - 83 because four points are being used to determine two parameters in equations 79 and 80 whereas the four points are being used to determine three parameters in equations 81 - 83. Equation 85 was obtained from four points and should be more reliable than equations 79 - 83 since equation 85 has only one parameter.

Since equations 81 - 83 were determined from only four points and the coefficients are of questionable reliability the use of a simpler linear equation might be preferred. The preference was decided with help of Gauss' criterion (65). This criterion states that the equation giving the closest fit yields a minimum for the function

$$\sigma = (y_o - y_c)^2 / (n-m) \tag{84}$$

where  $y_o$  and  $y_c$  represent the observed and calculated values of  $y$ , respectively. The quantities  $n$  and  $m$  represent, respectively, the number of points used for obtaining the equation, and the number of constants in the equation.

The following results were obtained for equation 81 - 83, where, in all cases,  $n = 4$ :

	$\sigma \times 10^3$	
	linear equation ( $m = 2$ )	quadratic equation ( $m = 3$ )
equation 81	0.15	0.11
equation 82	0.31	0.04
equation 83	0.30	0.12

Thus, the criterion shows that the quadratic forms give the closer fit to the data. However, since the criterion is reliable only when  $n \gg m$ , the evidence for using a quadratic equation is not overwhelming. Furthermore, cubic and higher order equations have not been excluded.

Explicit indication of the error in the predicted force constants can be obtained by calculating force constants from two different equations in a region far from the experimental points used to determine an equation. One such region is between the CH bond length ( $r = 1.083\text{\AA}$ ) and the SiH bond length ( $r = 1.484\text{\AA}$ ). Then the results obtained from quadratic equations (equations 81 - 83) and linear equations for the force constants are compared. Linear equations between the bending force constants and  $r$ , determined by the method of least squares are:

$$F_{SD} = -0.379 r + 0.801 \quad (81a)$$

$$F_{AD} = -0.599 r + 1.116 \quad (82a)$$

$$F_R = -0.357 r + 0.762 \quad (83a)$$

The results of the calculation of  $F_{SD}$ ,  $F_{AD}$ , and  $F_R$  from the quadratic equations (equation 81 - 83) and from the linear equations (equations 81a - 83a) for a bond length of  $1.30\text{\AA}$  are shown below.

calc. from	$F_{SD}$ (mdyn/Å)	$F_{AD}$ (mdyn/Å)	$F_R$ (mdyn/Å)
linear eqn.	0.308	0.337	0.298
quadratic eqn.	0.317	0.319	0.314

These calculations show that a variation of 6% might be expected in the predictions of unknown force constants.

## B. "Model" Force Constants and the Prediction of Vibrational Frequencies.

The principal force constant correlations (equations 79 - 83 and 85) discussed above can be used to calculate a set of "model" force constants for these molecules from the CH and XH bond lengths. The use of these "model" force constants, in combination with some model for estimating the interaction force constants within the CH<sub>3</sub> or XH<sub>3</sub> groups, can be tested by applying them to the prediction of vibrational frequencies for molecules within and outside the CH<sub>3</sub>XH<sub>3</sub> series. The HCH and HXH bond angles are assumed to be tetrahedral and all interactions between the CH<sub>3</sub> and XH<sub>3</sub> groups are assumed to be negligible, except for the interaction between the CH<sub>3</sub> rocking motion and the XH<sub>3</sub> rocking motion. For convenience, the equations used for calculating the "model" force constants are listed in Table XXX.

Using the values of the principal stretching force constants already obtained and the hybridization parameters for the orbitals forming the bonds,  $F_{SS-SD}$  and  $F_{SD-St}$  of the A<sub>1</sub> symmetry species and  $F_{AS-AD}$  and  $F_{AS-R}$  of the E symmetry species for the CH<sub>3</sub> group were estimated from equations 45-47 (Table XXX). The value of  $\partial r/\partial \lambda$  for the CH bond was estimated from the force constants for methane (20) using the relationship derived by Mills for regular tetrahedral molecules (47). The value of  $\partial R/\partial \lambda$  for the CSn bond can be calculated from equation 46 and the data in Table XIX. The interaction constants  $F_{AD-R}$  for the CH<sub>3</sub> group were estimated from equation 49. The interaction

Table XXX. The Equations Used for Calculating the "Model" Force Constants in mdyn/Å<sup>0</sup>. (Bond Lengths in Å<sup>0</sup>.)

$$F_{AS} = (6.51/r^2) - 0.060 \quad (79)$$

$$F_{SS} = (6.31/r^2) + 0.093 \quad (80)$$

$$F_{SD} = -0.1704r^2 + 0.08788r + 0.4910 \quad (81)$$

$$F_{AD} = 0.2955r^2 - 1.401r + 1.641 \quad (82)$$

$$F_R = -0.2718r^2 + 0.3802r + 0.2790 \quad (83)$$

$$F_{X-Y} = 10.16/r_{X-Y}^2 \quad (85)$$

$$F_{SS-SD} = \sqrt{3} (\partial r / \partial \lambda)_{XH} F_{SS} \quad (45)$$

$$F_{SD-St} = -3 (\partial R / \partial \lambda)_{CX} F_{St} \quad (46)$$

$$-F_{AS-R} = F_{AS-AD} = -\sqrt{6} (\partial r / \partial \lambda)_{XH} F_{AS} \quad (47)$$

$$F_{AD-R} = 0.00213Y - 0.2407 \quad (49)$$

(Y is the HXH bond angle.)

force constants for the  $\text{XH}_3$  group were also determined from equations 45-47 and equation 49. The  $\text{CH}_3$  rock- $\text{XH}_3$  rock interaction force constants present a problem because there are no relationships for determining them. They were estimated in this study by examining the values of this interaction force constant in similar molecules. For example, the  $\text{SiH}_3$  rock- $\text{GeH}_3$  rock interaction force constant of  $\text{SiH}_3\text{GeH}_3$  was estimated from the data on  $\text{CH}_3\text{SiH}_3$  and  $\text{CH}_3\text{GeH}_3$  obtained in this work, and from the data on  $\text{SiH}_3\text{SiH}_3$  (18).

The "model" force constants, calculated for  $\text{CH}_3\text{SiH}_3$ ,  $\text{CH}_3\text{GeH}_3$ , and  $\text{CH}_3\text{SnH}_3$ , are tabulated in Table XXXI. In Tables XXXII - XXXIV the vibrational frequencies calculated from the "model" force constants are listed. For comparison, the observed frequencies corrected for anharmonicity effects and the frequencies obtained from the force constant refinement are also listed. In the tables to follow, the frequencies listed as observed are the observed frequencies corrected for anharmonicity effects. In most cases the differences between the harmonic frequencies and the frequencies calculated from the "model" force constants are less than  $20 \text{ cm}^{-1}$ .

A study of the vibrational assignments made for several series of  $(\text{CH}_3)_n\text{XY}_{(4-n)}$  molecules, where  $\text{X}=\text{C}, \text{Si}, \text{Ge}, \text{Sn}$ , and  $\text{Y} = \text{H}, \text{Cl}$  (15, 16, 45, 59, 62), shows that assigned frequencies in the  $\text{XH}$  stretching vibration region may be in error by  $25\text{-}35 \text{ cm}^{-1}$  with a maximum error of  $50 \text{ cm}^{-1}$ . The assigned frequencies in the  $\text{XH}_3$  bending vibration region may be in error by  $15 - 25 \text{ cm}^{-1}$  with a maximum error of  $40 \text{ cm}^{-1}$ . The maximum

Table XXXI. "Model" Force Constants in mdyn/A.

Description		CH <sub>3</sub> SiH <sub>3</sub>	CH <sub>3</sub> GeH <sub>3</sub>	CH <sub>3</sub> SnH <sub>3</sub>	
CH sym. str.	F <sub>11</sub>	5.262	5.419	5.419	
XH sym. str.	F <sub>22</sub>	2.980	2.799	2.294	
CH <sub>3</sub> sym. deform.	F <sub>33</sub>	0.383	0.400	0.400	
XH <sub>3</sub> sym. deform.	F <sub>44</sub>	0.262	0.227	0.146	
CX str.	F <sub>55</sub>	2.954	2.760	2.124	
	F <sub>13</sub>	0.091	0.094	0.094	
	F <sub>24</sub>	0.032	0.041	0.032	
	F <sub>35</sub>	-0.302	-0.183	-0.236	
	F <sub>45</sub>	-0.090	-0.131	-0.026	
	CH asym. str.	F <sub>77</sub>	5.267	5.429	5.429
	XH asym. str.	F <sub>88</sub>	2.915	2.729	2.208
	CH <sub>3</sub> asym. deform.	F <sub>99</sub>	0.468	0.477	0.477
CH <sub>3</sub> rock	F <sub>1010</sub>	0.370	0.362	0.362	
XH <sub>3</sub> asym. deform.	F <sub>1111</sub>	0.224	0.196	0.109	
XH <sub>3</sub> rock	F <sub>1212</sub>	0.248	0.228	0.145	
	F <sub>79</sub> = -F <sub>710</sub>	-0.129	-0.133	-0.133	
	F <sub>811</sub> = -F <sub>812</sub>	-0.045	-0.058	-0.044	
	F <sub>910</sub>	0.020	0.010	0.012	
	F <sub>1112</sub>	-0.023	0.010	0.010	
	F <sub>1012</sub>	0.090	0.080	0.047	

TABLE XXXII. Harmonic Vibrational Frequencies ( $\text{Cm}^{-1}$ ) of  $\text{CH}_3\text{SiH}_3$  Calculated from the "Model" Force Constants.

Description	Observed	Calculated	
		Refinement	Model
$A_1$ Symmetry Species			
CH str.	3053.9	3050.6	3021.6
SiH str.	2252.3	2249.7	2254.6
$\text{CH}_3$ deform.	1295.1	1294.3	1236.0
$\text{SiH}_3$ deform.	973.0	973.9	989.5
C Si str.	701.0	700.1	699.8
$E$ Symmetry Species			
CH str.	3138.0	3138.0	3125.0
SiH str.	2249.2	2245.0	2265.1
$\text{CH}_3$ deform.	1466.0	1465.2	1473.2
$\text{CH}_3$ rock	893.5	886.2	888.9
$\text{SiH}_3$ deform.	983.4	972.8	988.8
$\text{SiH}_3$ rock	561.0	558.2	558.2

Table XXXIII. Harmonic Vibrational Frequencies ( $\text{Cm}^{-1}$ ) of  $\text{CH}_3\text{GeH}_3$  Calculated from the "Model" Force Constants.

Description	Observed	Calculated	
		Refinement	Model
$A_1$ Symmetry Species			
CH str.	3063.1	3026.1	3064.7
GeH str.	2158.8	2162.1	2176.5
$\text{CH}_3$ deform.	1272.4	1270.7	1283.7
$\text{GeH}_3$ deform.	870.3	877.3	891.4
C-Ge str.	601.6	603.2	603.8
$E$ Symmetry Species			
CH str.	3146.3	3145.1	3173.5
Ge str.	2158.3	2159.5	2162.9
$\text{CH}_3$ deform.	1474.4	1468.1	1481.4
$\text{CH}_3$ rock	861.5	845.6	825.8
$\text{GeH}_3$ deform.	930.0	960.1	971.7
$\text{GeH}_3$ rock	522.8	516.3	513.9

Table XXXIV. Harmonic Vibrational Frequencies ( $\text{Cm}^{-1}$ ) of  $\text{CH}_3\text{SnH}_3$  Calculated from the "Model" Force Constants.

Description	Observed	Calculated	
		Refinement	Model
<b>A<sub>1</sub> Symmetry Species</b>			
CH str.	3057.6	3061.5	3063.8
SnH str.	1934.5	1945.4	1968.7
CH <sub>3</sub> deform.	1242.0	1238.3	1262.1
SnH <sub>3</sub> deform.	716.1	715.5	707.5
C-Sn str.	526.9	516.8	517.0
<b>E Symmetry Species</b>			
CH str.	3156.9	3155.3	3173.8
SnH str.	1934.5	1943.5	1939.4
CH <sub>3</sub> deform.	1480.9	1472.5	1483.6
CH <sub>3</sub> rock	795.8	809.4	813.2
SnH <sub>3</sub> deform.	754.6	723.4	711.1
SnH <sub>3</sub> rock	429.5	428.2	429.1

errors are usually associated with the degenerate vibrations because the location of the band center for these vibrations are more uncertain than the location of the band center for the nondegenerate vibrations. The errors in the assigned frequencies for the nondegenerate vibrations are usually  $5-10 \text{ cm}^{-1}$  less than the corresponding degenerate vibrations. Usually the frequencies predicted from the model should not have errors greater than the above errors in the experimental frequencies. Occasionally, when it is uncertain to which of two modes a pair of frequencies belongs, predicted frequencies with even larger uncertainties would be useful. Thus, the data in Tables XXXII to XXXIV show that most "predicted" frequencies are sufficiently accurate for making assignments of observed frequencies.

The uncertainties in the predicted frequencies are due to the uncertainties in the force constants. The uncertainties in the force constants arise from the unreliability in the equations and the errors in the bond lengths. It has been previously shown that the variation in the predictions of unknown force constants can be as high as 6%. Variations in bond length by 1% would produce a change of 2% in the force constants. This 8% uncertainty in the force constants means an uncertainty of 3-4% in the frequencies.

The applicability of "model" force constants can be demonstrated by applying the method to molecules for which the infrared spectra have been reported but for which only tentative frequency assignments have been made. Such

tentative frequency assignments have been made for methyltriethyltin,  $\text{CH}_3\text{Sn}(\text{C}_2\text{H}_5)_3$  (15), and germylsilane,  $\text{GeH}_3\text{SiH}_3$  (58). It will now be shown that the "model" force constants can be used to support these assignments.

In the case of  $\text{CH}_3\text{Sn}(\text{C}_2\text{H}_5)_3$  only the  $\text{CH}_3$  group is of interest for the present discussion. The  $\text{Sn}(\text{C}_2\text{H}_5)_3$  moiety is assumed to be a point mass. The CH bond length and HCH bond angle of the  $\text{CH}_3$  group, and the CSn bond length were assumed to be the same as in methylstannane. The force constants obtained from these parameters are listed in Table XXXV. The frequencies and the vibrational assignments for the  $\text{CH}_3\text{Sn}$  part of methyltriethyltin are also given in Table XXXV. The frequencies and tentative assignments reported by Dillard and Lawson (15) for  $\text{CH}_3\text{Sn}(\text{C}_2\text{H}_5)_3$  are also given. The calculated frequencies for the asymmetric and symmetric deformation vibrations of methyltriethyltin are in good agreement with the observed values.

This agreement allows a way to distinguish between the  $\text{CH}_3$  vibrations due to the methyl group and to those of the ethyl group attached to the tin atom. For example, the  $\text{CH}_3$  deformation vibrations of  $\text{CH}_3\text{Sn}(\text{C}_2\text{H}_5)_3$  are reported as 1490 and 1437  $\text{cm}^{-1}$  for the asymmetric vibration, and 1268 and 1225  $\text{cm}^{-1}$  for the symmetric vibration. The "model" force constants show that the bands at 1490 and 1268  $\text{cm}^{-1}$  are probably due to the vibrations of the  $\text{CH}_3$  group attached to the tin atom. Since the combined errors in the predicted and observed frequencies could easily be as high as 40  $\text{cm}^{-1}$

the case for the first assignment ( $1490\text{ cm}^{-1}$ ) is not really a very strong one. (It was previously shown that a 3-4% uncertainty in the frequencies can be expected from the uncertainties in the "model" force constants.) The band assigned to the  $\text{CH}_3$  rocking vibration at  $683\text{ cm}^{-1}$  is apparently due to the terminal methyl group and the band due to the methyl group attached to the tin atom occurs at  $742\text{ cm}^{-1}$ .

The force constants for germylsilane were determined by the procedures outlined above. Since no bond lengths or bond angles have been reported for this molecule, the structural parameters for the  $\text{SiH}_3$  and  $\text{GeH}_3$  groups were assumed to be the same as those given for the groups in  $\text{CH}_3\text{SiH}_3$  (63) and  $\text{CH}_3\text{GeH}_3$  (26), respectively. The Ge-Si bond length was estimated from the covalent radii of the Ge and Si atoms (8). Equation 85 (Table XXX) was used to calculate the Ge-Si stretching force constant. The "model" force constants for  $\text{GeH}_3\text{SiH}_3$  are shown in Table XXXVI. The calculated and observed (58) frequencies and the vibrational assignments for this molecule are also shown in Table XXXVI. There is good agreement between the calculated and observed frequencies. The "model" force constants permit the assignment of the  $\text{GeH}_3$  symmetric deformation vibration to the absorption at  $916\text{ cm}^{-1}$  and the SiH and GeH stretching vibrations to the bands at  $2263$  and  $2175\text{ cm}^{-1}$ , respectively. The assignments of the stretching vibrations are in agreement with those made by Spanier and MacDiarmid (58).

A technique commonly used in the analysis of vibra-

Table XXXV. "Model" Force Constants and Calculated Frequencies for the Methyl Group in Methyltriethyltin.

Description	Force Constants (mdyn/A)		Frequencies (cm <sup>-1</sup> )	
		F	obs.	calc.
CH sym. str.	F <sub>11</sub>	5.419		3064
CH <sub>3</sub> sym. deform.	F <sub>22</sub>	0.400	1268 1225	1304
CSn str.	F <sub>33</sub>	2.124		535
CH asym. str.	F <sub>44</sub>	5.429		3174
CH <sub>3</sub> asym. deform.	F <sub>55</sub>	0.477	1525 1490 1437	1484
CH <sub>3</sub> rock	F <sub>66</sub>	0.360	742 683	773
	F <sub>12</sub>	0.094	675	
	F <sub>23</sub>	-0.236		
	F <sub>45</sub> = -F <sub>46</sub>	-0.133		
	F <sub>56</sub>	0.012		

tional spectra is to transfer frequencies between structurally similar groups of different molecules. For example, in the analysis of the infrared spectrum of  $\text{GeH}_3\text{SiH}_3$ , the frequencies for the vibrations of the  $\text{GeH}_3$  group in  $\text{CH}_3\text{GeH}_3$  and the  $\text{SiH}$  group in  $\text{CH}_3\text{SiH}_3$  could be transferred to the corresponding vibrations of  $\text{GeH}_3\text{SiH}_3$ . The results of this study indicate, not surprisingly, that vibrational frequencies can be obtained from the "model" force constants which are in better agreement with the observed frequencies than those frequencies which would be transferred from structurally similar molecules.

This can be seen by comparing the frequencies of  $\text{CH}_3\text{SiH}_3$  (Table XXXII) and  $\text{CH}_3\text{GeH}_3$  (Table XXXIII) with those of  $\text{GeH}_3\text{SiH}_3$  (Table XXXVI). For convenience, these are listed in Table XXXVII. The comparison also shows that using the more laborious "model" method for predicting vibrational frequencies in this case gives about equally good frequency assignments as the simpler "transfer" method.

The results of this study show that the set of empirical equations relating the symmetry force constants with bond lengths may be occasionally useful in vibrational analysis for the  $\text{CH}_3\text{XH}_3$  molecules ( $\text{X} = \text{Si}, \text{Ge}, \text{Sn}$ ) and their derivatives. It could be a useful starting point for tracing the frequency changes upon isotopic substitution.

Table XXXVI. "Model" Force Constants and Calculated Frequencies for Germysilane.

Description	Force Constants (mdyn/A)		Frequencies (cm <sup>-1</sup> )	
		F	obs.	calc.
SiH sym. str.	F <sub>11</sub>	2.980	2263	3354
GeH sym. str.	F <sub>22</sub>	2.799	2175	2176
SiH <sub>3</sub> sym. deform.	F <sub>33</sub>	0.262	1005	993
GeH <sub>3</sub> sym. deform.	F <sub>44</sub>	0.227	916	891
SiGe str.	F <sub>55</sub>	1.567		344
SiH asym. str.	F <sub>77</sub>	2.915	2263	2265
GeH asym. str.	F <sub>88</sub>	2.729	2175	2163
SiH <sub>3</sub> asym. deform.	F <sub>99</sub>	0.224	995	990
SiH <sub>3</sub> rock	F <sub>1010</sub>	0.252		690
GeH <sub>3</sub> asym. deform.	F <sub>1111</sub>	0.196	965	957
GeH <sub>3</sub> rock	F <sub>1212</sub>	0.221		466
	F <sub>13</sub>	0.032		
	F <sub>24</sub>	0.041		
	F <sub>35</sub>	-0.048		
	F <sub>45</sub>	-0.074		
	F <sub>79</sub> = -F <sub>710</sub>	-0.045		
	F <sub>811</sub> = -F <sub>812</sub>	-0.058		
	F <sub>910</sub>	-0.023		
	F <sub>1112</sub>	0.010		
	F <sub>1012</sub>	0.085		

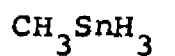
Table XXXVII. Vibrational Frequencies for Germysilane.

<u>Description</u>	<u>Frequencies (cm<sup>-1</sup>)</u>		
	<u>Transferred from CH<sub>3</sub>XH<sub>3</sub> Molecules</u>	<u>Calculated from "model" force constants</u>	<u>From Spanier and MacDiarmid (58)</u>
SiH sym. str.	2252	2254	2263
GeH sym. str.	2159	2176	2175
SiH <sub>3</sub> sym. deform.	973	993	1005
GeH <sub>3</sub> sym. deform.	870	891	916
SiH asym. str.	2249	2265	2263
GeH asym. str.	2158	2163	2175
SiH <sub>3</sub> asym. deform.	983	990	995
GeH <sub>3</sub> asym. deform.	930	957	965

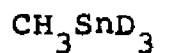
APPENDIX I

CALCULATED THERMODYNAMIC PROPERTIES OF METHYLSTANNANE

(CAL DEG<sup>-1</sup> MOLE<sup>-1</sup>)



$T(^{\circ}\text{K}):$	273.16	298.16	400	600	800	1000
	$\underline{C_p^{\circ}}$					
Translational	4.97	4.97	4.97	4.97	4.97	4.97
Rotational	2.98	2.98	2.98	2.98	2.98	2.98
Vibrational	7.24	8.27	11.91	17.36	21.26	24.10
Torsional	1.26	1.21	1.13	1.06	1.03	1.02
Total	16.45	17.43	20.99	26.37	30.24	33.07
	$\underline{(H^{\circ}-E_0^{\circ})/T}$					
Translational	4.97	4.97	4.97	4.97	4.97	4.97
Rotational	2.98	2.98	2.98	2.98	2.98	2.98
Vibrational	2.30	2.77	4.64	8.02	10.87	13.25
Torsional	1.27	1.27	1.25	1.20	1.16	1.13
Total	11.52	11.99	13.84	17.17	19.98	22.33
	$\underline{-(G^{\circ}-E_0^{\circ})/T}$					
Translational	35.25	35.68	37.14	39.16	40.59	41.70
Rotational	17.10	17.36	18.24	19.45	20.31	20.97
Vibrational	0.81	1.03	2.10	4.64	7.35	10.04
Torsional	1.75	1.87	2.25	2.83	3.18	3.43
Total	54.91	55.94	59.73	66.08	71.43	76.14
	$\underline{S^{\circ}}$					
Translational	40.22	40.65	42.11	44.13	45.56	46.67
Rotational	20.08	20.34	21.22	22.43	23.29	23.95
Vibrational	3.11	3.80	6.74	12.66	18.22	23.29
Torsional	3.02	3.14	3.50	4.03	4.34	4.56
Total	66.43	67.93	73.57	83.25	91.41	98.47



$T(^{\circ}\text{K}):$  273.16    298.16    400    600    800    1000

$\underline{C_p^{\circ}}$

Translational	4.97	4.97	4.97	4.97	4.97	4.97
Rotational	2.98	2.98	2.98	2.98	2.98	2.98
Vibrational	9.46	10.48	14.16	19.48	23.02	25.49
Torsional	1.27	1.23	1.13	1.06	1.03	1.02
Total	18.68	19.66	23.24	28.49	32.00	34.46

$\underline{(H^{\circ}-E_0^{\circ})/T}$

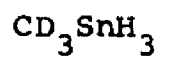
Translational	4.97	4.97	4.97	4.97	4.97	4.97
Rotational	2.98	2.98	2.98	2.98	2.98	2.98
Vibrational	3.52	4.06	6.18	9.79	12.68	15.01
Torsional	1.30	1.29	1.27	1.21	1.18	1.14
Total	12.77	13.30	15.40	18.95	21.81	24.10

$\underline{-(G^{\circ}-E_0^{\circ})/T}$

Translational	35.31	35.75	37.21	29.22	40.65	41.76
Rotational	17.81	18.07	18.95	20.16	21.01	21.68
Vibrational	1.50	1.83	3.33	6.54	9.77	12.86
Torsional	1.85	1.97	2.35	2.76	2.98	3.10
Total	56.47	57.62	61.84	68.68	74.41	79.40

$\underline{S^{\circ}}$

Translational	40.28	40.72	42.18	44.19	45.62	46.73
Rotational	20.79	21.05	21.93	23.14	23.99	24.66
Vibrational	5.02	5.89	9.51	16.33	22.45	27.87
Torsional	3.15	3.26	3.62	3.97	4.16	4.24
Total	69.24	70.92	77.24	87.63	96.22	103.50



T (°K):    273.16    298.16    400    600    800    1000

C<sub>p</sub><sup>o</sup>

Translational	4.97	4.97	4.97	4.97	4.97	4.97
Rotational	2.98	2.98	2.98	2.98	2.98	2.98
Vibrational	9.38	10.64	14.96	20.76	24.52	27.00
Torsional	1.27	1.23	1.14	1.06	1.03	1.02
Total	18.60	19.82	24.05	29.77	33.50	35.97

(H<sup>o</sup>-E<sub>o</sub><sup>o</sup>)/T

Translational	4.97	4.97	4.97	4.97	4.97	4.97
Rotational	2.98	2.98	2.98	2.98	2.98	2.98
Vibrational	3.01	3.59	5.96	10.01	13.20	15.73
Torsional	1.36	1.36	1.31	1.26	1.20	1.17
Total	12.32	12.90	15.22	19.22	22.35	24.85

-(G<sup>o</sup>-E<sub>o</sub><sup>o</sup>)/T

Translational	35.31	35.75	37.21	39.22	40.65	41.76
Rotational	17.77	18.03	18.91	20.12	20.98	21.64
Vibrational	1.07	1.36	2.75	5.96	9.30	12.52
Torsional	2.06	2.19	2.53	2.89	3.10	3.20
Total	56.21	57.33	61.40	68.19	74.03	79.12

S<sup>o</sup>

Translational	40.28	40.72	42.18	44.19	45.62	46.73
Rotational	20.75	21.01	21.89	23.10	23.96	24.62
Vibrational	4.08	4.95	8.71	15.97	22.50	28.25
Torsional	3.42	3.55	3.84	4.15	4.30	4.37
Total	68.53	70.23	76.62	87.41	96.38	103.97

APPENDIX II

TABLES OF ROTATION-VIBRATION LINES

CH asym. str. frequency,  $\nu_7$ , for  $\text{CH}_3\text{SnH}_3$  ( $\text{cm}^{-1}$ )

K	$R_{Q_K}$		$P_{Q_K}$	
	(Calc.)	(Obs.)	(Calc.)	(Obs.)
0	3006.6	3006.7		
1	3009.1	3008.9	3004.1	3004.3
2	3011.5	3010.9	3001.5	3001.9
3	3013.8	3013.3	2998.8	2999.4
4	3016.1	3015.3	2996.1	2996.0
5	3018.3	3018.1	2993.3	2993.6
6	3020.3	3020.5		
7	3022.4	3022.6		
8	3024.3			
		3025.3		
9	3026.2			
10	3028.0	3027.8		
11	3029.8	3029.9		
12	3031.5	3031.8		
13	3033.1			
14	3034.6	3034.5		
15	3036.1			
16	3037.5	3036.9		
17	3038.8	3039.0		

SnH asym. str. frequency,  $\nu_8$ , for  $\text{CH}_3\text{SnH}_3$  ( $\text{cm}^{-1}$ )

K	$R_{Q_K}$		$P_{Q_K}$	
	(Calc.)	(Obs.)	(Calc.)	(Obs.)
0	1876.0	1875.7		
1	1878.8	1878.6	1873.2	1873.0
2	1881.5	1881.8	1870.4	1870.3
3	1884.3	1884.5	1867.6	1866.7
4	1887.0	1886.8	1864.7	1864.1
5	1889.8	1889.8	1861.9	1861.8
6	1892.5	1892.4	1859.0	1858.5
7	1895.2	1894.4	1856.2	1856.1
8	1897.8	1897.7	1853.3	1853.4
9	1900.5	1900.6	1850.4	1850.3
10	1903.2	1902.6	1847.4	1846.8
11	1905.8	1905.9	1844.5	1844.0
12	1908.4	1908.7	1841.6	1841.1
13	1911.0		1838.6	1838.0
14	1913.6	1913.3	1835.6	
15	1916.2	1916.8	1832.6	1833.3
16	1918.8	1919.1		
17	1921.3			
18	1923.9	1923.5		

CH<sub>3</sub> asym. deform. frequency,  $\nu_9$ , for CH<sub>3</sub>SnH<sub>3</sub> (cm<sup>-1</sup>)

K	$R_{QK}$		$P_{QK}$	
	Calc.)	(Obs.)	(Calc.)	(Obs.)
0	1418.7	1419.5		
1	1421.7	1421.7	1415.7	1416.2
2	1424.7	1424.2	1412.7	1413.1
3	1427.6	1427.7	1409.6	1409.2
4	1430.6	1431.6	1406.6	1405.5
5	1433.5	1434.5	1403.5	1402.2
6	1436.4	1436.8	1400.4	1399.9
7	1439.3	1439.8	1397.3	
8	1442.2	1442.1	1394.2	1394.8
9	1445.1	1444.9	1391.1	1391.1
10	1448.0	1449.0		
11	1450.9	1452.5		
12	1453.8	1454.7		
13	1456.7	1456.5		

CH<sub>3</sub> rocking frequency,  $\nu_{10}$ , for CH<sub>3</sub>SnH<sub>3</sub> (Cm<sup>-1</sup>)

K	$R_{QK}$		$P_{QK}$	
	Calc.)	(Obs.)	(Calc.)	(Obs.)
0	775.1	775.3		
1	777.3	777.2	772.8	773.2
2	779.5	778.9	770.5	770.8
3	781.7	781.1	768.2	768.9
				767.5
4	783.9	783.2	765.9	765.3
		784.9		
5	786.1	787.0	763.6	763.1
6	788.2	788.8		
7	790.2	790.4		
8	792.3	792.4		
9	794.2	794.5		
10	796.2	796.5		
11	798.0	798.3		

SnH<sub>3</sub> asym. deform. frequency,  $\nu_{11}$ , for CH<sub>3</sub>SnH<sub>3</sub> (cm<sup>-1</sup>)

K	$R_{Q_K}$		$P_{Q_K}$	
	(Calc.)	(Obs.)	(Calc.)	(Obs.)
0	742.9	743.9		
1	745.9	747.0	740.0	740.4
2	748.9	749.2	737.1	737.3
3	751.9	751.9	734.2	734.8
4	754.9		731.3	731.4
5	757.9	757.3	728.4	728.3
6	761.0	760.0	725.6	725.4
7	764.2	763.1	722.8	722.2
8			720.0	720.5
9			717.2	718.0

SnH<sub>3</sub> rocking frequency,  $\nu_{12}$ , for CH<sub>3</sub>SnH<sub>3</sub> (cm<sup>-1</sup>)

K	$R_{O_K}$		$P_{O_K}$	
	(Calc.)	(Obs.)	(Calc.)	(Obs.)
0	416.8	417.0		
1	418.6	418.8	415.0	415.2
2	420.4	420.6	413.2	413.3
3	422.3	422.2	411.4	411.6
4	424.1	424.1	409.5	409.3
5	426.0	425.7	407.7	407.2
6	427.8	428.1	405.9	405.2
7	429.6	429.7	404.2	403.9
8	431.5	431.8	402.4	402.0
9	433.3	433.6	400.6	400.3
10	435.2	434.9	398.8	398.8
11	437.1	436.8	397.0	397.1
12	438.9	439.1	395.2	395.4
13			393.5	394.2
14			391.7	392.2
15			390.0	390.3

SnH asym. str. frequency,  $\nu_8$ , for  $\text{CD}_3\text{SnH}_3$  ( $\text{cm}^{-1}$ )

---

K	$R_{Q_K}$		$P_{Q_K}$	
	(Calc.)	(Obs.)	(Calc.)	(Obs.)
0	1890.1	1889.8		
1	1892.2	1891.9	1888.0	1886.6
2	1894.3	1894.0	1885.9	1884.8
3	1896.6	1897.6	1883.8	1883.0
4	1898.7	1900.0	1881.7	1880.9
5	1900.9	1902.0	1879.7	1878.5
6	1903.0	1904.5	1877.6	1876.7
7	1905.2	1906.0	1875.6	1874.2
8	1907.5	1908.2	1873.5	1872.9
9	1909.7	1910.2	1871.5	1870.5
10	1912.0	1912.3	1869.6	1869.6
11	1914.2	1914.2	1867.6	1868.0
12	1916.4	1916.8	1865.6	1866.0
13	1918.8	1920.2	1863.6	1864.9
14	1921.1	1922.6	1861.7	1863.0
15	1923.4	1924.6	1859.8	1859.6
16	1925.7	1926.1	1857.9	
17	1928.1	1928.9	1855.9	1856.5
18	1930.4	1931.1	1854.2	1854.5
19	1932.8	1933.5	1852.2	1852.9
20	1935.2		1850.4	1849.8
21	1937.6	1937.7	1848.6	
22	1939.9		1846.7	1846.7
23	1942.4	1942.2	1844.8	
24	1944.9	1944.9	1843.1	1843.2

SnH<sub>3</sub> asym. deform. frequency,  $\nu_{10}$ , for CD<sub>3</sub>SnH<sub>3</sub> (cm<sup>-1</sup>)

K	$R_{QK}$		$P_{QK}$	
	Calc.)	(Obs.)	(Calc.)	(Obs.)
0	739.5	739.3		
1	741.9	742.1	737.1	736.8
2	744.4	744.5	734.8	734.6
3	746.9	747.2	732.5	731.7
4	749.5	750.1	730.3	730.2
5	752.1	752.5	728.1	728.3
6	754.7	755.2	725.9	725.9
7	757.4	757.4	723.8	723.2
8	760.2	760.3		
9	763.0	762.3		
10	765.8	765.5		
11	768.7	768.0		
		770.2		
12	771.6	771.4		
		772.8		
13	774.6	775.2		
14	777.6	777.3		

CD<sub>3</sub> rocking frequency,  $\nu_{11}$ , for CD<sub>3</sub>SnH<sub>3</sub> (cm<sup>-1</sup>)

<u>K</u>	<u>(Calc.)</u>	<u>(Obs)</u>	<u>(Calc.)</u>	<u>(Obs.)</u>
0	628.8	628.6		
1	630.2	629.7	627.4	627.5
2	631.6	631.2	626.0	626.2
3	633.0	632.5	624.4	624.7
4	634.3	633.9	622.9	623.7
5	635.6	634.8	621.4	622.1
6	637.0	636.4	619.8	620.5
7	638.2	637.8	618.2	618.5
8	639.5	639.0	616.7	617.1
9	640.7	640.3	615.1	615.2
10	641.9	641.9		
11	643.1	643.4		
12	644.2	644.5		
13	645.3			
14	646.5	646.5		

APPENDIX III  
COMPUTER PROGRAMS

EJ

```

C      HOWARD KIMMEL.  VIBRATIONAL CONTRIBUTIONS TO THE
C      THERMODYNAMIC FUNCTIONS OF C(13)V MOLECULES.
-----
C      PX2=HEAT CAPACITY
C      QPX=HEAT CONTENT
C      QLX=FREE ENERGY
C
C      PRINT 101
101  FORMAT(34H KIMMEL.  VIB. CONTRIB. TO THE XVC. FONS./)
C      4 PRINT 121
121  FORMAT(34H TYPE IN THE NAME OF THE MOLECULE./)
C      ACCEPT 131
131  FORMAT(40H                                     /)
C      PRINT 103
103  FORMAT(27H ENTER TEMP. DATA CARDS./)
C      DIMENSION T(10), GNV(10)
C      READ 104,N
104  FORMAT(13)
C      DO 1 I=1,N
C      1 READ 105, T(I)
105  FORMAT(7./)
C      PRINT 106
106  FORMAT(27H ENTER FREQUENCY DATA CARDS./)
C      PRINT 111
111  FORMAT(/5H TEMP,AX,3H1LY,AX,3H2LY,AX,3H3LY,AX,3H4LY)
C      A=1.43884
C      B=1.9872
C      READ 107,N
107  FORMAT(13)
C      DO 8 J=1,N
C      8 READ 1-8, GNV(J)
108  FORMAT(=6.1)
C      DO 2 I=1,N
C      2 SX=0.
C      2 SLX=0.
C      2 SX2=0.
C      DO 3 J=1,N
C      3 YE=GNV(J)/T(I)
C      3 QX=SQY+Y/(EXP(Y)-1.)
C      3 SLX=SLX-LOG(1.-EXP(-Y))
C      3 SX2=SY2+Y**2+EXP(Y)/(1+EXP(Y)-1)**2)
C      PRINT 109, T(I),QX,SLX,SX2
109  FORMAT (/F7.2,3X,F9.5,3X,F9.5,3X,F9.5)
C      QPX=QX*SQY
C      QLX=QLX+SLX
C      PX2=PX2+SX2
C      2 PRINT 111, PLY,RLY,PLY2
111  FORMAT(/7H PRODS.,3X,F9.5,3X,F9.5,3X,F9.5)
C      PRINT 124
124  FORMAT(/12H END OF CASE.///)
C      PRINT 102
102  FORMAT (34H TURN ON P02 IF THERE IS MORE DATA.//)
C      PAUSE
C      IF (SENSE SWITCH 2) 4,5
C      5 STOP
C      END
-----

```

FOFI 428  
COMMENTS

WRITTEN BY W. T. THOMPSON AND C. S. SHOUP  
MODIFIED BY H. S. KIMMEL TO OPERATE ON AN  
IBM 7040 COMPUTER

FOFI 428 ADJUSTS AN INITIAL SET OF FORCE CONSTANTS UNTIL A LEAST SQUARES FIT OF THE OBSERVED FUNDAMENTAL FREQUENCIES OF A MOLECULE IS OBTAINED. FROM ONE TO THREE ISOTOPIC VERSIONS OF A GIVEN MOLECULE MAY BE RUN SIMULTANEOUSLY. THE MAXIMUM MOLECULE SIZE IS EIGHT ATOMS. THERE MAY BE NO MORE THAN EIGHT INDEPENDENT INTERACTION FORCE CONSTANTS. THE MAXIMUM NUMBER OF VARIABLE AND FIXED PRINCIPAL FORCE CONSTANTS IS SIX. ANY NUMBER OF SETS OF DATA MAY BE RUN SUCCESSIVELY.

-INPUT-

1. THE FIRST FOUR CARDS CONTAIN ALPHANUMERIC INFORMATION ABOUT THE MOLECULE TO BE USED AS A HEADING, PUNCHED IN COLUMNS 1-78
2. THE FIFTH CARD CONTAINS THE FIXED POINT NUMBERS DEFINED BELOW IN THE ORDER GIVEN IN SUCCESSIVE TWO COLUMN FIELDS BEGINNING IN COLUMN 1. ALL FIXED POINT NUMBERS MUST BE RIGHT JUSTIFIED

IN	NUMBER OF SYMMETRY COORDINATES.	COL. 1-2.
IL	NUMBER OF INTERNAL COORDINATES.	COL. 3-4.
IR	NUMBER OF CARTESIAN COORDINATES.	COL. 5-6.
IM	NUMBER OF INDEPENDENT VARIABLE PRINCIPAL FORCE CONSTANTS.	COL. 7-8.
IH	NUMBER OF INDEPENDENT VARIABLE INTERACTION FORCE CONSTANTS.	COL. 9-10.
NISP	NUMBER OF ISOTOPIC MOLECULES.	COL. 11-12.
NI	THE MAXIMUM NUMBER OF ITERATIONS TO BE ALLOWED IS EQUAL TO 8*(NI-1). IF NI = 0 THE INITIAL FREQUENCY CALCULATION AND THE STATISTICAL ANALYSIS ARE MADE AND PRINTED.	COL. 13-14.
ISCF	IF IT IS DESIRED THAT THE FORCE CONSTANT CORRECTIONS CALCULATED AT THE END OF EACH ITERATION BE SCALED DOWN BY SOME FACTOR, A NON-ZERO VALUE OF ISCF IS ENTERED. THE CORRECTIONS WILL THEN EACH BE SCALED DOWN BY A FACTOR EQUAL TO 1/ISCF BEFORE BEING APPLIED TO THE EXISTING SET OF FORCE CONSTANTS.	COL. 15-16.
IFFC	NUMBER OF FORCE CONSTANTS IN THE COLUMN WHICH ARE TO BE INVARIANT IN THE ITERATION.	COL. 17-18.
IW	ZERO IF THE WEIGHTING FACTORS IN THE VARIANCE ARE TO BE UNITY, OTHERWISE NON-ZERO.	COL. 19-20.
IB	A NON-ZERO NUMBER IF THE B MATRIX INPUT IS TO BE IN THE FORMAT PUNCHED OUT BY THE BMAT PROGRAM, OTHERWISE ZERO.	COL. 21-22.
ISYM	IF THE C MATRICES ARE TO BE ENTERED IN UNSYMMETRIZED FORM, A NON-ZERO VALUE IS ENTERED, AND THE PROGRAM WILL SYMMETRIZE THEM AND PRINT THEM OUT IN SYMMETRIZED FORM. OTHERWISE A ZERO VALUE IS ENTERED.	COL. 23-24.
IDEG	NUMBER OF COORDINATES IN THE DEGENERATE SPECIES (THE FIRST SET ONLY) IF CORIOLIS CONSTANTS ARE TO BE FITTED, OTHERWISE ZERO.	COL. 25-26.
LW	DEFINES THE METHOD OF WEIGHTING	COL. 27-28.

LW=0 W(I) ARE ALL UNITY.

LW=1 W(I) = 1/LAMBDA(I)

LW=2 W(I) = 1/((LAMBDA(I))\*\*2

LW=3 W(I) = 1/(DELTA LAMBDA)\*\*2

THE DELTA LAMBDA'S ARE DEFINED BY THE ELEMENTS OF

W(1). THE UNCERTAINTIES IN NUS (IN WAVE NUMBERS)  
AND ZETAS ARE ENTERED DIRECTLY.

NOTE THAT IF LW = 3, IW CANNOT BE ZERO.

3. THE SIXTH CARD CONTAINS THE NUMBER OF SYMMETRY SPECIES IN THE FIRST UP TO THE NISP-TH ISOTOPIC DERIVATIVE IN SUCCESSIVE TWO COLUMN FIXED-POINT FIELDS, BEGINNING IN COLUMN 1.

4. THE SEVENTH CARD CONTAINS THE DIMENSIONS OF THE SYMMETRY SPECIES OF THE FIRST ISOTOPIC DERIVATIVE IN THE ORDER IN WHICH THE SYMMETRY BLOCKS APPEAR GOING DOWN THE PRINCIPAL DIAGONAL OF THE G MATRIX. THESE NUMBERS ARE IN SUCCESSIVE TWO COLUMN FIXED POINT FIELDS, BEGINNING IN COLUMN 1.

5. IF THERE ARE MORE ISOTOPIC DERIVATIVES, CARDS SIMILAR TO THE PREVIOUS CARD ARE INCLUDED FOR EACH, IN THE PROPER ORDER.

6. THE C MATRIX IN INDEX FORM. I. E. THE VALUE OF A NON-ZERO ELEMENT OF C APPEARS IN THE FIRST TWELVE COLUMNS IN FLOATING POINT FORMAT AND IS FOLLOWED BY THE I AND J INDICES OF ALL ELEMENTS OF C WITH THAT VALUE IN SUCCESSIVE TWO-COLUMN FIXED POINT FIELDS, BEGINNING IN COLUMN 13, IN THE ORDER I, J, I, J, ETC. THERE WILL BE AS MANY CARDS AS THERE ARE DIFFERENT NON-ZERO VALUES OF MATRIX ELEMENTS. ZERO ELEMENTS NEED NOT

BE ENTERED. THE NUMBER OF C MATRICES WILL BE EQUAL TO IH+IFFC, AND A BLANK CARD MUST FOLLOW EACH. ELEMENTS OF THE C MATRICES BELOW THE PRINCIPAL DIAGONAL NEED NOT BE ENTERED EXPLICITLY. THE C MATRICES ARE USED TO CONSTRUCT THE INTERACTION TERMS OF THE F MATRIX. A GIVEN C MATRIX CONTAINS THE COEFFICIENTS IN THE F MATRIX OF THE CORRESPONDING INTERACTION CONSTANT. IN THE CASE OF FIXED FORCE CONSTANTS, IF THERE ARE MORE THAN ONE OF THEM, IT IS MORE EFFICIENT TO PUT THE VALUES OF THE CONSTANTS IN A SINGLE C MATRIX AND ENTER UNITY AS THE CORRESPONDING CONSTANT IN THE COLUMN OF INITIAL CONSTANTS. FIXED PRINCIPAL AS WELL AS FIXED INTERACTION CONSTANTS MUST ALWAYS BE ENTERED VIA THE C MATRICES RATHER

THAN THE G MATRIX.

8. THE Q MATRIX IN INDEX FORM, FOLLOWED BY A BLANK CARD. THERE MUST ALWAYS BE A Q MATRIX. IT IS USED TO ARRANGE THE PRINCIPAL VARIABLE FORCE CONSTANTS ALONG THE DIAGONAL OF THE F MATRIX, WHICH IS EQUAL TO THE COLUMN OF PRINCIPAL VARIABLE CONSTANTS MULTIPLIED ON THE LEFT BY THE Q MATRIX.

9. THE G MATRIX BY INDICES FOR EACH ISOTOPIC SPECIES. EACH G MATRIX IS TERMINATED BY A BLANK CARD.

10. OBSERVED FREQUENCIES IN SUCCESSIVE TEN-COLUMN FLOATING POINT FIELDS BEGINNING WITH COLUMN 1. UP TO SIX FREQUENCIES MAY APPEAR ON A CARD, AND THEY MUST BE ARRANGED IN DESCENDING MAGNITUDE WITHIN EACH SYMMETRY SPECIES. THE SYMMETRY SPECIES MUST BE IN THE SAME ORDER AS IN THE F AND G MATRICES. IF AN ISOTOPIC DERIVATIVE IS BEING USED, ALL THE FREQUENCIES FOR IT FOLLOW THE COMPLETE SET FOR THE NORMAL MOLECULE USING THE SAME RULES FOR ORDERING.

11. IF IW IS NON-ZERO CARDS FOR THE ALTERED WEIGHTING FACTORS COME NEXT. EACH OF THESE CARDS CONTAINS AN ALTERED WEIGHTING FACTOR IN FLOATING POINT IN COLUMNS 1-12, FOLLOWED BY TWO-COLUMN FIXED POINT NUMBERS I, J, K, ETC. BEGINNING IN COLUMN 13 AND CORRESPONDING TO THE NUMBERS OF THE FREQUENCIES IN THE COLUMN OF OBSERVED FREQUENCIES TO BE GIVEN THAT WEIGHTING FACTOR. A BLANK CARD FOLLOWS THE LAST CARD. IF IW IS ZERO, NO DATA ARE ENTERED HERE AND NO BLANK CARD.

13. THE COLUMN OF INITIAL FORCE CONSTANTS. EACH CONSTANT IS PUNCHED ON A SEPARATE CARD IN COLUMNS 1-10 IN FLOATING POINT. COLUMNS 11-34 MAY CONTAIN ALPHANUMERIC INFORMATION TO LABEL EACH CONSTANT. IN ORDERING THE FORCE CONSTANTS, THE PRINCIPAL CONSTANTS MUST COME FIRST AND IN AN ORDER CORRESPONDING

TO THE ORDER OF THE COLUMNS OF THE Q MATRIX. THE VARIABLE INTERACTION CONSTANTS FOLLOW IN AN ORDER CORRESPONDING TO THE ORDER OF THE C MATRICES. FIXED FORCE CONSTANTS COME LAST, AND THEIR ORDER MUST ALSO AGREE WITH THAT OF THEIR CORRESPONDING C MATRICES.

14. A CARD WITH A NON-ZERO FIXED POINT NUMBER PUNCHED IN COLUMNS 1-2 IF THIS IS THE LAST SET OF DATA. IF THERE ARE ADDITIONAL DATA SETS TO BE RUN, A BLANK CARD IS INCLUDED HERE.

-OUTPUT-

ALL THE INPUT DATA IS PRINTED OUT EXCEPT ITEM 14. IN ITEM 2, THE NUMBERS PRINTED HAVE LABELS WHICH OMIT THE LETTER I WHICH IS THE FIRST LETTER IN EACH VARIABLE NAME. THE C MATRICES PRINTED ARE THE SYMMETRIZED ONES WHETHER OR NOT THE INPUT C MATRICES WERE SYMMETRIZED.

G MATRIX OR MATRICES TOGETHER WITH THE DETERMINANT OF EACH BLOCK FOR USE WITH THE PRODUCT RULE.

INITIALLY AND AFTER EACH ITERATION THE F MATRIX, CALCULATED FREQUENCIES WITH THEIR OBSERVED VALUES, ERRORS AND PERCENT ERRORS,

THE AVERAGE PERCENT ERROR OVER ALL FREQUENCIES, THE FORCE CONSTANTS USED, THE FREQUENCY JACOBIAN, AND A SINGULARITY CRITERION FOR THE PRODUCT MATRIX,  $(J-TRANSPOSE)(W)(J)$ , ARE PRINTED. THIS CRITERION IS THE RATIO OF THE DETERMINANT OF THE MATRIX TO THE PRODUCT OF ITS DIAGONAL ELEMENTS. THE NEARER THE CRITERION IS TO UNITY, THE FARTHER THE MATRIX IS FROM BEING SINGULAR PROVIDED IT HAS NO DIAGONAL ELEMENTS NEARLY ZERO.

AFTER EACH SET OF EIGHT ITERATIONS, SUMMARIES OF THE FORCE CONSTANTS, CALCULATED FREQUENCIES WITH THEIR OBSERVED VALUES AND ERRORS, THE AVERAGE PERCENT ERROR, AND THE VARIANCE IS PRINTED. WHEN CONVERGENCE OCCURS OR WHEN THE MAXIMUM NUMBER OF ITERATIONS HAS BEEN REACHED, SUMMARIES AS ABOVE FOR THE LAST GROUP OF ITERATIONS ARE PRINTED, FOLLOWED BY THE L MATRICES, THE P. E. DISTRIBUTION, THE FINAL CALCULATED FREQUENCIES WITH THEIR OBSERVED VALUES, ERRORS, PERCENT ERRORS, AND DISPERSIONS, THE FINAL FORCE CONSTANTS WITH THEIR DISPERSIONS, THE VARIANCE AND AVERAGE PERCENT ERROR OVER ALL FREQUENCIES, AND THE CORRELATION MATRIX FOR FORCE CONSTANTS.

-STOPS-

DURING EXECUTION OF A GIVEN SET OF DATA, THE PROGRAM WILL STOP AND AUTOMATICALLY PROCEED TO THE NEXT SET OF DATA IF ONE OF THE FOLLOWING SITUATIONS IS ENCOUNTERED.

1. NONE OF THE CALCULATED FREQUENCIES OR CORIOLIS CONSTANTS DIFFER FROM THEIR VALUES IN THE PRECEDING ITERATION BY MORE THAN 0.01 PERCENT.
2. THE MAXIMUM NUMBER OF ITERATIONS SPECIFIED IS REACHED.
3. A NEGATIVE EIGENVALUE IS CALCULATED.
4. THE AVERAGE PERCENT ERROR EXCEEDS FIFTY PERCENT.
5. THE SINGULARITY CRITERION IS LESS THAN 0.001.

IN CASES 1 AND 2 THE FINAL RESULTS ARE PRINTED. IN CASES 3, 4, AND 5, ONLY THE CALCULATIONS FOR THOSE ITERATIONS SUCCESSFULLY COMPLETED ARE PRINTED. IN CASE 3, THE NEGATIVE EIGENVALUE IS MADE POSITIVE AND A MESSAGE IS PRINTED GIVING ITS NUMBER. IN CASE 5 THE MESSAGE - NO INVERSE EXISTS FOR THIS CASE - IS PRINTED.

\$IRJOB DECK,MAP

\$CHAIN FOFI

\$IBFTC FOFI DECK

C

C PROGRAM FOFI 428

C

DIMENSION IDENT(13,4),VOBS(18),W(18),C(6,6,8),  
1Q(6,6),DK(14),TEMP(18,14),G(6,6,3),VN(18),XI(18),  
2EL(6,6,3),H(6),F(6,6),V(18),VYR(18,8),XXX(18,8),X(18),  
3TKR(14,8),AJ(18,14),DELK(14),SUMT(2,8),AJWJ(14,14),  
4INEG(18),ELIN(6,6,3),SIGK(14),SIGV(18),  
6KIDENT(33,3),NFAC(3),ID(8,3)  
DIMENSION FLMOBS(18),FLMC(18)  
COMMON D,EL,ELIN,AJWJ,C,AJ,Q

COMMON /B1/IN,IL,IR,IM,IH,NISP,NI,ISCF,IFFC,IW,IB,ISYM,IDEG,N2,LW,  
1MPH,NUMB,ITER,NEG,MPHT,IHT,VAR/B2/VOBS,X,V/B3/VYR,TKR,XXX,SUMT/  
2B4/TEMP/B5/G/B6/XI,INEG/B7/F,H,DK/B8/IDENT,KIDENT,W,ID,NFAC/B9/  
3CZ,ZM/B10/SIGK,SIGV/B11/FLMOBS,FLMC

C

1 FORMAT(13A6)

C

C READ IDENTIFICATION

C

1002 READ 1,((IDENT(I,J),I=1,13),J=1,4)

C

CALL CHAIN(1)

CALL CHAIN(2)

CALL CHAIN(3)

C

C IS THIS THE LAST SET OF DATA

C

READ (5,2) NND

2 FORMAT(24I2)

IF (NND) 1001,1002,1001

1001 CONTINUE

C

END FOFI 428

CALL EXIT

C

C THE FOLLOWING I/O STATEMENTS ARE USED IN THE LINKS. THEY MUST  
C BE INCLUDED TO DEFINE FILES

C

READ 100,LIST

READ (5,100) LIST

PRINT 100,LIST

WRITE (6,100) LIST

100 FORMAT (I1)

END

\$ENTRY

\$LINK FIRST

\$IBFTC FIRST DECK

C

C READ IN DATA

C

DIMENSION IDENT(13,4),VOBS(18),W(18),C(6,6,8),  
1Q(6,6),DK(14),TEMP(18,14),G(6,6,3),VN(18),XI(18),  
2EL(6,6,3),H(6),F(6,6),V(18),VYR(18,8),XXX(18,8),X(18),  
3TKR(14,8),AJ(18,14),DELK(14),SUMT(2,8),AJWJ(14,14),  
4INEG(18),ELIN(6,6,3),SIGK(14),SIGV(18),  
6KIDENT(33,3),NFAC(3),ID(8,3)  
DIMENSION FLMOBS(18),FLMC(18)  
COMMON D,EL,ELIN,AJWJ,C,AJ,Q

```
COMMON /B1/IN,IL,IR,IM,IH,NISP,NI,ISCF,IFFC,IW,IB,ISYM,IDEG,N2,LW,  
1MPH,NUMB,ITER,NEG,MPHT,IHT,VAR/B2/VOBS,X,V/B3/VYR,TKR,XXX,SUMT/  
2B4/TEMP/B5/G/B6/XI,INEG/B7/F,H,DK/B8/IDENT,KIDENT,W,ID,NFAC/B9/  
3CZ,ZM/B10/SIGK,SIGV/B11/FLMOBS,FLMC
```

```
C  
C READ MATRIX DIMENSIONS AND CHECK WORDS  
C
```

```
READ2,IN,IL,IR,IM,IH,NISP,NI,ISCF,IFFC,IW,IB,ISYM,IDEG,LW,ISENT
```

```
READ 2,(NFAC(I),I=1,NISP)
```

```
DO 25 I=1,NISP
```

```
K=NFAC(I)
```

```
READ 2,(ID(J,I),J=1,K)
```

```
25 CONTINUE
```

```
2 FORMAT(24I2)
```

```
IF(NI)4,3,4
```

```
3 NII=1
```

```
GO TO 420
```

```
4 NII=NI
```

```
420 CONTINUE
```

```
IF (ISYM) 104,104,105
```

```
105 ND=IL
```

```
GO TO 106
```

```
104 ND=IN
```

```
106 IHT=IH+IFFC
```

```
IF (IHT) 801,801,800
```

```
800 DO 112 I=1,IHT
```

```
C  
C READ C MATRICES  
C
```

```
CALL READFL (TEMP,ND,ND,0)
```

```
IF (ISYM) 109,109,110
```

```
110 DO 108 J=1,IN
```

```
DO 108 K=1,IL
```

```
ELIN(J,K,2)=0.
```

```
DO 108 L=1,IL
```

```
108 ELIN(J,K,2)=ELIN(J,K,2)+ELIN(J,L,1)*TEMP(L,K)
```

```
DO 111 J=1,IN
```

```
DO 111 K=1,IN
```

```
TEMP(J,K)=0.
```

```
DO 111 L=1,IL
```

```
111 TEMP(J,K)=TEMP(J,K)+ELIN(J,L,2)*ELIN(K,L,1)
```

```
109 DO 112 J=1,IN
```

```
DO 112 K=1,IN
```

```
112 C(J,K,I)=TEMP(J,K)
```

```
C  
C READ Q MATRIX  
C
```

```
801 CALL READFL (TEMP,IN,IM,1)
```

```
DO 107 I=1,IN
```

```
DO 107 J=1,IM
```

```
107 Q(I,J)=TEMP(I,J)
```

```
DO 152 L=1,NISP
```

```
C  
C READ G MATRICES  
C
```

```
ND=IN
```

```
CALL READFL (TEMP,ND,ND,0)
```

```
DO 152 I=1,ND
```

```
DO 152 J=1,ND
```

```
152 G(I,J,L)=TEMP(I,J)
```

81 FNISP=NISP  
SCF=1./FNISP

GOTO83

82 XYZ=NISP\*ISCF  
SCF=1./XYZ

83 FLN2=SCF  
N2=NISP\*(IN+IDEG)

READ OBSERVED FREQUENCIES AND ZETA CONSTANTS

READ 111.(VOBS(I),I=1,N2)

N3=NISP\*IN

DO901I=1,N3

901 FLMOBS(I)=(VOBS(I)/1303.0)\*\*2

IF(IDEQ)915,915,916

916 KAP=N3+1

DO912I=KAP,N2

912 FLMOBS(I)=VOBS(I)

118 FORMAT (6F10.8)

915 DOBJ=1,N2

8 W(J)=1.

IF(IW)87,913,87

87 CALL READDM(VN,N2)

DO 89 I=1,N2

IF(VN(I))88,89,88

88 W(I)=VN(I)

89 CONTINUE

913 IF(LW)90,90,904

904 IF(LW-1)905,905,910

905 DO907I=1,N2

907 W(I)=W(I)\*1.0/ABS(FLMOBS(I))

GOTO90

910 IF(LW-2)906,906,908

906 DO930I=1,N2

930 W(I)=W(I)\*1.0/FLMOBS(I)\*\*2

GOTO90

908 DO909I=1,N3

IF(VN(I))920,920,921

920 W(I)=0.0

GOTO909

921 W(I)=(848904.5/(VOBS(I)\*VN(I)))\*\*2

909 CONTINUE

IF(IDEQ)90,90,918

918 DO911I=KAP,N2

IF(VN(I))925,925,926

925 W(I)=0.0

GOTO911

926 W(I)=1.0/VN(I)\*\*2

911 CONTINUE

90 CONTINUE

MPH=IM+IH

N2G=IN\*NISP

MPHT=M?H+IFFC

DO 103 I=1,N2G

103 INEG(I)=0

READ INITIAL FORCE CONSTANTS

DO 77 I=1,MPHT

77 READ 78,DK(I),(KIDENT(I,J),J=1,3)

78 FORMAT (F10.5,4A6)

C  
C LIST INPUT DATA  
C

C  
C CALL WINPI  
10 CONTINUE  
CALL CHNXIT  
END

C  
\$IBFTC READDM DECK

SUBROUTINE READDM (D,IR)

C  
C READS MASSES IN ATOMIC WEIGHT UNITS AND MODIFIED WEIGHT FACTORS  
C

DIMENSION D(33),IH(24)  
DO 1 I=1,IR

1 D(I)=0.  
2 READ (5,3) DH,(IH(I),I=1,24)  
3 FORMAT (F12.8,24I2)  
IF(DH)4,7,4  
4 DO 6 K=1,24  
IF(IH(K))5,2,5  
5 IST=IH(K)  
6 D(IST)=DH  
GO TO 2  
7 RETURN  
END

\$IBFTC READFL DECK

SUBROUTINE READFL(D,M1,M2,IX)

C  
C READS MATRICES.  
C

DIMENSION D(18,14),IH(15),JH(15)  
DO 10 I=1,M1

DO 10 J=1,M2  
10 D(I,J)=0.  
5 READ (5,1) DH,(IH(I),JH(I),I=1,15)  
1 FORMAT(E12.8,30I2)  
IF (DH)2,3,2  
2 DO 6 K=1,15  
IF (IH(K))4,5,4  
4 I=IH(K)  
J=JH(K)  
6 D(I,J)=DH  
GO TO 5  
3 IF (IX)22,23,22  
23 DO 20 I=1,M1  
DO 20 J=1,M1  
IF (I-J) 21,20,21  
21 IF(D(I,J))11,20,11  
11 D(J,I)=D(I,J)  
20 CONTINUE  
22 RETURN  
END

\$IBFTC WTEMP DECK

SUBROUTINE WTEMP (NR,NC)

C  
C PRINTS UNSYMMETRIC MATRIX(60,60)  
C

DIMENSION TEMP(18,14)  
COMMON/B4/TEMP  
INC=1  
IL=9

```

DO 1 I=1,3
IF (NC-IL) 2,2,3
2 IL=NC
3 PRINT 4,(J,J=INC,IL)
4 FORMAT (1H0,3HI/J,I7,8I13,7IH )
DO 7 J=1,NR
7 PRINT 10,J,(TEMP(J,K),K=INC,IL)
10 FORMAT (13,9F13.8)

```

```

IF (NC-IL) 5,5,6
6 INC=INC+9
1 IL=IL+9
5 RETURN
END

```

\$IBFTC WINPI DECK

SUBROUTINE WINPI

C  
C PRINTS INPUT DATA  
C

```

DIMENSION IDENT(13,4),NFAC(3),VOBS(18),w(18),C(6,6,8),
1Q(6,6),DK(14),TEMP(18,14),G(6,6,3),EL(6,6,3),M(6),F(6,6),
2V(18),X(18),AJ(18,14),AJWJ(14,14),ELIN(6,6,3),KIDENT(33,3)
3, ID(8,3)

```

```

DIMENSION FLMOBS(18),FLMC(18)
COMMON D,EL,ELIN,AJWJ,C,AJ,G
COMMON /B1/IN,IL,IR,IM,IH,NISP,NI,ISCF,IFFC,IW,IB,ISYM,IDEG,N2,LW,
1MPH,NUMB,ITER,NEG,MPHT,IHT,VAR/92/VORS,X,V/94/TEMP/B5/G/87/F,H,DK
2/B8/IDENT,KIDENT,w,IO,NFAC
COMMON /B11/FLMOBS,FLMC

```

C  
WRITE (6,1) ((IDENT(I,J), I=1,13), J=1,4)  
1 FORMAT (1H1,22X,13A6/(1H ,22X,13A6))  
PRINT 7,IN,IL,IR,IM,IH,NISP,NI,ISCF,IFFC,IW,IB,ISYM,IDEG,LW

```

7 FORMAT(1H0,4X,1HN,4X,1HL,4X,1HR,4X,1HW,4X,1HH,2X,4HNISP,
13X,2HNI,2X,3HSCF,2X,3HFFC,3X,1HW,4X,1HB,3X,3HSYM,2X,
24HIDEG,2X,2HLW/16,13I5)
PRINT 2

```

```

2 FORMAT (///70H ISOTOPE NO. FACTORS FACTOR DIMENSIONS
1 FOFI-428 )

```

```

DO 3 I=1,NISP
K=NFAC(I)
PRINT 4,I,K,(ID(J,I),J=1,K)
3 CONTINUE
4 FORMAT (/I9,I14,I15,7I3)
WRITE (6,11)

```

```

11 FORMAT (1H0,56X,5HINPUT/1H0)
PRINT 34

```

```

34 FORMAT (1H0,55X,10HG MATRICES)
DO 13 L=1,NISP
DO 14 I=1,IN
DO 14 J=1,IN

```

```

14 TEMP(I,J)=G(I,J,L)
PRINT 17,L
17 FORMAT (///59X,I2)
CALL WTEMP (IN,IN)

```

```

13 CONTINUE
DO 35 I=1,IN
DO 35 J=I,IM

```

```

35 TEMP(I,J)=Q(I,J)
WRITE (6,36)
36 FORMAT (///58X,1HQ)
CALL WTEMP(IN,IM)

```

```

IF (MPHT-IM) 56,56,55
55 PRINT 38
38 FORMAT (1H1,55X,10HC MATRICES)
DO 37 L=1,IHT
DO 39 I=1,IN
DO 39 J=1,IN
39 TEMP(I,J)=C(I,J,L)
PRINT 40,L
40 FORMAT (///59X,12)
CALL WTEMP(IN,IN)
37 CONTINUE
56 WRITE (6,48)
48 FORMAT (1H1,2H 1,9X,2HM1,12X,2HM2,12X,2HM3,12X,2HM4//)
PRINT 43
43 FORMAT (///3H 1,6X,4HVOBS,1(X,1HW,12X,1HK)
IMAX=AMAX0(N2,MPHT)
DO 44 I=1,IMAX
IF (MPHT-I) 45,46,46
46 PRINT 47,I,VOBS(I),W(I),DK(I),(KIDENT(I,J),J=1,3)
GO TO 44
45 PRINT 47,I,VOBS(I),W(I)
44 CONTINUE
47 FORMAT (13,F11.3,F13.6,F13.5,4X,4A6)
RETURN
END

```

```
SENTRY FIRST
```

```
$LINK GMAT
```

```
$IBFTC GMAT DECK
```

```
C
```

```
C CALCULATE EIGENVALUES OF G MATRICES
```

```
C
```

```
DIMENSION IDENT(13,4),VOBS(18),W(18),C(6,6,8),
```

```
IQ(6,6),DK(14),TEMP(18,14),G(6,6,3),VNT(8),XI(18),
```

```
2EL(6,6,3),H(6),F(6,6),V(18),VYR(18,8),XXX(18,8),X(18),
```

```
3TKR(14,8),AJ(18,14),DFLK(14),SUMT(2,8),AJWJ(14,14),
```

```
4INEG(18),ELIN(6,6,3),SIGK(14),SIGV(18),
```

```
6KIDENT(33,3),NFAC(3),ID(8,3)
```

```
DIMENSION FLMOBS(18),FLMC(18)
```

```
COMMON D,FL,ELIN,AJWJ,C,AJ,G
```

```
COMMON /B1/IN,IL,IR,IM,IH,NISP,NI,ISCF,IFFC,IW,IB,ISYM,IDEG,N2,LW,
```

```
1MPH,NUMB,ITER,NEG,MPHT,IHT,VAR/B2/VOBS,X,V/B3/VYR,TKR,XXX,SUMT/
```

```
2B4/TEMP/B5/G/B6/XI,INEG/B7/F,H,DK/B8/IDENT,KIDENT,W,ID,NFAC/B9/
```

```
3CZ,ZM/B10/SIGK,SIGV/B11/FLMOBS,FLMC
```

```
DO 24 I=1,N2
```

```
24 VN(I)=FLMOBS(I)
```

```
DO 33 L=1,NISP
```

```
DO 20 I=1,IN
```

```
DO 20 J=1,IN
```

```
20 TEMP(I,J)=G(I,J,L)
```

```
PRINT 500,L
```

```
600 FORMAT (17HIIISOTOPIC SPECIES,14,///55X,8HG MATRIX//)
```

```
CALL WTEMP(IN,IN)
```

```
C
```

```
C EIGENVALUES OF G MATRICES BY FACTORED SYMMETRY SPECIES
```

```
C
```

```
92 ISC = 0
```

```
DO 151 I=1,IN
```

```
DO 151 J=1,IN
```

```
AJWJ(I,J)=G(I,J,L)
```

```
151 EL(I,J,L)=0.
```

```
M=0
```

```

      N=0
      INI=IN*(L-1)
      K=NFAC(L)
      DO 32 IDX=1,K
      IF (IDX-1) 1000,26,27
26  M=1
      GOTO28
27  M=M+ID(IDX-1,L)
28  N=N+ID(IDX,L)
      LL=L
      CALL SYMAS (AJWJ,XI,ISC,INI,M,N,LL,G)
      DET=1.
      DO 29 J=M,N
      JI=J+INI
      DET=DET*XI(JI)
      DO 29 I=M,N
29  G(I,J,L)=AJWJ(I,J)*SORT(XI(JI))
32  PRINT 601,IDX,DET
601  FORMAT (///30H DETERMINANT OF G MATRIX ELOCK,I3,2H =,E14.6)
33  CONTINUE
      N2G=IN*NISP
      DO 34 J=1,N2G
34  XI(J)=1./XI(J)
      DO 555 I=1,IN
      DO 555 J=1,IN
      DO 555 L=1,NISP
555  ELIN(I,J,L)=0.
1000 CONTINUE
      CALL CHNXIT
      FND
$IBFTC WTEMP  DECK
      SUBROUTINE WTEMP (NR,NC)
C
C      PRINTS UNSYMMETRIC MATRIX(60,60)
C
      DIMENSION TEMP(18,14)
      COMMON/B4/TEMP
      INC=1
      IL=9
      DO 1 I=1,3
      IF (NC-IL) 2,2,3
2  IL=NC
3  PRINT 4,(J,J=INC,IL)
4  FORMAT (1H0,3HI/J,I7,8I13,/,1H )
      DO 7 J=1,NR
7  PRINT 10,J,(TEMP(J,K),K=INC,IL)
10  FORMAT (I3,9F13.8)
      IF (NC-IL) 5,5,6
6  INC=INC+9
1  IL=IL+9
5  RETURN
      FND
$IBFTC SYMAS  DECK
      SUBROUTINE SYMAS (A,Z,ISC,INI,MMM,NNN,L,G)
C
C      CALCULATES EIGENVECTORS AND EIGENVALUES OF FACTORED A MATRIX
C      CORRESPONDING TO G OR GF). EIGENVALUES ARE STORED IN Z AND
C      EIGENVECTORS (OF GF) ARE STORED IN D(FACTORED).
C
      DIMENSION EL(6,6,3),ELIN(6,6,3),AJWJ(14,14),C(6,
16,8),AJ(18,14),G(6,6),VORS(18),X(18),V(18),TEMP(18,14),XI(18),

```

Z(INEG(18),G(6,6,3),Z(18),A(14,14),XNIT(14,14))

DIMENSION FLMOBS(18),FLMC(18)

COMMON D,EL,ELIN,AJWJ,C,AJ,Q

COMMON /B1/IN,IL,IR,IM,IH,NISP,NI,ISCF,IFFC,IW,IB,ISYM,IDEG,N2,LW,  
IMPH,NUMB,ITER,NEG,MPHT,IHT,VAR/82/VOBS,X,V/B4/TEMP/B6/XI,INEG

COMMON /B11/FLMOBS,FLMC

LL=L

M=MMM

N=NNN

IF(ISC)1,4,1

C CHECK FOR (IXI) SPECIES

1 IF(N-M)145,142,145

142 INM=INI+M

Z(INM)=G(M,M,LL)\*A(M,M)\*G(M,M,LL)

IF (Z(INM)) 143,144,144

143 NEG=NFG+1

INEG(NEG)=INM

Z(INM)=-Z(INM)

144 FLMC(INM)=Z(INM)

X(INM)=FLMC(INM)-FLMOBS(INM)

EL(M,M,LL)=G(M,M,LL)

ELIN(M,M,LL)=1./EL(M,M,LL)

RETURN

145 DO 2 I=M,N

DO 2 J=M,N

EL(I,J,LL)=0.

DO 2 K=M,N

2 EL(I,J,LL)=EL(I,J,LL)+A(I,K)\*G(K,J,LL)

DO 3 I=M,N

DO 3 J=M,N

A(I,J)=0.

DO 3 K=M,N

3 A(I,J)=A(I,J)+G(K,I,LL)\*EL(K,J,LL)

C A IS NOW (GTRANSPOSE)(F)(G) WHERE G IS DEFINED IN MAIN PROGRAM

C AFTER STATEMENT NO. 32.

C CALCULATE EIGENVALUES -

4 IF(N-M)5,6,5

6 INM=INI+M

Z(INM)=A(M,M)

A(M,M)=1.

RETURN

5 E=0.

DO 101 I=M,N

101 E=E+ABS(A(I,I))

R=N-M+1

E=E/(5.\*R)

DO 102 I=M,N

DO 102 J=M,N

IF(I-J)103,104,103

104 XNIT(I,J)=1.

GO TO 102

103 XNIT(I,J)=0.

102 CONTINUE

105 M2=M+1

DO 106 J=M2,N

L=J-1

DO 106 I=M,L

IF (ABS(A(I,J))-F) 106,106,126

126 IF(A(I,I)-A(J,J))107,125,107

125 QX=A(I,J)

GO TO 109

```

107 QX=A(I,J)/(2.*(A(I,I)-A(J,J)))
IF (ABS(QX)-0.41421) 108,109,109
108 S=2.*QX/(1.+(QX*QX))
CO=(1.-(QX*QX))/(1.+(QX*QX))
GO TO 110
109 S=.70710678
CO=.70710678
IF(QX)111,110,110
111 S=-S
110 CC=CO*CO
SS=S*S
CS=CO*S
QX=A(I,J)*(CC-SS)+CS*(A(J,J)-A(I,I))
R=A(I,I)*CC+A(J,J)*SS+2.*CS*A(I,J)
A(J,J)=SS*A(I,I)+CC*A(J,J)-(2.*CS*A(I,J))
A(I,J)=QX
A(I,I)=R
A(J,I)=A(I,J)
DO 112 K=M,N
IF(K-I)113,114,113
113 IF(K-J)115,114,115
115 R=A(I,K)*CO+A(J,K)*S
A(J,K)=A(J,K)*CO-A(I,K)*S
A(K,J)=A(J,K)
A(I,K)=R
A(K,I)=A(I,K)
114 R=XNIT(K,I)*CO+XNIT(K,J)*S
XNIT(K,J)=XNIT(K,J)*CO-XNIT(K,I)*S
112 XNIT(K,I)=R
106 CONTINUE
DO 116 J=M2,N
L=J-1
DO 116 I=M,L
IF (ABS(A(I,J))-E) 116,116,105
116 CONTINUE
IF(E-1.0E-010)117,117,118
118 E=E/10.
GO TO 105
117 DO 119 I=M,N
INII=INI+I
Z(INII)=A(I,I)
DO 119 J=M,N
119 A(I,J)=XNIT(I,J)
IF(ISC)120,122,120
120 DO 121 I=M,N
INII=INI+I
IF (Z(INII)) 140,141,141
140 Z(INII)=-Z(INII)
NEG=NEG+1
INEG(INII)=1
141 FLMC(INII)=Z(INII)
DO 121 J=M,N
TEMP(I,J)=0
EL(I,J,LL)=0.
DO 121 K=M,N
INK=INI+K
TEMP(I,J)=TEMP(I,J)+A(K,I)*XI(INK)*G(J,K,LL)
121 EL(I,J,LL)=EL(I,J,LL)+G(I,K,LL)*A(K,J)
EL IS NOW THE MATRIX OF EIGENVECTORS OF GF.
DO 135 J=M,N
DO 135 I=M,N

```

```
      K=INI + I
      IF (I-N) 139,135,135
```

```
139 IF (FLMC(K)-FLMC(K+1)) 137,135,135
```

```
137 R=FLMC(K)
    FLMC(K)=FLMC(K+1)
    FLMC(K+1)=R
    IT=INEG(K)
    INEG(K)=INEG(K+1)
```

```
    INEG(K+1)=IT
    DO 138 L=M,N
      R=EL(L,I,LL)
      EL(L,I,LL)=EL(L,I+1,LL)
      EL(L,I+1,LL)=R
      R=TEMP(I,L)
```

```
    TEMP(I,L)=TEMP(I+1,L)
138 TEMP(I+1,L)=R
135 X(K)=FLMC(K)-FLMOBS(K)
    DO136 I=M,N
    DO136 J=M,N
136 ELIN(I,J,LL)=TEMP(I,J)
```

```
122 RETURN
```

```
    END
```

```
$ENTRY          GMAT
```

```
$LINK LAST
```

```
$IBFTC LAST    DECK
```

```
C
```

```
C DO ITERATIONS
```

```
C
```

```
    DIMENSION IDENT(13,4),VOBS(18),W(18),C(6,6,8),
    1Q(6,6),DK(14),TEMP(18,14),G(6,6,3),VN(18),XI(18),
    2EL(6,6,3),H(6),F(6,6),V(18),VYR(18,8),XXX(18,8),X(18),
    3TKR(14,8),AJ(18,14),DELK(14),SUMT(2,8),AJWJ(14,14),
```

```
4INEG(18),ELIN(6,6,3),SIGK(14),SIGV(18),
```

```
6KIDENT(33,3),NFAC(2),ID(8,3)
```

```
    DIMENSION FLMOBS(18),FLMC(18)
```

```
    COMMON D,EL,ELIN,AJWJ,C,AJ,Q
```

```
    COMMON /B1/IN,IL,IR,IM,IH,NISP,NI,ISCF,IFFC,IW,IB,ISYM,IDEG,N2,LW,
    1MPH,NUMB,ITER,NEG,MPHT,IHT,VAR/B2/VOBS,X,V/B3/VYR,TKR,XXX,SUMT/
```

```
2B4/TEMP/B5/G/B6/XI,INEG/B7/F,H,DK/B8/IDENT,KIDENT,W,ID,NFAC/B9/
```

```
3CZ,ZM/B10/SIGK,SIGV/B11/FLMOBS,FLMC
```

```
C
```

```
C START ITERATION
```

```
C
```

```
    IF (NI) 4,3,4
```

```
3 NII=1
```

```
    GO TO 5
```

```
4 NII=NI
```

```
5 ISENT=1
```

```
    ITER=-1
```

```
    ICOUNT=1
```

```
    DO72 ITERX=1,NII
```

```
    DO 70 KOUNT=1,ICOUNT
```

```
    NUMB=KOUNT
```

```
    ITER=ITER+1
```

```
    DO 35 I=1,IN
```

```
    H(I)=C.
```

```
    DO 35 J=1,IM
```

```
35 H(I)=H(I) + O(I,J)*DK(J)
```

```
    CALL FCALC1
```

```
    DO 31 I=1,IN
```

```
    DO 31 J=1,IN
```

```

31 TEMP(I,J)=F(I,J)
   IF(ITER)1000,36,37
36 WRITE (6,602)
602 FORMAT(1H1,51X,16HINITIAL F MATRIX/1H )
   GOTO38
37 WRITE (6,603) ITER
603 FORMAT(1H1,48X,22HF MATRIX FOR ITERATION,13/1H )
38 CALL WTEMP(IN,IN)
   NEG=0
   DO 30 L=1,NISP
     M=0
     N=0
     INI=IN*(L-1)
     K=NFAC(L)
     DO 45 IDX=1,K
       IF (IDX-1) 1000,40,41
40 M=M+1
     GOTO42
41 M=M+ID(IDX-1,L)
42 N=N+ID(IDX,L)
     DO 43 I=M,N
       DO 43 J=M,N
43 AJWJ(I,J)=F(I,J)
     LI=L
     CALL SYMAS (AJWJ,X,IN,INI,M,N,LL,G)
45 CONTINUE
30 CONTINUE
   IF(ISENT)931,931,932
932 WRITE (6,853) ITER
853 FORMAT(28H0EIGENVECTORS FROM ITERATION14)
   DO854K=1,NISP
   DO854I=1,IN
854 WRITE (6,855) (EL(I,J,K), J=1,IN)
855 FORMAT(1H010F11.5)
931 IF(NEG)76,46,76
76 CALL WNUOUT
   PRINT 610,NEG
610 FORMAT (1H0,13,24H NEGATIVE EIGENVALUES -/1H0)
   N2G=IN*NISP
   DO 121 I = 1,N2G
     IF (INEG(I)) 122,121,122
122 PRINT 123,I
123 FORMAT (I10)
121 CONTINUE
   GO TO 1000
46 N3=NISP*IN
   DO47I=1,N3
   VYR(I,KOUNT)=1303.0*SQRT(FLMC(I))
47 XXX(I,KOUNT)=1303.0*(SQRT(FLMC(I))-SQRT(FLMOBS(I)))
   IF(IDEG)950,950,960
960 KAP=N3+1
   DO965I=KAP,N2
   VYR(I,KOUNT)=FLMC(I)
965 XXX(I,KOUNT)=X(I)
950 DO48I=1,MPHT
48 TKR(I,KOUNT)=DK(I)
C
C   CALCULATE JACOBIAN (AJ) FROM EIGENVECTORS
C
49 DO 50 I=1,N2
   DO 50 J=1,MPHT

```

```

50 AJ(I,J)=0.
DO 51 I=1,N1SP
M=(L-1)*IN+1
N=M+IN-1
CALL EIGJAC (M,N,L)
51 CONTINUE
CALL WNUOUT (AVE)
97 DO 55 I=1,N2
Y1=0.
DO 54 J=1,MPHT
TEMP(I,J)=AJ(I,J)*DK(J)/FLMC(I)
54 Y1=Y1+ABS(TEMP(I,J))
DO 55 J=1,MPHT
55 TEMP(I,J)=TEMP(I,J)*100.0/Y1
IF(ITER)57,53,57
53 PRINT 605
605 FORMAT (////29X,29HPOTENTIAL ENERGY DISTRIBUTION,
932H - CONTRIBUTION OF K(J) TO NU(I)/1H )
CALL WTEMP(N2,MPHT)
57 DO 98 I=1,N2
DO 98 J=1,MPHT
98 TEMP(I,J)=AJ(I,J)
WRITE (6,604) ITER
604 FORMAT(1H1,47X,23HJACOBIAN FROM ITERATION,I3/1H )
CALL WTEMP(N2,MPHT)
IF(AVE-100.)201,201,200
200 WRITE (6,202)
202 FORMAT(66H CALCULATION TERMINATED BECAUSE AVERAGE ERROR EXCEEDS 1
10 PER CENT)
GO TO 1000
C
C TRANSPOSE JACOBIAN AND FORM (JTRANSPOSE)(W)(J)INVERSE AS XNIT
C
201 DO 58 I=1,N2
DO 58 J=1,MPH
58 TEMP(I,J)=W(I)*AJ(I,J)
DO 59 I=1,MPH
DO 59 J=1,MPH
AJWJ(I,J)=0.
DO 59 K=1,N2
59 AJWJ(I,J)=AJWJ(I,J)+AJ(K,I)*TEMP(K,J)
IF(ISENT)933,933,934
934 WRITE (6,856) ITER
856 FORMAT(22HOMATRIX FROM ITERATIONI4)
DO 456 I=1,MPH
456 WRITE (6,855) (AJWJ(I,J), J=1,MPH)
933 PROD=1.0
DO 119 I=1,MPH
119 PROD=PROD*AJWJ(I,I)
WRITE (6,615) PROD
615 FORMAT (1H0,46X,16HA(1,I)***A(N,N)=,E11.2)
NEROR=0
CALLINVERT(AJWJ,MPH,1.0E-03,NEROR,DET,PROD)
IF(ISENT)935,935,936
936 WRITE (6,857) ITER
857 FORMAT(30HUIVERSE MATRIX FROM ITERATIONI4)
DO 858 I=1,MPH
858 WRITE (6,855) (AJWJ(I,J), J=1,MPH)
935 CONTINUE
WRITE (6,120) PROD
120 FORMAT (1H0,46X,24HDET(A)/A(1,1)***A(N,N) =,E11.2)

```

```

      IF (NEROR) 75, 63, 75
63 DO 64 I=1, N2
      IF (ABS((FLMC(I)-VN(I))/FLMC(I))- .0001) 64, 64, 65
64 CONTINUE
      WRITE (6, 606)
606 FORMAT(1H0, 46X, 27H THIS IS THE FINAL JACCOBIAN.)
      GOTO 73
65 DO 66 I=1, N2
66 VN(I)=FLMC(I)
      DO 67 I=1, MPH
      DO 67 J=1, N2
      TEMP(J, I)=0.
      DO 67 K=1, MPH
67 TEMP(J, I)=TEMP(J, I)+AJWJ(I, K)*AJ(J, K)*W(J)
      DO 69 I=1, MPH
      DELK(I)=0.
      DO 68 J=1, N2
68 DFLK(I)=DELK(I)-TEMP(J, I)*(FLMC(J)-FLMOBS(J))
69 DK(I)=DK(I)+DFLK(I)
      IF (ISENT) 70, 70, 937
937 WRITE (6, 860) ITER
860 FORMAT(32H PARAMETER INCREMENTS, ITERATION I4)
      DO 859 I=1, MPH
859 WRITE (6, 855) DELK(I)
70 CONTINUE
      IF (NI) 991, 991, 990
990 ICOUNT=8
      ICOUNT=8
      M=ITER-NUMB+1
      CALL SUMS
      IF (ITER) 71, 72, 71
71 CALL WDKNUX(M)
72 CONTINUE
      DO 56 I=1, MPH
56 DK(I)=DK(I)-DELK(I)
      VAR=SUMT(2, NUMB)
      CALL STAT
991 WRITE (6, 607)
607 FORMAT (777710X, 29HDID NOT CONVERGE.....)
      GOTO 1000
73 CALL SUMS
      M=ITER-NUMB+1
      CALL WDKNUX(M)
      VAR=SUMT(2, NUMB)
      CALL STAT
74 WRITE (6, 608)
608 FORMAT (777710X, 29HEND OF CASE.....)
      GOTO 1000
75 WRITE (6, 609)
609 FORMAT(32H NO INVERSE EXISTS FOR THIS CASE)
1000 CONTINUE
      CALL CHNXIT
      END
$IBFTC SUMS DECK
      SUBROUTINE SUMS
C
C CALCULATES AVERAGE PER CENT ERROR AND VARIANCE
C
      DIMENSION VOBS(18), X(18), V(18), VYR(18, 8), XXX(18, 8), TKR(14, 8),
      1SUMT(2, 8), IDENT(13, 4), KIDENT(33, 3), W(18), ID(8, 3), NFAC(3)
      DIMENSION FIMOBS(18), FLMC(18)

```

```
COMMON /B1/IN,IL,IR,IM,IH,NISP,NI,ISCF,IFFC,IW,IB,ISYM,IDEG,N2,LW,  
1MPH,NUMB,ITER,NEG,MPHT,IHT,VAR/R2/VOBS,X,V/B3/VYR,TKR,XXX,SUMT
```

```
2/B8/IDENT,KIDENT,W,ID,NFAC
```

```
COMMON /B11/FLMOBS,FLMC
```

```
N3=NISP*IN
```

```
KAP=N3+1
```

```
XN=N2
```

```
DO 1 I=1,NUMB
```

```
SUM1=0.
```

```
SUM2=0.
```

```
DO 2 J=1,N3
```

```
SUM1=SUM1+ABS(XXX(J,I)/VOBS(J))
```

```
2 SUM2=SUM2+W(J)*((VYR(J,I)**2-VOPS(J)**2)/1303.0**2)**2
```

```
IF(IDEG)5,5,4
```

```
4 DO3J=KAP,N2
```

```
SUM1=SUM1+ABS(XXX(J,I)/VOBS(J))
```

```
3 SUM2=SUM2+W(J)*XXX(J,I)**2
```

```
5 SUMT(1,I)=SUM1*100./XN
```

```
1 SUMT(2,I)=SUM2
```

```
RETURN
```

```
END
```

```
$IBFTC INVERT DECK
```

```
SUBROUTINE INVERT(A,N,EPS,NEROR,DELTA,PRODI)
```

```
C MATRIX INVERSION BY GAUSS-JORDAN ELIMINATION
```

```
DIMENSION A(14,14),B(14),C(14),LZ(14)
```

```
DELTA=.0
```

```
NEROR=0
```

```
DO 10 J=1,N
```

```
10 LZ(J)=J
```

```
DO 20 I=1,N
```

```
K=I
```

```
Y=A(I,I)
```

```
L=I-1
```

```
LP=I+1
```

```
IF(N-LP)14,11,11
```

```
11 DO 13 J=LP,N
```

```
W=A(I,J)
```

```
IF (ABS(W)-ABS(Y)) 13,13,12
```

```
12 K=J
```

```
Y=W
```

```
13 CONTINUE
```

```
14 DELTA=DELTA*Y
```

```
DO 15 J=1,N
```

```
C(J)=A(J,K)
```

```
A(J,K)=A(J,I)
```

```
A(J,I)=-C(J)/Y
```

```
A(I,J)=A(I,J)/Y
```

```
15 B(J)=A(I,J)
```

```
A(I,I)=1.0/Y
```

```
J=LZ(I)
```

```
LZ(I)=LZ(K)
```

```
LZ(K)=J
```

```
DO 19 K=1,N
```

```
IF(I-K)16,19,16
```

```
16 DO 18 J=1,N
```

```
IF(I-J)17,18,17
```

```
17 A(K,J)=A(K,J)-B(J)*C(K)
```

```
18 CONTINUE
```

```
19 CONTINUE
```

```
20 CONTINUE
```

```
WRITE (4,11) DELTA
```

```

1 FORMAT (1H0,46X,7HDET(A)=,E11.2)
  PROD=DELTA/PROD
  WRITE (6,120) PROD
120 FORMAT (1H0,46X,24HDET(A)/A(1,1)***A(N,N) =,E11.2)
  IF (ABS(PROD)-EPS) 80,80,81
 80 NEROR=1
  GO TO 82
 81 DO 200 I=1,N
    IF(I-LZ(I))100,200,100
 100 K=I+1
    IF(I-N)800,200,200
 800 DO 500 J=K,N
    IF(I-LZ(J))500,600,500
 600 M=LZ(I)
    LZ(I)=LZ(J)
    LZ(J)=M
    DELTA=-DELTA
    DO 700 L=1,N
    C(L)=A(I,L)
    A(I,L)=A(J,L)
 700 A(J,L)=C(L)
 500 CONTINUE
 200 CONTINUE
 82 RETURN
  END

```

```

$IBFTC FCALCI DECK
  SUBROUTINE FCALCI

```

```

  C
  C   CALCULATES F MATRIX FROM Q, DK, AND C MATRICES
  C
  DIMENSION F(6,6),H(6),Q(6,6),C(6,6,6),
  1EL(6,6,3),ELIN(6,6,3),AJ(18,14),AJWJ(14,14),DK(14)
  COMMON D,EL,ELIN,AJWJ,C,AJ,G
  COMMON /B1/IN,IL,IR,IM,IH,NISP,NI,ISCF,IFFC,IW,IB,ISYM,IDEG,N2,LW,
  IMPH,NUMB,ITER,NEG,MPHT,IHT,VAR/B7/F,H,DK
  DO 6 I=1,IN
  DO 6 J=1,IN
  F(I,J)=0.
  IF(I-J)2,1,2
  1 F(I,J)=F(I,J)+H(J)
  2 IF (MPHT-IM) 6,6,7
  7 DO 3 K=1,I,IT
  IMK=IM+K
  3 F(I,J)=F(I,J)+C(I,J,K)*DK(IMK)
  6 CONTINUE
  RETURN
  END

```

```

$IBFTC WTEMP DECK
  SUBROUTINE WTEMP (NR,NC)

```

```

  C
  C   PRINTS UNSYMMETRIC MATRIX(60,60)
  C
  DIMENSION TEMP(18,14)
  COMMON/B4/TEMP
  INC=1
  IL=9
  DO 1 I=1,3
  IF (NC-IL) 2,2,3
  2 IL=NC
  3 PRINT 4,(J,J=INC,IL)
  4 FORMAT (1H0,3HI/J,17,8I13,/1H )

```

```
DO 7 J=1,NR
7 PRINT 10,J,(TEMP(J,K),K=INC,IL)
10 FORMAT (13,9F13.8)
IF (NC-IL) 5,5,6
6 INC=INC+9
1 IL=IL+9
5 RETURN
END
```

```
$IBFTC WNUX DECK
SUBROUTINE WNUX(A,SUMT,M,KC)
```

```
C
C PRINTS NU AND X COLUMNS AFTER EACH SET OF EIGHT ITERATIONS
C
```

```
DIMENSION A(18,8),SUMT(2,8),VOBS(18),X(18),V(18)
```

```
DIMENSION FLMOBS(18),FLMC(18)
```

```
COMMON /B1/IN,IL,IR,IM,IH,NISP,NI,ISCF,IFFC,IW,IB,ISYM,IDEG,N2,LW,
1MPH,NUMB,ITER,NEG,MPHT,IHT,VAR/B2/VOBS,X,V
```

```
COMMON /B11/FLMOBS,FLMC
```

```
JD=0
```

```
WRITE (6,1) (JJJ, JJJ=M,ITER), JD
```

```
1 FORMAT(1H0,111,8113/1H )
```

```
DO 3 JD=1,N2
```

```
4 PRINT 2,JD,(A(JD,K),K=1,NUMB),VOBS(JD)
```

```
3 CONTINUE
```

```
2 FORMAT(1H ,12,9F13.5)
```

```
IF(KC)9,10,9
```

```
9 WRITE (6,11)
```

```
11 FORMAT(1H0,45X,27HPER CENT ERROR AND VARIANCE)
```

```
DO 12 JD=1,2
```

```
12 WRITE (6,16) JD, (SUMT(JD,K), K=1,NUMB)
```

```
16 FORMAT(1H ,12,8F13.7)
```

```
10 RETURN
```

```
END
```

```
$IBFTC WDKNUX DECK
SUBROUTINE WDKNUX(M)
```

```
C
C PRINTS K, NU, AND X COLUMNS AFTER EACH SET OF EIGHT ITERATIONS.
C CALLS SUBROUTINES WDK, AND WNUX
```

```
DIMENSION VYR(18,8),XXX(18,8),TKR(14,8),SUMT(2,8)
```

```
COMMON /B1/IN,IL,IR,IM,IH,NISP,NI,ISCF,IFFC,IW,IB,ISYM,IDEG,N2,LW,
1MPH,NUMB,ITER,NEG,MPHT,IHT,VAR/B3/VYR,TKR,XXX,SUMT
```

```
WRITE (6,449) M, ITER
```

```
449 FORMAT(1H1,39X,25HK COLUMNS FROM ITERATIONS,13,8H THROUGH,13)
```

```
CALL WDK(M)
```

```
WRITE (6,450) M, ITER
```

```
450 FORMAT (////34X,19HNUS FROM ITERATIONS,13,8H THROUGH,13,
917H PLUS NU OBSERVED)
```

```
KC=0
```

```
CALL WNUX(VYR,SUMT,M,KC)
```

```
WRITE (6,451) M, ITER
```

```
451 FORMAT (////18X,45HX(NU CALC. - NU OBS.) COLUMNS FROM ITERATIONS,
913,8H THROUGH,13,24H FOLLOWED BY NU OBSERVED)
```

```
KC=1
```

```
CALL WNUX(XXX,SUMT,M,KC)
```

```
RETURN
```

```
END
```

```
$IBFTC WDK DECK
SUBROUTINE WDK(M)
```

```
C
C PRINTS K COLUMNS AFTER EACH SET OF EIGHT ITERATIONS
```

C

DIMENSION VYR(18,8),XXX(18,8),TKR(14,8),SUMT(2,8)

COMMON /B1/IN,IL,IR,IM,IH,NISP,NI,ISCF,IFFC,IW,IB,ISYM,IDEG,N2,LW,  
1MPH,NUMB,ITER,NEG,MPHT,IHT,VAR/B3/VYR,TKR,XXX,SUMT

WRITE (6,1) (J, J=M,ITER)

WRITE (6,4)

DO 3 JD=1,MPHT

3 WRITE (6,2) JD, (TKR(JD,K), K=1,NUMB)

1 FORMAT(1H0,I11,7I14)

2 FORMAT(1H ,12,8F14.7)

4 FORMAT(1H )

RETURN

END

SIBFTC SYMAS DECK

SUBROUTINE SYMAS (A,Z,ISC,INI,MMM,NNN,L,G)

C

C

C

C

C

CALCULATES EIGENVECTORS AND EIGENVALUES OF FACTORED A MATRIX  
(CORRESPONDING TO G OR GF). EIGENVALUES ARE STORED IN Z AND  
EIGENVECTORS (OF GF) ARE STORED IN D(FACTORED).

DIMENSION EL(6,6,3),ELIN(6,6,3),AJWJ(14,14),C(6,  
16,8),AJ(18,14),G(6,6),VOBS(18),X(18),V(18),TEMP(18,14),XI(18),  
2INEG(13),G(6,6,3),Z(18),A(14,14),XNIT(14,14)

DIMENSION FLMOBS(18),FLMC(18)

COMMON D,EL,ELIN,AJWJ,C,AJ,G

COMMON /B1/IN,IL,IR,IM,IH,NISP,NI,ISCF,IFFC,IW,IB,ISYM,IDEG,N2,LW,  
1MPH,NUMB,ITER,NEG,MPHT,IHT,VAR/B2/VOBS,X,V/B4/TEMP/B6/XI,INEG

COMMON /B11/FLMOBS,FLMC

LL=L

M=MMM

N=NNN

IF(ISC)1,4,1

C

CHECK FOR (1X1) SPECIES

1 IF(N-M)145,142,145

142 INM=INI+M

Z(INM)=G(M,M,LL)\*A(M,M)\*G(M,M,LL)

IF (Z(INM)) 143,144,144

143 NEG=NEG+1

INEG(NEG)=INM

Z(INM)=-Z(INM)

144 FLMC(INM)=Z(INM)

X(INM)=FLMC(INM)-FLMOBS(INM)

EL(M,M,LL)=G(M,M,LL)

ELIN(M,M,LL)=1./EL(M,M,LL)

RETURN

145 DO 2 I=M,N

DO 2 J=M,N

EL(I,J,LL)=0.

DO 2 K=M,N

2 EL(I,J,LL)=EL(I,J,LL)+A(I,K)\*G(K,J,LL)

DO 3 I=M,N

DO 3 J=M,N

A(I,J)=0.

DO 3 K=M,N

3 A(I,J)=A(I,J)+G(K,I,LL)\*EL(K,J,LL)

C

A IS NOW (GTRANSPOSE)(F)(G) WHERE G IS DEFINED IN MAIN PROGRAM

C

AFTER STATEMENT NO. 32.

C

CALCULATE EIGENVALUES -

4 IF(N-M)5,6,5

6 INM=INI+M

Z(INM)=A(M,M)

```

A(M,M)=1.
RETURN
5 E=0.
DO 101 I=M,N
101 F=E+ABS(A(I,I))
R=N-M+1
E=E/(5.*R)
DO 102 I=M,N
DO 102 J=M,N
IF(I-J)103,104,103
104 XNIT(I,J)=1.
GO TO 102
103 XNIT(I,J)=0.
102 CONTINUE
105 M2=M+1
DO 106 J=M2,N
L=J-1
DO 106 I=M,L
IF (ABS(A(I,J))-E) 106,106,126
126 IF(A(I,I)-A(J,J))107,125,107
125 QX=A(I,J)
GO TO 109
107 QX=A(I,J)/(2.*(A(I,I)-A(J,J)))
IF (ABS(QX)-0.41421) 108,109,109
108 S=2.*QX/(1.+(QX*QX))
CO=(1.-(QX*QX))/(1.+(QX*QX))
GO TO 110
109 S=-.70710678
CO=.70710678
IF(QX)111,110,110
111 S=-S
110 CC=CO*CO
SS=S*S
CS=CO*S
QX=A(I,J)*(CC-SS)+CS*(A(J,J)-A(I,I))
R=A(I,I)*CC+A(J,J)*SS+2.*CS*A(I,J)
A(J,J)=SS*A(I,I)+CC*A(J,J)-(2.*CS*A(I,J))
A(I,J)=QX
A(I,I)=R
A(J,I)=A(I,J)
DO 112 K=M,N
IF(K-I)113,114,113
113 IF(K-J)115,114,115
115 R=A(I,K)*CO+A(J,K)*S
A(J,K)=A(J,K)*CO-A(I,K)*S
A(K,J)=A(J,K)
A(I,K)=R
A(K,I)=A(I,K)
114 R=XNIT(K,I)*CC+XNIT(K,J)*S
XNIT(K,J)=XNIT(K,J)*CO-XNIT(K,I)*S
112 XNIT(K,I)=R
106 CONTINUE
DO 116 J=M2,N
L=J-1
DO 116 I=M,L
IF (ABS(A(I,J))-E) 116,116,105
116 CONTINUE
IF(E-1.0E-010)117,117,118
118 E=E/10.
GO TO 105
117 DO 119 I=M,N

```

```

      INII=INI+I
      Z(INII)=A(I,I)
      DO 119 J=M,N
119  A(I,J)=XNIT(I,J)
      IF(ISC)120,122,120
120  DO 121 I=M,N
      INII=INI+I
      IF (Z(INII)) 140,141,141
140  Z(INII)=-Z(INII)
      NEG=NEG+1
      INEG(INII)=1
141  FLMC(INII)=Z(INII)
      DO 121 J=M,N
      TEMP(I,J)=0
      EL(I,J,LL)=0.
      DO 121 K=M,N
      INK=INI+K
      TEMP(I,J)=TEMP(I,J)+A(K,I)*XI(INK)*G(J,K,LL)
121  EL(I,J,LL)=EL(I,J,LL)+G(I,K,LL)*A(K,J)
      C  EL IS NOW THE MATRIX OF EIGENVECTORS OF GF.
      DO 135 J=M,N
      DO 135 I=M,N
      K=INI + I
      IF (I-N) 139,135,135
139  IF (FLMC(K)-FLMC(K+1))137,135,135
137  R=FLMC(K)
      FLMC(K)=FLMC(K+1)
      FLMC(K+1)=R
      IT=INEG(K)
      INEG(K)=INEG(K+1)
      INEG(K+1)=IT
      DO 138 L=M,N
      R=EL(L,I,LL)
      EL(L,I,LL)=EL(L,I+1,LL)
      EL(L,I+1,LL)=R
      R=TEMP(I,L)
      TEMP(I,L)=TEMP(I+1,L)
138  TEMP(I+1,L)=R
135  X(K)=FLMC(K)-FLMOBS(K)
      DO136 I=M,N
      DO136 J=M,N
136  ELIN(I,J,LL)=TEMP(I,J)
      WRITE (6,200) ITER
200  FORMAT (26HELIN MATRIX FROM ITERATION, I4)
      DO 201 I=M,N
201  WRITE (6,202) (ELIN(I,J,LL), J=M,N)
202  FORMAT (1H0,10F11.5)
122  RETURN
      END
      $IBFTC WNUOUT DECK
      SUBROUTINE WNUOUT (AVE)
      C
      C  WRITES NU OBS., NU CALC., X, PCT. ERROR, K AFTER EACH ITERATION
      C
      DIMENSION VOPS(18),X(18),V(18),F(6,6),H(6),DK(14),
1 IDENT(13,4),KIDENT(33,3),W(18),ID(8,3),NFAC(3)
      DIMENSION FLMOBS(18),FLMC(18)
      COMMON /B1/IN,IL,IR,IM,IH,NISP,NI,ISCF,IFFC,IW,IB,ISYM,IDEG,N2,LW
1 MPH,NUMB,ITER,NEG,MPHT,IHT,VAR/B2/VOBS,X,V/B7/F,H,DK/B8/IDENT,
2 KIDENT,W,ID,NFAC
      COMMON /B11/FLMOBS,FLMC

```

```

N3=NISP*IN
DO10I=1,N3
V(I)=1303.0*SQRT(FLMC(I))
10 X(I)=1303.0*(SQRT(FLMC(I))-SQRT(FLMOBS(I)))
N4=N3+1
DO11I=N4,N2
11 V(I)=FLMC(I)
WRITE (6,1) ITER
1 FORMAT (///35X,16HITERATION NUMBER,13)
WRITE (6,2)
2 FORMAT(1H0,3HNO.,3X,7HNU OBS.,7X,8HNU CALC.,5X,8HDELTA NU,
94X,10HPCT. ERROR,12X,3HNO.,5X,1HK/1H )
AVE=0.
DO 3 I=1,MPHT
PCT=X(I)*100./VOBS(I)
PRINT 4,I,VOBS(I),V(I),X(I),PCT,I,PK(I),(KIDFNT(I,J),J=1,3)
3 AVE=AVE+ABS(PCT)
4 FORMAT (1H ,12,F13.3,3F13.5,12X,12,F13.7,2X,4A6)
IF (N2-MPHT) 7,7,5
5 II=MPHT+1
DO 6 I=II,N2
PCT=X(I)*100./VOBS(I)
WRITE (6,4) I, VOBS(I), V(I), X(I), PCT
6 AVE=AVE+ABS(PCT)
7 FN2=N2
AVE=AVE/FN2
WRITE (6,8) AVE
8 FORMAT(1H0,15HAVERAGE ERROR =,F10.5,9H PER CENT)
RETURN
END
$IBFTC EIGJAC DECK
SUBROUTINE EIGJAC (II,IE,L)
C
C CALCULATES FREQUENCY JACOBIAN FROM EIGENVECTORS
C
DIMENSION EL(6,6,3),ELIN(6,6,3),AJWJ(14,14),
1C(6,6,8),AJ(18,14),Q(6,6),VOBS(18),X(18),V(18)
DIMENSION FLMOBS(18),FLMC(18)
COMMON D,EL,ELIN,AJWJ,C,AJ,Q
COMMON /B1/IN,IL,IR,IM,IH,NISP,NI,ISCF,IFFC,IW,IB,ISYM,IDEG,N2,LW,
1MPH,NUMB,ITER,NEG,MPHT,IHT,VAR/32/VOBS,X,V
COMMON /B11/FLMOBS,FLMC
IG=0
DO 2 I=II,IE
IG=IG+1
DO 2 J=1,IM
DO 2 K=1,IN
2 AJ(I,J)=AJ(I,J)+EL(K,IG,L)*EL(K,IG,L)*Q(K,J)
IF(MPHT-IM)1000,1000,3
3 IG=0
DO 9 I=II,IE
IG=IG+1
DO 9 K=1,IN
DO 9 IP=1,IN
DO 9 J=1,IHT
IMJ=IM+J
9 AJ(I,IMJ)=AJ(I,IMJ)+EL(K,IG,L)*EL(IP,IG,L)*C(K,IP,J)
1000 RETURN
END
$IRFTC STAT DECK
SUBROUTINE STAT

```

C  
C  
C  
CALCULATES AND PRINTS STATISTICAL ANALYSIS OF FINAL RESULTS

C  
C  
C  
DIMENSION FL(6,6,3),ELIN(6,6,3),C(6,6,8),  
1AJWJ(14,14),AJ(18,14),Q(6,6),VOBS(18),X(18),V(18),TEMP(18,14),  
2F(6,6),H(6),DK(14),IDENT(13,4),KIDENT(33,3),W(18),  
3ID(8,3),NFAC(3),SIGK(14),SIGV(18)  
DIMENSION FLMOBS(18),FLMC(18)

C  
C  
C  
DIMENSION VYR(18,8),TKR(14,8),XXX(18,8),SUMT(2,8)  
COMMON D,EL,ELIN,AJWJ,C,AJ,Q  
COMMON /B1/IN,IL,IR,IM,IH,NISP,NI,ISCF,IFFC,IW,IB,ISYM,IDEG,N2,LW,  
1MPH,NUMB,ITER,NEG,MPHT,IHT,VAR/B2/VOBS,X,V/B4/TEMP/B7/F,H,DK  
2/B8/IDENT,KIDENT,W,ID,NFAC/B10/SIGK,SIGV  
COMMON /B11/FLMOBS,FLMC  
COMMON /B3/VYR,TKR,XXX,SUMT

C  
C  
C  
PRINT EIGENVECTORS

C  
C  
C  
PRINT 15  
15 FORMAT (1H1,54X,10HL MATRICES)

C  
C  
C  
DO 1 L=1,NISP  
PRINT 2,L  
2 FORMAT (///59X,I2)  
DO 3 I=1,IN  
DO 3 J=1,IN  
3 TEMP(I,J)=EL(I,J,L)

C  
C  
C  
CALL WTEMP(IN,IN)  
1 CONTINUE

C  
C  
C  
POTENTIAL ENERGY DISTRIBUTION

C  
C  
C  
18 DO 24 I=1,N2  
Y1=0.  
DO 23 J=1,MPHT  
TEMP(I,J)=AJ(I,J)\*DK(J)/FLMC(I)  
23 Y1=Y1+ABS(TEMP(I,J))  
DO 24 J=1,MPHT  
24 TEMP(I,J)=TEMP(I,J)\*100./Y1

C  
C  
C  
WRITE (6,25)  
25 FORMAT(1H1,29X,44HPOTENTIAL ENERGY DISTRIBUTION - CONTRIBUTION,  
117H OF K(J) TO NU(I)/1H )  
CALL WTEMP(N2,MPHT)

C  
C  
C  
OVERALL DISPERSION(SIGMA) AND DISPERSIONS FOR FORCE CONSTANTS  
AND FREQUENCIES

C  
C  
C  
SIGMA=VAR  
DIF=N2-MPHT  
IF(DIF)26,26,27  
26 DIF=1.0  
27 SIGSQ=SIGMA/DIF  
SIGMA=SQRT(SIGSQ)  
DO 28 I=1,MPH  
28 SIGK(I)=SIGMA\*SQRT(AJWJ(I,I))  
DO 29 I=1,N2  
DO 29 J=1,MPH  
TEMP(I,J)=0.  
DO 29 K=1,MPH  
29 TEMP(I,J)=TEMP(I,J)+AJ(I,K)\*AJWJ(K,J)  
DO 31 I=1,N2  
Y1=0.

```
DO 30 K=1,MPH
30 Y1=Y1+TEMP(I,K)*AJ(I,K)
31 SIGV(I)=SIGMA*SQRT(Y1)
N3=NISP*IN
D050I=1,N3
50 SIGV(I)=848904.5/VYR(I,NUMB)*SIGV(I)
```

```
C
C PRINT FINAL FREQUENCIES, FORCE CONSTANTS, AND DISPERSIONS
C
```

```
32 WRITE (6,33)
33 FORMAT (///3HNO.,2X,7HNU OBS.,6X,8HNU CALC.,7X,8HDELTA NU,
94X,10HPCT. ERROR,4X,9HSIGMA(NU),6X,1HK,10X,8HSIGMA(K)/1H )
AVE=0.
DO 37 I=1,N2
```

```
DIF=(X(I)/VOBS(I))*100.
AVE=AVE+ABS(DIF)
IF (I-MPHT) 34,34,36
34 WRITE (6,35) I, VOBS(I), V(I), X(I), DIF, SIGV(I),
9DK(I),SIGK(I),(KIDENT(I,J),J=1,3)
GO TO 37
```

```
35 FORMAT (1H ,I2,F10.3,F16.7,3F13.5,4X,F10.7,F11.5,1X,4A6)
36 WRITE (6,35) I, VOBS(I), V(I), X(I), DIF, SIGV(I)
37 CONTINUE
```

```
FN2=N2
AVE=AVE/FN2
WRITE (6,38) SIGMA, AVE
38 FORMAT(1H0,20X,30HSQRT(SUM(I*(O-C)**2)/(NO-NV))=F10.6,10X,
925HAVERAGE PER CENT ERROR = ,F10.6)
```

```
C
C CORRELATION MATRICES
C
```

```
WRITE (6,39)
39 FORMAT(1H1,40X,38HCORRELATION MATRIX FOR FORCE CONSTANTS/1H )
DO 40 I=1,MPH
DO 40 J=1,MPH
40 TEMP(I,J)=AJWJ(I,J)*SIGSQ/(SIGK(I)*SIGK(J))
CALL WTFMP(MPH,MPH)
RETURN
```

```
END
SENTRY LAST
SENDCH
```

```

C CORIOLIS COEFFICIENTS PROGRAM
C INVERTS THE L VECTOR MATRIX AND THEN CALCULATES THE CORIOLIS
C COEFFICIENTS.
C DATA INPUT
C FIRST CARD CONTAINS N, THE ORDER OF THE MATRIX, AS A THREE
C DIGIT NUMBER.
C THE NEXT (N**2) CARDS CONTAINS THE ELEMENTS OF THE L-MATRIX
C (ONE ELEMENT PER CARD) USING THE FOLLOWING FORMAT
C COL. 1-3 I,
C COL. 4, BLANK SPACE,
C COL. 5-7 J,
C COL. 8-10 BLANK SPACES,
C COL. 11-22 MATRIX ELEMENT AS A FLOATING POINT NUMBER.
C INON AS A THREE DIGIT NUMBER
C SET INON=01 IF INVERTED MATRIX IS DESIRED IN OUTPUT.
C OTHERWISE SET INON=00.
C THE NEXT (N*(N+1)/2) CARDS CONTAINS THE ELEMENTS OF THE C-MAT
C USING THE SAME FORMAT AS FOR THE L-MATRIX.
C ANY NUMBER OF SETS OF DAT MAY BE RUN SUCCESSIVELY.
C THE LAST CARD OF THE LAST SET OF DATA HAS 000 IN COL. 1-3.

```

```

C DIMENSION A(6,6),B(6),C(6),LZ(6)
C DIMENSION CZ(6,6),TEMP(6,6),ZM(6,6),FLMC(6)
1 READ 101,N
101 FORMAT (I3)
IF (N) 99,99,2
2 KMAX=N**2
DO 3 K=1,KMAX
READ 102,I,J,A(I,J)
102 FORMAT (I3,1X,I3,3X,F12.8)
3 CONTINUE
READ 500,INON
500 FORMAT (I2)
202 LMAX=(N*(N+1))/2
DO 203 L=1,LMAX
READ 102,I,J,CZ(I,J)
203 CONTINUE
DO 230 I=1,N
DO 230 J=1,N
230 CZ(J,I)=CZ(I,J)
299 PRINT 300
300 FORMAT (25HTYPE IN NAME OF MOLECULE.//)
ACCEPT 301
301 FORMAT (40H /)
PRINT 501
PUNCH 501
501 FORMAT (/12H INPUT DATA.//)
298 PUNCH 502
PRINT 502
502 FORMAT (24H L MATRIX AND CZ MATRIX.)
PUNCH 304
304 FORMAT (///39H I J A(I,J) CZ(I,J))
DO 204 I=1,N
DO 204 J=1,N
PUNCH 305,I,J,A(I,J),CZ(I,J)
305 FORMAT (/I3,1X,I3,3X,E15.8,3X,E15.8)
204 CONTINUE
296 PUNCH 103,N
PRINT 103,N

```

```

103 FORMAT (//28HINVERSION OF MATRIX OF ORDER,13,4H FOR)
PRINT 301
PUNCH 301
C MATRIX INVERSION BY GAUSS-JORDAN ELIMINATION
DELTA=1.0
DO 10 J=1,N
10 LZ(J)=J
DO 20 I=1,N
K=I
Y=A(I,I)
L=I-1
LP=I+1
IF (N-LP) 14,11,11
11 DO 13 J=LP,N
W=A(I,J)
IF (ABS(W)-ABS(Y)) 13,13,12
12 K=J
Y=W
13 CONTINUE
14 DELTA=DELTA*Y
DO 15 J=1,N
C(J)=A(J,K)
A(J,K)=A(J,I)
A(J,I)=-C(J)/Y
A(I,J)=A(I,J)/Y
15 B(J)=A(I,J)
A(I,I)=1.0/Y
J=LZ(I)
LZ(I)=LZ(K)
LZ(K)=J
DO 19 K=1,N
IF (I-K) 16,19,16
16 DO 18 J=1,N
IF (I-J) 17,18,17
17 A(K,J)=A(K,J)-B(J)*C(K)
18 CONTINUE
19 CONTINUE
20 CONTINUE
IF (INON) 530,530,529
529 DO 30 K=1,N
DO 30 J=1,N
PUNCH 105,K,J,A(K,J)
105 FORMAT (/13,1X,13,3X,E15.8)
30 CONTINUE
C CALCULATE CORIOLIS COEFFICIENTS.
530 PUNCH 303
PRINT 303
303 FORMAT (//37HCALCULATED CORIOLIS COEFFICIENTS FOR )
PUNCH 301
PRINT 301
DO 211 I=1,N
DO 211 J=1,N
TEMP(I,J)=0.
DO 211 K=1,N
211 TEMP(I,J)=TEMP(I,J)+CZ(I,K)*A(J,K)
DO 212 I=1,N
DO 212 J=1,N
ZM(I,J)=0.
DO 212 K=1,N
212 ZM(I,J)=ZM(I,J)+A(I,K)*TEMP(K,J)

```

```
      PUNCH 400
400  FORMAT (///22H  I  J      ZETA(I,J))
      DO 430 I=1,N
      DO 430 J=1,N
      PUNCH 105,I,J,ZM(I,J)
430  CONTINUE
      DO 214 I=1,N
214  FLMC(I)=ZM(I,I)
      PUNCH 401
401  FORMAT (///)
      DO 450 I=1,N
      PUNCH 402,I,FLMC(I)
      PRINT 402,I,FLMC(I)
402  FORMAT (5HZETA ,I3,4H = ,E15.8/)
450  CONTINUE
503  PRINT 106
      PUNCH 106
106  FORMAT (///12HEND OF CASE./)
      PAUSE
      GO TO 1
99   STOP
      END
```

BIBLIOGRAPHY

1. Aldous, J. and Mills, I. M., Spectrochim. Acta, 18, 1073 (1961).
2. Aldous, J. and Mills, I. M., Spectrochim. Acta, 19, 1567 (1963).
3. Allen, Jr., H. C. and Cross, P. C., Molecular Vib-Rotors, John Wiley & Sons, Inc., New York, 1963.
4. Arnett, R. L. and Crawford, Jr., B. L., J. Chem. Phys., 18, 118 (1950).
5. Ball, D. F., Goggin, P. L., McKean, D. C. and Woodward, L. A., Spectrochim. Acta, 16, 1358, (1961).
6. Blaine, L. R., Plyler, E. K. and Benedict, W. S., J. Research Natl. Bur. Standards, 66A, 223, (1962).
7. Boyd, D. R. J. and Longuet-Higgins, H. C., Proc. Roy. Soc. (London), A213, 55 (1952).
8. Brockway, L. O. and Jenkins, H. O., J. Am. Chem. Soc., 58, 2036 (1936).
9. Cahill, P. and Butcher, S., J. Chem. Phys., 35, 2255 (1961).
10. Chem. Eng. News, 39, 42 (November 20, 1961).
- 11a. Coulson, C. A., Victor Henri Memorial Volume, Desoer, Liege, 1947, p. 15.
- 11b. Coulson, C. A., Duchesne, J. and Manneback, C., Victor Henri Memorial Volume, Desoer, Liege, 1947, p.33.
12. deHeer, J., J. Chem. Phys., 20, 637 (1952).
13. Dennison, D. M., Rev. Mod. Phys., 3, 280 (1931).
14. Dennison, D. M., Rev. Mod. Phys., 12, 175 (1940).
15. Dillard, C. R. and Lawson, J. R., J. Opt. Soc. Am., 50, 1271, (1960).
16. Dillard, C. R. and May, L., J. Mol. Spectry., 14, 250 (1964).
17. Duncan, J. L., Spectrochim. Acta, 20, 1197 (1964).
18. Duncan, J. L., Spectrochim. Acta, 20, 1807 (1964).
19. Duncan, J. L., J. Mol. Spectry., 18, 62 (1965).

20. Duncan, J. L., and Mills, I. M., Spectrochim. Acta, 20, 523 (1964).
21. Fately, W. G. and Miller, F. A., Spectrochim. Acta, 17, 857 (1961).
22. Finholt, A. E., Bond, Jr., A. C., Wilzbach, K. E. and Schlesinger, H. I., J. Am. Chem. Soc., 69, 2692 (1947).
23. Gerhard, S. L. and Dennison, D. M., Phys. Rev., 43, 197 (1933).
24. Glass, W. K. and Pullin, A. D. E., Trans. Faraday Soc., 59, 25 (1963).
25. Goldfarb, T. D., J. Chem. Phys., 39, 2860 (1963).
26. Griffiths, J. E., J. Chem. Phys., 38, 2879 (1963).
27. Hansen, G. E. and Dennison, D. M., J. Chem. Phys., 20, 313 (1952).
28. Heath, D. F. and Linnett, J. W., Trans. Faraday Soc., 44, 873, 878 (1948).
29. Heath, D. F. and Linnett, J. W., Trans. Faraday Soc., 44, 884, (1948).
30. Heath, D. F., Linnett, J. W., and Wheatley, P. J., Trans. Faraday Soc., 46, 137 (1950).
31. Herschbach, D. R., Tables for the Internal Rotation Problem, Department of Chemistry, Harvard University, (1957).
32. Herzberg, G., Molecular Spectra and Molecular Structure, Vol. II, D. Van Nostrand Co., Inc., Princeton, New Jersey, 1945.
33. IBM Library Program #7.0.002, "Polynomial Curve Fitting by the Least Square Technique."
34. I.U.P.A.C., Table of Wavenumbers for the Calibration of Infra-Red Spectrometers, Butterworths, Washington, D.C., 1961.
- 34a. Kim, H. J. and Parr, R. G., J. Chem. Phys., 41, 2892 (1964).
35. Laurie, V. W. and Herschbach, D. R., J. Chem. Phys., 37, 1687 (1962).
36. Levin, I. W. and Ziffer, H., J. Chem. Phys., 43, 4023 (1965).

37. Lewis, G. N. and Randall, M., revised by Pitzer, K. and Brewer, L., Thermodynamics, Second Edition, McGraw-Hill Book Co., New York, 1961, Chapter 27.
38. Lide, Jr., D. R., J. Chem. Phys., 19, 1605 (1951).
39. Linnett, J. W., Quart. Rev., 1, 73 (1947).
40. Linnett, J. W., and Wheatley, P. J., Trans. Faraday Soc., 45, 33 (1949).
41. Linnett, J. W. and Wheatley, P. J., Trans. Faraday Soc., 45, 39 (1949).
42. Long, D. A., Gravenor, R. B. and Jones, D. T. L., Trans. Faraday Soc., 60, 1509 (1964).
43. Lord, R. C. and Merrifield, R. E., J. Chem. Phys., 20, 1348 (1952).
44. Lord, R. C. and Venkateswarlu, P., J. Chem. Phys., 20, 1237 (1952).
45. Markova, S. V., Ois Supplement on MOLECULAR SPECTROSCOPY, Optical Society of America, Washington, D.C., 1966, p. 88.
46. Meal, J. E. and Polo, S. R., J. Chem. Phys., 24, 1119, 1126 (1956).
47. Mills, I. M., Spectrochim. Acta, 19, 1585 (1963).
48. Moore, P. W., PhD Thesis, Purdue University, 1961.
49. Nielsen, H. H., J. Opt. Soc. Am., 34, 521 (1944).
50. Nielsen, H. H., Rev. Mod. Phys., 23, 90 (1951).
51. Overend, J. and Crawford, Jr., B. L., J. Chem. Phys., 29, 1002 (1958).
52. Overend, J. and Scherer, J. R., J. Chem. Phys., 32, 1289 (1960).
53. Plyler, E. K., Dante, A., Blaine, L. R., and Tidwell, E. D., J. Research Natl. Bur. Standards, 64A, 29 (1960).
54. Randic, M., Spectrochim. Acta, 18, 115 (1962).
55. Randic, M., J. Chem. Phys., 36, 567 (1962).
56. Salem, L., J. Chem. Phys., 38, 1227 (1963):
57. Shimanouchi, T., J. Chem. Phys., 17, 848 (1949).

58. Spanier, E. J. and MacDiarmid, A. G., Inorg. Chem., 2, 215 (1963).
59. Tobin, M. C., J. Am. Chem. Soc., 75, 1788 (1953).
60. Urey, H. C., and Bradley, C. A., Phys. Rev., 38, 1969 (1931).
61. Van Riet, R., Bull. Classe Sci., Acad. Roy. Belg., 41, 188 (1955).
62. Ward, C. H., PhD Thesis, Purdue University, 1954.
63. Wilde, R. E., PhD Thesis, University of Washington, 1961.
64. Wilson, Jr., E. B., Decius, J. C., and Cross, P. C., Molecular Vibrations, McGraw-Hill Book Co., New York, 1955..
65. Worthing, A. G. and Geffner, J., Treatment of Experimental Data, John Wiley & Sons, Inc., New York, 1943, Chapter IX.